WestVirginiaUniversity
THE RESEARCH REPOSITORY @ WVU

Graduate Theses, Dissertations, and Problem Reports

2013

Nanoclay-Based Solid-Amine Adsorbents for Carbon Dioxide Capture

Elliot A. Roth
West Virginia University

Follow this and additional works at: https://researchrepository.wvu.edu/etd

Recommended Citation

Roth, Elliot A., "Nanoclay-Based Solid-Amine Adsorbents for Carbon Dioxide Capture" (2013). *Graduate Theses, Dissertations, and Problem Reports*. 279.
https://researchrepository.wvu.edu/etd/279

This Dissertation is protected by copyright and/or related rights. It has been brought to you by the The Research Repository @ WVU with permission from the rights-holder(s). You are free to use this Dissertation in any way that is permitted by the copyright and related rights legislation that applies to your use. For other uses you must obtain permission from the rights-holder(s) directly, unless additional rights are indicated by a Creative Commons license in the record and/ or on the work itself. This Dissertation has been accepted for inclusion in WVU Graduate Theses, Dissertations, and Problem Reports collection by an authorized administrator of The Research Repository @ WVU. For more information, please contact researchrepository@mail.wvu.edu.

Nanoclay-Based Solid-Amine Adsorbents for Carbon Dioxide Capture

Elliot A. Roth

Dissertation submitted to the
Benjamin M. Statler College of Engineering and Mineral Resources
at West Virginia University
in partial fulfillment of the requirements
for the degree of

Doctor of Philosophy
in
Chemical Engineering

Rakesh Gupta, Ph.D., Chair
Sushant Agarwal, Ph.D.
Charter Stinespring, Ph.D.
Evan Granite, Ph.D.
Karl Haider, Ph.D.

Department of Chemical Engineering

Morgantown, West Virginia
2013

Keywords: Carbon Dioxide Capture; Amine; Solid Adsorbent
Copyright 2013 Elliot A. Roth

ABSTRACT

Nanoclay-Based Solid-Amine Adsorbents for Carbon Dioxide Capture

Elliot A. Roth

The objective of this research was to develop an efficient, low cost, recyclable solid sorbent for carbon dioxide adsorption from large point sources, such as coal-fired power plants. The current commercial way to adsorb CO_2 is to use a liquid amine or ammonia process. These processes are used in industry in the "sweetening" of natural gas, but liquid based technologies are not economically viable in the adsorption of CO_2 from power plants due to the extremely large volume of CO_2 and the inherent high regeneration costs of cycling the sorbent. Therefore, one of the main objectives of this research was to develop a novel sorbent that can be cycled and uses very little energy for regeneration.

The sorbent developed here is composed of a nanoclay (montmorillonite), commonly used in the production of polymer nanocomposites, grafted with commercially available amines. (3-aminopropyl) trimethoxysilane (APTMS) was chemically grafted to the edge hydroxyl groups of the clay. While another amine, polyethylenimine (PEI), was attached to the surface of the clay by electrostatic interactions. To confirm the attachment of amines to the clay, the samples were characterized using FTIR and the corresponding peaks for amines were observed. The amount of amine loaded onto the support was determined by TGA techniques. The treated clay was initially analyzed for CO_2 adsorption in a pure CO_2 stream. The adsorption temperatures that had the highest adsorption capacity were determined to be between 75°C and 100°C for all of the samples tested at atmospheric pressure. The maximum CO_2 adsorption capacity observed was with nanoclay treated with both APTMS and PEI at 85°C. In a more realistic flue gas of 10% CO_2 and 90% N_2, the adsorbents had essentially the same overall CO_2 adsorption capacity indicating that the presence of nitrogen did not hinder the adsorption of CO_2. Adsorption studies in pure CO_2 at room temperature under pressure from 40-300 PSI were also conducted. The average adsorption capacity for the adsorbents did not change significantly over the range of pressures studied, indicating that the uptake of CO_2 was due mainly to chemical reaction and not to the physical absorption of CO_2. The average CO_2 adsorption capacity at 300 psi and room temperature for clay treated with APTMS alone was 7.6 wt% CO_2. The combination of APTMS and PEI treatment increased the average adsorption capacity to 11.4 wt% CO_2.

The regeneration method for the majority of the adsorption tests employed pure N_2 at 100°C as a sweep gas, and it was successful in regenerating the adsorbent. The regeneration of the adsorbent was also studied with pure and humid CO_2 at 155°C. Using CO_2 as a sweep gas for regeneration is more commercially relevant and was able to regenerate the sorbents.

Vacuum regeneration and the stability of the adsorbents to water vapor were also studied. Our studies showed that the developed adsorbents were able to adsorb CO_2 at atmospheric conditions using pure CO_2 as well as 10% CO_2 and 90% nitrogen. Additionally, the adsorbents developed have the potential to be cycled using commercially applicable regeneration schemes. While these results are comparable to results of other emerging CO_2 adsorption technologies, our adsorbent has the benefit of a very cheap support, and it could provide a commercially useful CO_2 adsorbent.

ACKNOWLEDGEMENT

I would like to thank my advisor, Dr. Rakesh Gupta, for all of his enthusiasm, advice, motivation, and help he provided me with throughout my graduate studies. He helped me with not only my research and classwork, but also helped me become a better person in general. I would like to thank Dr. Sushant Agarwal for all of his expertise in the laboratory, and his help with everyday problems that tend to occur with experimental research. I would like to thank Dr. Evan Granite for his unwavering support, enthusiasm, and advice with my research, and giving me a chance to see his laboratory at the Department of Energy, which was very exciting in many ways. My appreciations are extended to Dr. Karl Haider who helped organize my internship at Bayer MaterialScience, and provide a vast amount of knowledge with the chemistry and other areas of my research. I would also like to thank Dr. Charter Stinespring for his advice and guidance during my studies.

My sincere gratitude goes out to Dr. John Zondlo and Dr. Gloria Oporto for allowing me to use their equipment and laboratory space, which was instrumental to my research. Additionally, I would like to thank Adam Finniss, Matthew Thompson, Jeremy Hardinger, and everyone else who helped me with laboratory techniques, with technical problems, and with proofreading anything that I needed. Finally I would like to thank the Bayer Foundation for the fellowship it provided me for the duration of my studies, and Center for Advanced Separation Technology (CAST) for funding.

Table of Contents

List of Figures

List of Tables

Chapter 1

1. Introduction

Almost all the energy produced in the world comes from the burning of fossil fuels such as oil, coal and natural gas. Since no clean and renewable energy source, (i.e. solar, wind, hydro, geothermal) seems likely to make a major impact in world energy demands in the near future, it is foreseeable that the amount of anthropogenic (i.e., human caused) carbon dioxide emission is only going to rise. The growing concern with global warming and its effects on climate change is almost certain to drive government regulation to reduce the amount of greenhouse gases allowed to be emitted into the atmosphere. Although CO_2 is not the worst greenhouse gas, it is by far the most released with the current world-wide emission rate of approximately 28 gigatonnes of CO_2 per year. [1]

The most logical way to capture vast amounts of CO_2 is by focusing on large point sources like coal-fired power plants. Commercially available CO_2 capture processes exist due to industrial processes which require the removal of CO_2 from natural gas streams or from hydrogen production streams. These typically use either liquid physical solvents, which absorb CO_2 without reactions, or liquid chemical solvents, which are usually amines that react with CO_2. One problem with both of these processes is that they require a large amount of energy to regenerate the sorbent.

Solid sorbents have also been studied for adsorption of CO_2 and typically use a porous support material which can adsorb CO_2 itself. Alternatively a chemical that can adsorb CO_2 (usually an amine) is either attached to the surface of the substrate by chemical reaction or is

impregnated into the pores. Once the amine is attached to the support material, the sorbent can adsorb CO_2 by reacting with the attached amines. After the sorbent has adsorbed the CO_2 from the gas stream, it can then be regenerated by thermal treatment, reduction in pressure, or a combination of both processes. This cycle can be repeated multiple times. Some possible advantages that solid amines have over conventional liquid amines are reduced energy requirement for regeneration, less corrosion problems, and less environmental impacts from loss of evaporated toxic amines.

1.1 Coal-fired Power Plants and Carbon Dioxide Emissions

There has been a growing concern with the rise in the amount of CO_2 in the atmosphere and its possible effects on the environment over the past several years. One possible reason for this sharp increase in the amount of atmospheric CO_2 could be the enormous amount of CO_2 that is released into the atmosphere from the burning of fossil fuels for energy. Electricity and heat generation produced 41% of the world CO_2 emissions in 2009 with transport and industry contributing the majority of the other CO_2 emissions. [2] Figure 1-1 is a representation of the amount of CO_2 emissions produced from different sources in 2009.

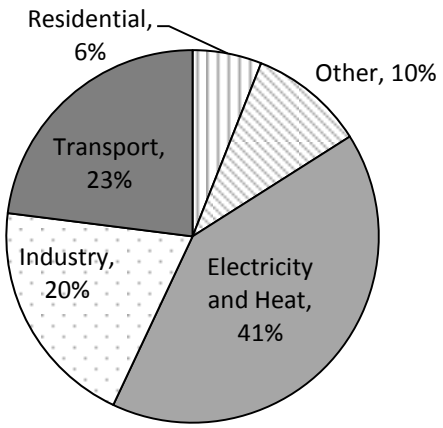

Figure 1-1: World CO_2 emissions by sector in 2009; Other, includes commercial/public services, agriculture/forestry, fishing and other emissions not specified elsewhere. [2]

Processes where large amounts of CO_2 are released at a single point source would seem to be the most logical and easiest place to start to explore the possibility for CO_2 capture and sequestration. Some important information to consider is that approximately 25% of the world's primary energy demand is satisfied by coal, and about 50% of the power produced in the United States comes from coal-fired power plants. [3] Recently the decrease in natural gas prices has decreased the amount of electricity being produced from coal. In August 2012 only 39% of the power produced in the U.S. came from coal. [4] Worldwide, approximately 12.5 billion metric tons of CO_2 is produced from the combustion of coal which is about 43% of the world's CO_2 emissions in 2009. [2] Since coal CO_2 emissions are so large and the equivalent of one hundred 500 MW coal-fired power plants are built in China each year, CO_2 capture at coal-fired power plants is an ideal place to reduce emissions. [5] CO_2 capture at this point source would obviously result in significant reduction of the anthropogenic CO_2 emitted each year.

For each ton of coal burned, over 3 tons of CO_2 are produced, and this generates about 3MM ton/year of CO_2 for a 500 MW power plant. [5] A $25 per ton target cost for capturing CO_2 would imply about $75 in additional costs per ton of coal burned, which is close to the cost of coal itself. [5] With the equivalent of about five hundred 500 MW coal-fired power plants in the U.S. it can be seen that to capture all of the CO_2 emitted by coal-fired power plants in the U.S. would amount to billions of dollars per year in CO_2 capture cost. Therefore a low cost, efficient, and robust technology is needed for CO_2 capture in the quantities needed at coal-fired power plants.

1.1.1 Post-combustion capture of CO_2

The majority of coal-fired power plants in the U.S. traditionally burn coal with excess air to create heat. This process creates a flue gas stream of mostly nitrogen and carbon dioxide, with some leftover oxygen, water, acid gases and other impurities. Traditional coal combustion creates a flue stream with a huge volumetric flow rate, at about atmospheric pressure, and relatively low temperature as compared to other coal combustion technologies. As a result, it is necessary to capture CO_2 by the use of post-combustion technology, and it would be ideal to develop a CO_2 sorbent and process that can be retrofitted onto these existing plants. Figure 1-2 shows the estimated amount of CO_2 released from existing coal-fired power plants versus coal-fired power plants being built.

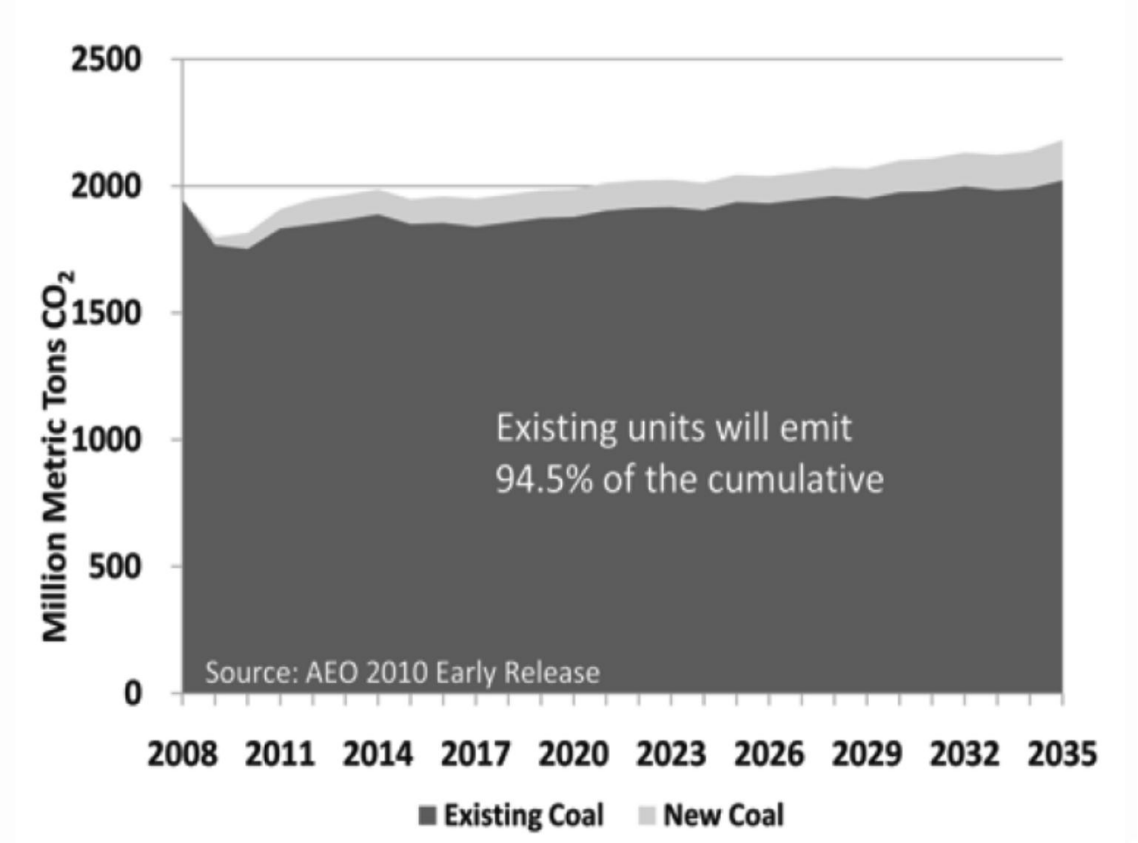

Figure 1-2: U.S. projection of CO_2 emissions for existing coal-fired power plants versus new coal-fired power plants [6]

From Figure 1-2, it can be seen that the vast amount of CO_2 emission from coal-fired power plants is projected to occur from existing plants in the United States. Therefore it is necessary to develop a sorbent for the conditions that occur in pre-existing plants. The conditions and composition of the flue gas in post-combustion power plants are compared with other technologies in section 1.1.2.

1.1.2 Pre-Combustion capture of CO_2

In pre-combustion capture of CO_2 the coal is first gasified to create a synthesis gas composed of CO and H_2. The CO is then converted to CO_2 by a shift reaction, which produces more H_2. The CO_2 would then be removed before the burning of H_2. Integrated gasification combined cycle (IGCC) is a process in which CO_2 can be captured before the combustion of coal.

In an IGCC process, the coal is reacted with H_2O and O_2. The reaction of coal and the H_2O produces the syngas. The combustion reaction with O_2 and coal is used to produce heat to drive the predominantly endothermic gasification reactions [7]. The main reactions that occur in the gasification of coal are shown in Equations 1-4. [7]

$$C + O_2 \rightarrow CO_2 \qquad \Delta H_{rxn} = -394 \text{ kJ/mol} \qquad (1)$$

$$C + \tfrac{1}{2} O_2 \rightarrow CO \qquad \Delta H_{rxn} = -111 \text{ kJ/mol} \qquad (2)$$

$$C + H_2O \rightarrow CO + H_2 \qquad \Delta H_{rxn} = -131 \text{ kJ/mol} \qquad (3)$$

$$C + CO_2 \rightarrow 2CO \qquad \Delta H_{rxn} = 173 \text{ kJ/mol} \qquad (4)$$

Table 1-1 lists typical conditions for a 500 MW coal fired power plant using traditional post-combustion technology versus the conditions from pre-combustion capture fuel stream.

Table 1-1: Typical process conditions for combustion and gasification of coal in a 500 MW power plant [5]

	Post-Combustion	Gasification or Pre-Combustion
Coal Feed (kg/h)	284,000	228,000
Gas Mass Flow (kg/h)	3,210,000	607,000
Pressure (bar)	1-1.5	25-100
Temperature (°C)	40-160	40-300
Volumetric Flow Rate (m^3/h)	2,568,000	21,274

The typical gas composition of a coal combustion flue stream versus pre-combustion fuel stream is shown in Table 1-2. The pre-combustion fuel stream has a greater concentration in CO_2 and H_2 while simultaneously having a significantly smaller concentration of N_2.

Table 1-2: Typical Composition of Coal Combustion Flue Gas and Gasification Fuel Gas [5]

		Post-Combustion	Gasification or Pre-combustion
Composition	MW	Volume %	Volume %
H_2	2	0	50
H_2O	18	15	10
N_2	28	65	4
O_2	32	4	0
NO	32	0.06	0
H_2S	34	0	0.5
CO_2	44	14.8	35.5
SO_2	64	0.14	0
Hydrocarbon	Various	Some	Some

In pre-combustion capture of CO_2, the gas stream is at considerably higher pressures, has a higher concentration of CO_2, and has a much lower flow rate than post-combustion capture. This is the preferred technology for coal efficiency, but there are few IGCC power plants operating at present.

1.1.3 Oxy-fuel Combustion

Oxy-fuel combustion is a process where pure oxygen is used instead of air to burn the coal. This technology creates a flue gas with almost no N_2 and a very high concentration of CO_2.

Using this combustion process would produce an almost sequestration-ready CO_2 flue gas with drying probably being the only separation needed. [7] Problems with this process are that it requires an expensive air separation unit, and concerns with conventional boilers and gas turbines handling the high flame temperature of coal burned in pure O_2. [7] To alleviate the high flame temperature caused by burning in a pure oxygen environment, CO_2 could possibly be recycled and mixed with the pure O_2 and coal prior to combustion in existing coal-fired power plants. Theoretical gas compositions for a 500 MW power plant for this process are compared with air-blown combustion in Table 1-3.

Table 1-3: Theoretical gas compositions for a 500 MW power plant flue gas for Air-Blown versus Oxyfuel Combustion [7]

	Air-Blown	Oxyfuel (99% O_2 / 1% CO_2)
Flue Gas Flow Rate (kg/s)	552	178
Nitrogen (% v/v)	74	0.6
Carbon Dioxide (%v/v)	14	63
Water (% v/v)	8	32
Oxygen (% v/v)	3	4.5
Argon (% v/v)	1	0.3
Sulfur Oxides (% v/v)	0.07	0.3
Nitrogen Oxides (% v/v)	0.02	0.07

Table 1-3 shows that the combustion of coal in pure oxygen would possibly create a flue gas stream that would only need the removal of water to be sequestered. If this technology could

be economically achieved it would greatly reduce the need for an adsorbent that could capture CO_2 from post-combustion coal-fired power plants.

1.2 Sequestration of CO_2

The capture of CO_2 is a challenging and expensive problem, but it is only the first step in the process of carbon capture and sequestration. [6] After the capture of CO_2, the next step is to transport the CO_2 through a pipeline for sequestration. The three major geologic formations considered to be good candidates for CO_2 sequestration are depleted oil and gas reservoirs, deep unmineable coal seams, and saline formations. [1] With the large amount of CO_2 that could be potentially captured from coal-fired power plants, an enormous amount of storage capacity is needed. Fortunately the estimated worldwide capacity of CO_2 in geologic formations is in the range of 100-10,000 gigatonnes. [8]

1.2.1 Storage of CO_2 in Oil and Gas Reservoirs

Storage of CO_2 in oil and gas reservoirs is a good place to sequester CO_2 because they have contained oil and gas for millions of years with minimum leakage. Also, their geology is well understood and CO_2 can be used to help increase the production of oil and gas, which can offset some of the costs of capturing CO_2. The process of using CO_2 for enhanced oil recovery (EOR) has been shown to work and is currently being conducted. In North Dakota there is a major CO_2 pipeline that transports CO_2 to the Weyburn enhanced oil recovery (EOR) project in Canada. The CO_2 is 95% pure, has a flow rate of 5,000 tonnes per day and is in the form of a supercritical fluid at a pressure of about 150 atm. [1] This project shows the possibility for CO_2

sequestration in oil formations. The estimated capacity for CO_2 storage in the U.S. and Canada within oil and gas fields is 138 billion tonnes. [9]

1.2.2 Storage in Unmineable Coal Seams

Another geologic formation for CO_2 sequestration is unmineable coal seams. Unmineable coal seams are seams that are either too deep or too thin to be mined economically. By sequestering CO_2 in coal seams, it is possible to recover methane that is commonly found in coal seams. This process of recovering methane by sequestering CO_2 is called enhanced coal-bed methane (ECBM) recovery. Since the geology of coal seams is well known, this process could provide a good option for long term storage for CO_2. The rank of the coal determines the amount of CO_2 molecules that are adsorbed for each molecule of methane released. The estimation for the capacity of CO_2 that can be sequestered in unmineable coal seams is in the range of 60-117 billion metric tons in the U.S and Canada. [10] Just like EOR, sequestration in unmineable coal seams would not only be a good place for long term sequestration, but it could also offset some of the cost for CO_2 capture by recovering methane.

1.2.3 Saline Formations

Saline formations are layers of porous rock that are saturated in salt water that was either trapped from the ocean during the rock formation or had salt leach into the water from the surrounding rocks. These formations are possibly huge sinks for CO_2 sequestration. Unlike oil, gas and coal reservoirs for sequestration, there is no added cost benefit from the recovery of methane or oil. Another disadvantage of saline formations is the limited characterization experience from industry compared to oil and coal reservoirs. All of the saline formations in the U.S. have not been documented, but enough have been documented to form an estimate for

CO_2 storage. In the U.S. there is an estimated CO_2 storage capacity of 1,653 to more than 20,213 billion metric tons in saline formations. [10] This is enough storage capacity to sequester more than 450 years of current CO_2 emissions. [10]

1.3 Objective of Research

With billions of tons of CO_2 being released into the atmosphere every year from the combustion of fossil fuels to produce electricity, the need for a cheap and efficient process to capture CO_2 is key to the reduction of anthropogenic greenhouse gas emissions. Therefore, the objective of the current research is to develop an efficient, low cost, highly recyclable solid sorbent for carbon dioxide adsorption from large point sources, such as coal-fired power plants. The solid support used is to be available in large quantities and be modified using commercial amines. Once the amine is grafted to the support, the amount of amine grafted onto the support and the CO_2 adsorption capacity need to be studied.

The sorbent developed here is composed of a nanoclay (montmorillonite), commonly used in the production of polymer nanocomposites, grafted with commercially available amines. The goal was to react (3-aminopropyl) trimethoxysilane to the edge hydroxyl groups of the clay. Additionally polyethylenimine was attached to the flat surface of the clay by electrostatic interactions. The combination of both treatments was also studied to determine if there was an increase in the adsorption of CO_2.

For the adsorption of CO_2, the objective is to first study the sorbents in a pure CO_2 atmosphere to determine the adsorption capacity. Different temperatures and pressures for CO_2 adsorption will be used to determine the dependence on each variable and its applicability to post-combustion or pre-combustions conditions. Desorption of the adsorbed CO_2 will also

be tested to determine the ability for multiple CO_2 adsorption steps. Additionally a realistic reaction gas with 10% CO_2 will be used to determine the CO_2 adsorption capacity in a mixed gas stream.

Once the adsorption and desorption of the adsorbents has been studied the objective is to determine more industrially realistic conditions for cycling of the adsorbent. The stability of the adsorbents in water vapor will be studied and so will the ability to desorb CO_2 in an industrially realistic process such as vacuum or temperature swing desorption using a sweep gas.

Chapter 2

2. Literature Review

Carbon dioxide capture technologies exist due to commercial processes that require separation of CO_2, like the purification of natural gas. Commercial purification of natural gas, the possibility of carbon emission taxes or regulations in the U.S., and the possibility of successful carbon capture and sequestration to reduce or stop global warming have created many research opportunities for the capture of CO_2. The main research areas are for work on improving existing CO_2 capture technologies and creating completely new sorbents to separate or capture CO_2. Some of these processes being researched to capture carbon dioxide are conventional physical and chemical solvents, aqueous ammonia, metal organic frame works (MOFs), membranes, solid amine sorbents, zeolites and compounds of alkali and alkali earth metals, hydrates, and chemical-looping. Solid amine adsorbents, which is the category of the adsorbent developed in this research, contain a vast amount of different supports and amines to capture CO_2 with various advantages and disadvantages.

2.1 Physical and Chemical Solvents for CO_2 Capture

Physical solvents capture CO_2 by selectively absorbing CO_2 from the flue stream without chemical reaction. The amount of CO_2 that can be absorbed using physical solvents depends on the partial pressure of CO_2 and temperature of the flue gas. Higher loadings are achieved with low temperatures and high partial pressures of CO_2. The maximum loading of CO_2 for physical solvents are approximately proportional to the partial pressure of CO_2. [1] Henry's law is an approximation for the amount of CO_2 that can be absorbed into a physical solvent.

$$X_{CO_2} = P_{CO_2} \times \frac{1}{H_{CO_2}(T)} \qquad 2\text{-}1$$

Where X_{CO_2} is the mole fraction of CO_2 in the liquid phase, P_{CO_2} is the partial pressure of CO_2, and $H_{CO_2}(T)$is the Henry's constant for CO_2 in the solvent at a given temperature. [7] Since the absorption capacity depends on the partial pressure of CO_2, physical solvents work best for pre-combustion capture of carbon dioxide where the pressures are much higher and the concentration of CO_2 is higher than post-combustion conditions. Physical solvents are regenerated by either pressure reduction or addition of heat, and since the Van der Waal's forces or electrostatic forces that bind the CO_2 molecules to the solvent are much weaker than the chemical bonds with CO_2 in chemical solvents, the regeneration energy required for physical solvents is much less than for chemical solvents. [7] A major problem with physical solvents is that they usually require cooling of the syngas before carbon capture. [1] Two conventional physical processes for acid gas removal are Selexol™ and Rectisol®, which rely on dimethyl ethers of polyethylene glycol (DMPEG) and chilled methanol respectively, as the solvents. [11]

Chemical solvents differ from physical solvents in that they chemically react with CO_2 to separate CO_2 from the flue gas. Chemical solvents can capture carbon dioxide at low partial pressures, and the loading capacity depends on chemical equilibrium and concentration of the amine in the solvent. [1] The ability to capture CO_2 at low partial pressures makes chemical solvents capable of capturing CO_2 from traditional coal fired power plants. Commonly used amines in chemical solvents are a primary amine, monoethanol amine (MEA), a secondary amine, diethanol amine (DEA), and a tertiary amine, methyl diethanol amine (MDEA), with primary amines forming the strongest bonds with acid gases. Problems with chemical amine solvents are that amine concentration is usually limited to approximately 30%, due to corrosion

problems, which increases the heat input for regeneration, formation of stable compounds with impurities like COS, SO_2, SO_3, and NO_x, degradation of the amine by oxygen in the flue gas, and loss of the amine due to vaporization. Adsorption capacity for MEA processes can reach up to 1.20 kg CO_2/ kg NH_3 or 0.40 kg CO_2/ kg of MEA based on 30% amine solution. [12]

2.2 Aqueous Ammonia

Aqueous ammonia sorbents work in the same way that amine chemical solvents work, but they have the advantage of lower regeneration energy, potential for higher CO_2 capacity, and no degradation due to oxygen. Also when reacted with SO_x and NO_x, ammonium sulfate and ammonium nitrate can be produced and sold as fertilizer. [1] One significant problem is the higher volatility of ammonia compared to MEA, requiring the flue gas to be cooled between 0-25°C. [1] This technology has not been sufficiently developed for commercial deployment. [7]

2.3 Metal organic Frameworks (MOFs)

Metal organic frameworks are a class of nanoporous materials that are synthesized using organic linker molecules and metal joints that self-assemble into well-defined crystalline forms with high surface areas. [13] An example of the formation of a MOF is shown in Figure 2-1. Figure 2-1 shows a well-organized structure that is composed of an organic linker and produces a nanoporous material.

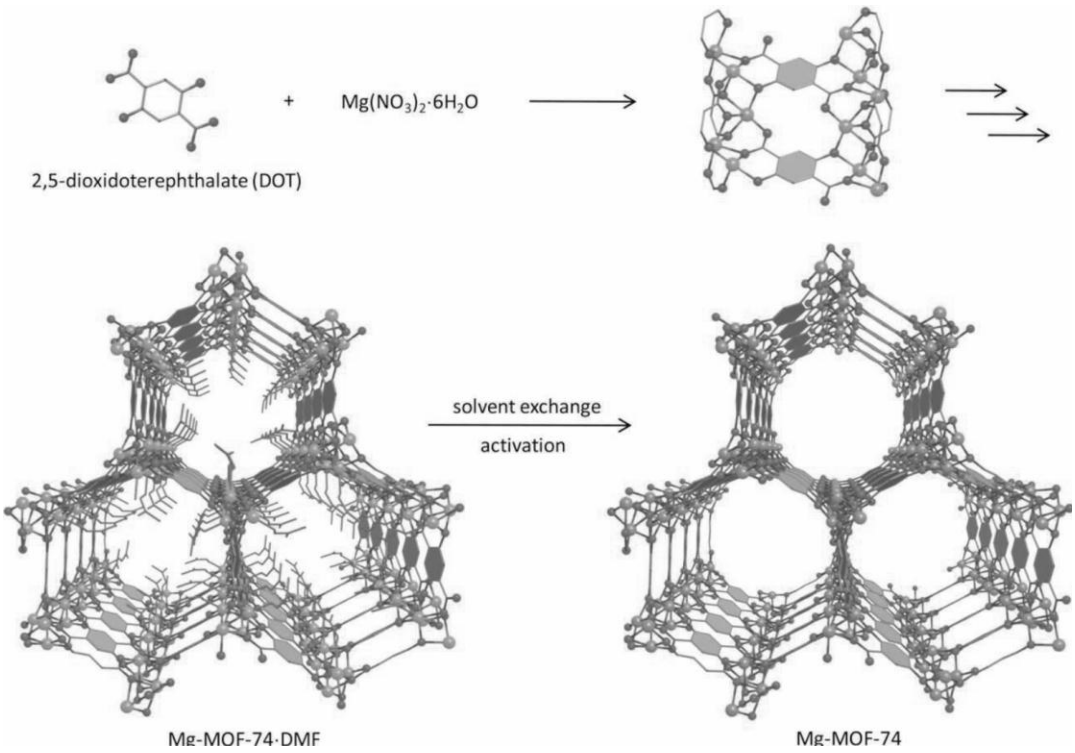

Figure 2-1: Single crystal structure of Mg-MOF-74, formed by reaction of the DOT linker with $Mg(NO_3)_2 \cdot 6H_2O$ [14]

There are a vast amount of MOFs that can be formed with different chemical functionalities, which potentially make MOFs excellent candidates for CO_2 adsorption. [13] With the possibility of thousands of combinations of MOFs, there is a significant potential for modeling and simulation to determine the best MOF for carbon dioxide capture. Therefore, there has been a large amount of research on simulating MOFs for CO_2 capture. [13] [15], [16] MOFs have been shown to adsorb CO_2 at pressures as low as 0.1 bar and at room temperature with an adsorption capacity of 236 mg CO_2/ g sorbent (23.6% wt gain). [15] Problems with MOFs for CO_2 capture are low selectivity for CO_2 in nitrogen and CO_2 streams, unfavorable adsorption isotherms at low pressure, and large reduction of CO_2 adsorption with an increase in temperature.

2.4 Zeolites and compounds composed of alkali and alkali earth metals

Zeolites are highly organized microporous crystalline materials that have also been studied for CO_2 capture. The interests of zeolites for carbon dioxide capture are the different adsorption capacities observed based on the pore size, chemical make-up and structure of the zeolite. Zeolites with low Si/Al ratio have been reported to have the best CO_2 adsorption capacity. [17] One commonly studied zeolite is 13X and has shown to have a high CO_2 adsorption capacity at higher pressures and low temperatures. [18] Figure 2-2 shows a diagram of different frameworks of typical zeolites.

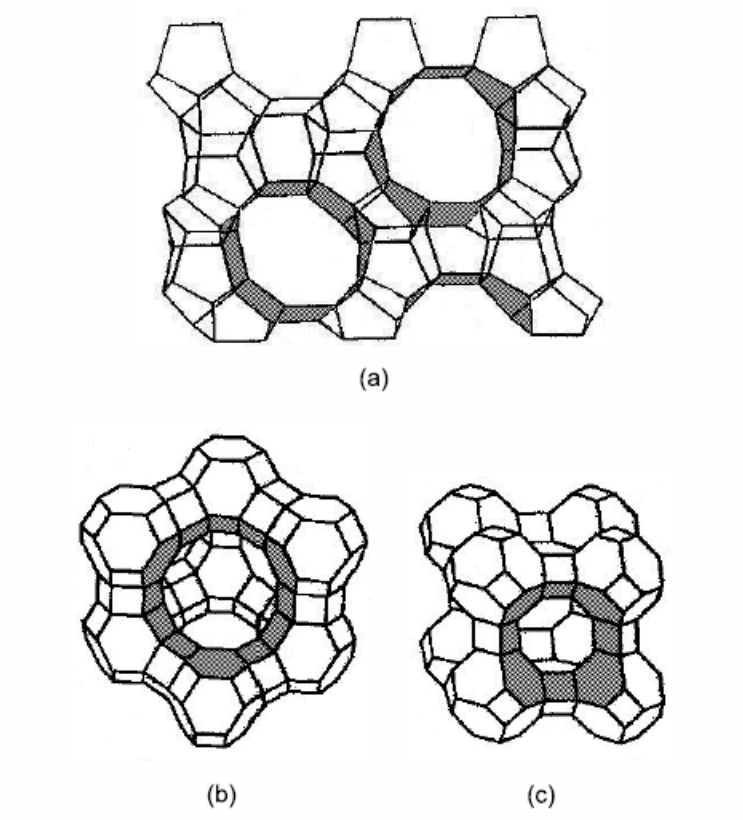

Figure 2-2: Structures of different zeolite frameworks (a) silicalite, (b) 13X and (c) 5A [19]

Zeolites consist of tetrahedrons as the primary building units, were a silicon or aluminum atom is surrounded by four oxygen atoms. [19] The internal pore surfaces are made by linkages of secondary building units in different geometries, which can be seen in Figure 2-2 for three different zeolites. [19] The inner surfaces of the zeolites can be made up of triangles, squares, rectangles and regular hexagons, which can also be seen in Figure 2-2. [19] Although zeolites can be tunable, one problem with zeolites is the severe reduction of CO_2 adsorption capacity in the presence of water. [20]

Compounds of alkali metals can be used to chemically react with CO_2. An example of this is an alkali metal carbonate reacting with CO_2 and H_2O to form alkali metal bicarbonate as shown in Equation 5.

$$X_2CO_3 + CO_2 + H_2O \leftrightarrow 2XHCO_3 \quad (5)$$

(X = Li, Na, K, etc.)

Alkaline earth metals react with CO_2 to form alkaline earth metal carbonate. Equation 6 is an example of this reaction.

$$XO + CO_2 \leftrightarrow XCO_3 \quad (X = Mg, Ca, etc.) \quad (6)$$

Alkali metals can react with CO_2 in the temperature range of 373-473 K, which is suitable for flue gas carbon capture. The alkaline earth metal (CaO, MgO) can also react with CO_2 in the temperature range of 773-1173 K, which can be utilized in process streams at elevated temperature, such as integrated gasification combined cycle (IGCC). [12]

2.5 Gas Hydrates

Carbon dioxide can also be captured by the formation of hydrates. Gas hydrates are crystalline solids where low molecular weight molecules are trapped inside cages of hydrogen-bonded water molecules. [21] In this process the exhaust gas containing CO_2 is exposed to water under high pressure and a hydrate is formed, which captures the carbon. The hydrate is separated and dissociated to release the CO_2. This process has shown to have a potential energy penalty as small as 6-8%. [22] This process is an interesting process to capture CO_2, but has not been extensively studied as a viable option for CO_2 capture from coal-fired power plants.

2.6 Chemical Looping

Chemical looping is a process where a particle acts as an oxygen carrier, and is used in place of air to combust the fuel. By using a metal oxide as the oxygen source instead of air, an exhaust stream of CO_2 and H_2O is formed which can easily be separated by drying. The success of chemical looping is strongly dependent on the chemical looping particles or oxygen carrier particles, and it has been used to create hydrogen in industrial processes. [23] The chemical looping process can be applied to combustion (CLC) or gasification (CLG) of carbon-based materials and can be more energetically efficient than conventional power generation processes. [23] Figure 2-3 is a simplified representation of chemical looping in direct combustion of coal using iron as the chemical looping particle.

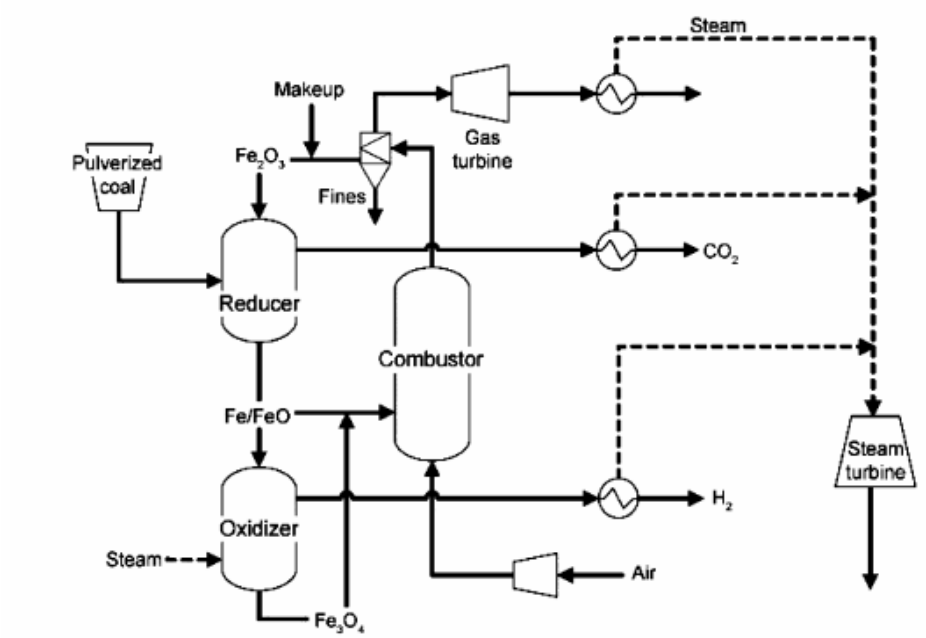

Figure 2-3: Schematic of direct coal combustion using chemical looping with iron. [23]

This technology is an alternative to separating oxygen from nitrogen in air for oxyfuel combustion, and it is a very interesting process for CO_2 capture. Using this process a stream of CO_2 pure enough for sequestration could possibly be created by simply condensing out water in the flue gas. The reason this process is not in commercial operation is high product cost due to low reactivity and recyclability of the chemical looping particles. [23]

2.7 Membranes for CO_2 Separation

Membranes have been used for many industrial separation applications and have been used to separate CO_2 from natural gas. Membranes separate CO_2 from other gases by either size exclusion or by chemical affinity. Problems with polymer membranes for CO_2 separation include the chemically harsh environment and high temperatures of fuel and flue gases. Also the low pressure of traditional flue does not provide a large driving force for membrane processes. The ideal membrane is one with high permeability and a high selectivity, but a highly

permeable membrane tends to have a low selectivity and a highly selective membrane tends to have low selectivity. [24] Polyimide based membranes have shown some of the best permeability and selectivity properties for purely polymeric membranes and are resistant to thermal, chemical and plasticization degradation. [24] The development of a membrane process that could separate CO_2 from a gas stream with a huge volumetric flow rate at low pressure and a low concentration of CO_2 is a very difficult task. If a membrane could be developed for these conditions, this would seem to be a simple commercial system for cheap retrofitting of existing coal-fired power plants and the separation of CO_2.

2.8 Solid Amine Sorbents

Solid amine adsorbents use an amine to chemically react with CO_2 to adsorb CO_2. Solid amine sorbents for CO_2 capture are usually made up of a porous large surface area support that is either impregnated or reacted with an amine that can absorb CO_2. Solid amine sorbents have an advantage over liquid amine processes in that they do not have corrosion problems, and they need less energy to regenerate because they are not diluted in an aqueous solution like liquid amine processes. Some problems with solid amine sorbents that were initially reported are low CO_2 capacity, lack of stability over regeneration cycles and poisoning from other flue gases. [25]

It has been reported that for a solid CO_2 adsorbent to be economically competitive against other technologies, the adsorbent would have to adsorb approximately 2-4 mmol/g sorbent. [26] Many solid amine sorbents described in the literature have not been able to reach this capacity, but some more recently studied solid amine sorbents have been reported to have a CO_2 capture capacity as high as to 5.55 mmol CO_2/g sorbent (24.4 wt.% CO_2). [27] The ability of

some solid amine adsorbents to adsorb a relatively large amount of CO_2 shows the possibility for these sorbents to work in the CO_2 capture from coal-fired power plants. Besides the key requirement for these adsorbents to adsorb CO_2, they should also be able to desorb CO_2 with minimal amount of energy. The proposed reaction for CO_2 using liquid amines is shown in Figure 2-4. It is expected that solid amine adsorbents would follow the same reaction

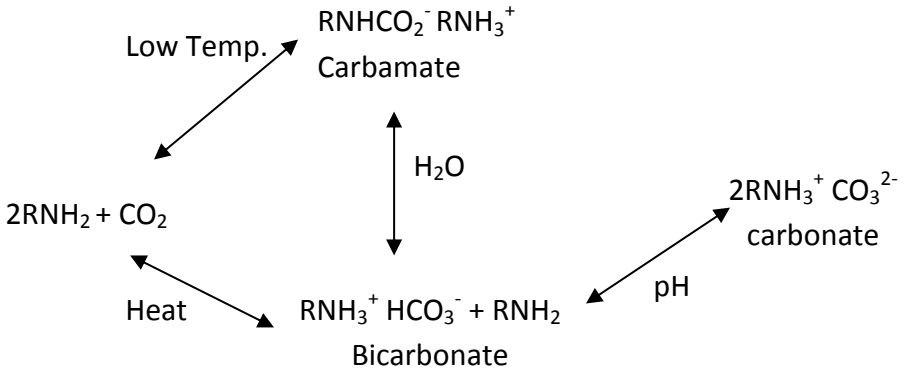

mechanism. [28]

Figure 2-4: Proposed reaction mechanism for carbon dioxide and amines [28]

Three different types of solid amine adsorbents have been reported for the capture of CO_2 at relatively low temperatures and atmospheric pressures. The first class of solid amine adsorbents uses a porous support that is impregnated with an amine such as PEI. Significant amount of research for this support was conducted by Song and was first reported in 2002. [29], [30], [31], [32], [33] The second class of solid amine adsorbents is based on amines that are covalently attached to the solid support such as (3-trimethoxysilylpropyl)diethylenetriamine (TRI). Sayari's group published a large amount of the research conducted on this type of adsorbent. [34], [35], [36], [37] The third class of solid amine adsorbents is aminopolymers that are polymerized *in situ* onto a porous support. These solid amine adsorbents have been called hyperbranched aminosilicas

(HAS), and work on them was first published by Drese et al. in 2008. [38], [39], [40] Figure 2-5 is a representation of each class of adsorbent with porous silica as a support.

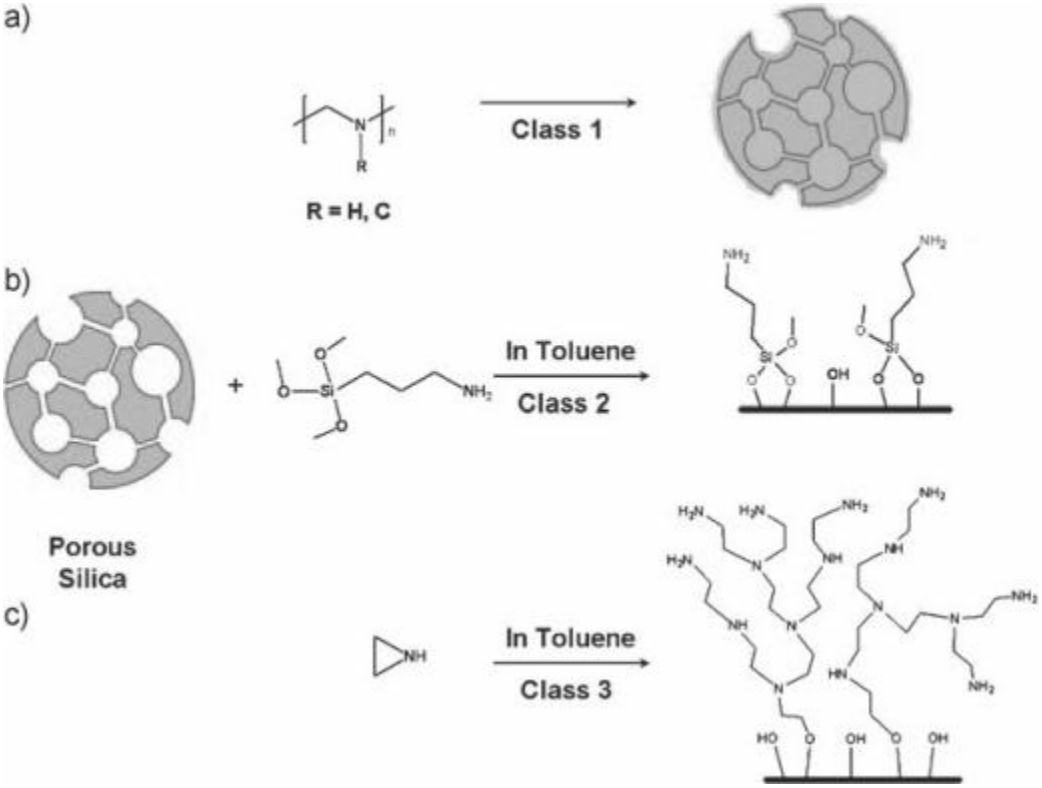

Figure 2-5: a) Class 1 amine impregnated solid amine adsorbent, b) Class 2 covalently attached solid amine adsorbent, c) Class 3 polymerized solid amine adsorbent [40]

In Figure 2-5 it can be seen that the class 1 adsorbents are just the physical impregnation of an amine into a porous support, while the class 2 and 3 adsorbents are chemically attached amines. The class 1 adsorbents usually use a porous silica support such as MCM-41 or SBA-15 and impregnate the support with a low molecular weight poly(ethyleneimine) (PEI). [30], [41] Class 2 solid amine adsorbents use a variety of aminosilanes such as, 3-[2-(2-aminoethylamino)ethylamino]propyl trimethoxysilane (TRI), grafted to porous silica supports such as MCM-41 or SBA-15. [34], [42] Class 3 amine adsorbents typically use

aziridine monomer attached to a silica support such as SBA-15. [25] The aziridine is then polymerized to produce amine groups for CO_2 capture.

2.8.1 Amine Impregnated Solid Adsorbents

Amine impregnated solid adsorbents have been designated as Class 1 amine adsorbents in the literature, and they typically consist of a low molecular weight PEI impregnated into a porous silica support. [43] Song et. al. have conducted a significant amount of work using this type of adsorbent. [29], [30], [31], [32], [33] This type of adsorbent is also known as a "molecular basket", and was initially reported to increase the CO_2 adsorption capacity of pure PEI by a factor of 2.3. [30] The increase of the CO_2 adsorption capacity of PEI when it was impregnated into a porous silica support indicated that there were some synergistic effects occurring with the incorporation of PEI into the pores. This synergistic effect was the greatest when the support was loaded with 50% PEI. [30]

The procedure described in the literature for impregnating the PEI into the support is to dissolve the PEI in methanol, add the support, and then dry the mixture in a vacuum oven at 70°C for 16 hours. [30] The addition of PEI into the pores of MCM-41 was reported to continually reduce the surface area and pore volume of the support with increased loading of PEI, but resulted in an increased amount of CO_2 adsorbed per gram of adsorbent. [30] The highest initial adsorption capacity reported for MCM-41 that was loaded with 75% PEI was 133 (mg CO_2/g-adsorbent) in pure CO_2 at 75°C. [30] Thermal gravimetric analysis (TGA) was used to measure the amount of CO_2 adsorbed on the sample; the procedure for CO_2 adsorption used was to heat the sample to 100°C in nitrogen for 30 minutes, then cool the sample to 75°C and switch the reaction gas to pure CO_2. [30] Another interesting finding for MCM-41 impregnated

with PEI was that the CO_2 adsorption capacity increased with increasing temperature up to 75°C. [44] The authors attributed this phenomenon to a diffusion limited reaction at lower temperatures. [44] The increase of the temperature is suspected to increase the diffusion of CO_2 into PEI on the support causing more amine reaction sites to be exposed for CO_2 adsorption. To show that the adsorption of CO_2 was diffusion limited at lower temperatures, CO_2 was adsorbed at 75°C and the temperature was then reduced and the CO_2 adsorption capacity monitored. [44] When the temperature was reduced, the CO_2 adsorption capacity did not decrease to the adsorption capacity recorded at the lower temperatures, but in fact it continued to very slowly increase. This indicated that the CO_2 adsorption at lower temperatures was diffusion limited.

The influence of moisture on the CO_2 adsorption capacity has been studied using this type adsorbent. [31], [32] In the presence of moisture in the reaction gases, the CO_2 adsorption capacity was shown to increase. [31] In one study, the effect of increased moisture concentration on CO_2 adsorption capacity was examined. [31] The addition of 6% moisture to a simulated flue gas that contained 14.9% CO_2 increased the CO_2 adsorption capacity by approximately 20%. [31] Using the same concentration of CO_2 and increasing the moisture to 10%, the CO_2 adsorption capacity was observed to increase approximately by 40%, but, when the moisture content was 16%, the adsorption capacity only increased 5% from the adsorption capacity using 10% moisture. [31] The authors concluded from this study that a moisture content that is the same as the concentration of CO_2 had the most influence on enhanced CO_2 adsorption. [31]

Degradation in the presence of acid gases in the flue gas is a concern for all CO_2 adsorbents. MCM-41 loaded with 50% PEI has also been studied using flue gas from a natural gas-fired boiler that contained 7.4-7.7% CO_2, 14.6% H_2O, oxygen, CO, ppm of NO_x, and nitrogen. [32] In this study, it was reported that very little NO_x is desorbed after adsorption, and therefore reduces the CO_2 adsorption capacity of the adsorbent. [32] This may indicate that the removal of NO_x is necessary for the commercial use of this type of adsorbent in coal-fired power plants.

Another application of this type of adsorbent has recently been studied in the capture of CO_2 from air using a porous silica support (SBA-15) and PEI. [33] In this study SBA-15 was loaded with 50 weight percent PEI and was able to capture CO_2 from a stream containing 1% CO_2 at 75°C. The CO_2 saturation capacity of 63.1 and 66.7 mg/g adsorbent was achieved and regeneration was stable for 20 cycles using helium purge and heating to 105°C. [33] This study indicated that this type of adsorbent could be used for the adsorption of CO_2 from coal-fired power plants, and for CO_2 adsorption from air.

2.8.2 Covalently Attached Amines to Solid Sorbents

Many different amines have been covalently attached to solid supports. Primary, secondary, and tertiary amines have all been used for covalently binding to solid supports. [45] One of the first reports of an amine grafted support for CO_2 capture was an amine attached to a silica gel from Leal et. al. in 1995. [43], [46] Since then some of the typical amines are that are grafted to silica supports are (3-amniopropyl)trimethoxsilane (APTMS) [45], [47], (3-trimethoxysilylpropyl)diethylenetriamine (TRI) [48], and *N*-[3-(trimethoxysily)propyl] ethylenediamine (EDA) [43], [49] These amines are typically attached to porous silica supports such as hexagonal mesoporous silicas (HMS) [47], mesoporous silica MCM-41, [36], [37] pore expanded

PE-MCM-41, [35] MCM-48, [50] and SBA-15. [51], [52] Amine grafted sorbents have been studied in a wide range of conditions, including temperatures from 20-60°C, [43] various concentrations of CO_2 in dry and humid reaction streams, [43] and using different types of stability and regeneration tests. [40], [53], [54]

The addition of water in the reaction gas has generally shown an increase in the CO_2 adsorption capacity of the sorbent. One study observed an increase in CO_2 adsorption from 0.41 to 0.89 (mmol/g) when using 100% relative humidity (RH) in a CO_2 stream at room temperature. [55] Similarly, another group observed a 10% increase in CO_2 adsorption from 2.65 mmol/g to 2.94 mmol/g when using a 27% relative humidity stream consisting of 5% CO_2 balanced with nitrogen. [35] Although typically there is an increase in the CO_2 adsorption capacity with the presence of water, it has also been reported in some cases that water had little to no effect on the CO_2 adsorption capacities. One study using amines grafted to SBA-15 with a reaction gas of 15 kPa CO_2 and 12 kPa H_2O and balance nitrogen at 333K showed little to no effect on the CO_2 adsorption capacity in the presence of water. [52]

Table 2-1 shows some CO_2 adsorption capacities for different types of amines and supports used in amine grafted supports. The data in Table 2-1 shows the some of the many different conditions, supports, and amines used to study amine grafted CO_2 adsorbents. The highest CO_2 adsorption capacity shown in Table 2-1 is 2.94 mmol/g or 12.9 weight percent gained.

Table 2-1: CO_2 adsorption capacities for amine grafted adsorbents at atmospheric pressure

Support	Amine	CO_2 Capacity (mmol/g)	Experimental Conditions: Percent CO_2	T (°C)	Reference	Year
Silica Gel	APTMS	0.89 (3.9wt %)	100% (100% RH)	50	[55]	1995
SBA-15	TRI	1.80 (7.9wt %)	15%(humid)	60	[52]	2005
MCM-48	APTMS	2.3 (10.1wt %)	10% (100% RH)	25	[50]	2003
PE-MCM-41	TRI	2.94 (12.9wt %)	5% (27% RH)	25	[35]	2007
SBA-16	EDA	1.4 (6.2wt %)	100%	27	[49]	2007
HMS	APTMS	1.59 (7.0wt %)	90%	20	[47]	2005

One significant problem that has been reported for amine grafted materials is loss of CO_2 adsorption capacity when the adsorbent is exposed to SO_2. [56], [57] It has been reported that the CO_2 adsorption capacity of TRI-PE-MCM-41 in a stream of 10% CO_2 at 50°C decreased from 6.9 weight percent to 3.9 weight percent after exposure to pure SO_2 at 323K using vacuum regeneration at 373K. [57] Although exposure to pure SO_2 is extreme, the degradation of amine grafted adsorbents after exposure to SO_2 would indicate that the flue gas from a coal-fired power plant would have to be processed for removal of SO_2, or at the least taken into consideration.

Another concern for this type of amine adsorbent and other amine adsorbents is oxidative degradation of the amine. Since coal-fired power plants are typically operated using excess air, the adsorbents will be exposed to oxygen during the adsorption cycle. A study of primary, secondary, and tertiary monoamines, and a primary-secondary diamine was conducted under accelerated oxidation conditions using pure O_2 at reaction temperatures of

25-135°C for 24 hours. [45] In this study, it was reported that primary and tertiary amines on propyl linkers were found to be more stable to accelerated oxidative degradation compared to secondary amines. [45] Additionally, functional groups that had a primary amine separated from a secondary amine ($RNHCH_2CH_2NH_2$), which are seen in poly(ethyleneimine), also showed oxidative degradation. [45] Although this study was conducted under extreme oxidative conditions, the degradation of these types of amines should be considered when adsorbents have to be stable over thousands of cycles in a flue stream that contains oxygen.

2.8.3 Hyperbranched Aminosilicas

Hyperbranched aminosilicas to adsorb CO_2 were reported in the literature in 2008, and these were prepared by polymerizing aziridine inside the pores of SBA-15. [25] This adsorbent was initially reported as having a CO_2 adsorption capacity of 3.11 mmol/g using a water saturated reaction gas of 10% CO_2 in argon at 25°C. [25] A different study with an increase in the loading of hyperbranched amines reported CO_2 adsorption capacity of 4 mmol/g, using humid 10% CO_2 in nitrogen. [27]

The effect of the support structure on the CO_2 adsorption properties was studied using pore-expanded SBA-15, mesocellular foam, and a large-pore commercial silica. [58] In this study with the larger pore diameter silica, the amount of amine loaded by the polymerization of aziridine was lower than the loading using standard SBA-15, and therefore also had a lower CO_2 adsorption capacity. [58] This type of solid amine adsorbent is very interesting and has been shown to have a high CO_2 adsorption capacity and could possibly be a better option than the PEI loaded sorbents since the amine is covalently attached to the solid sorbent.

2.8.4 Regeneration and Stability of Amine Solid Sorbents

One of the most important properties of an adsorbent for CO_2 capture from coal-fired power plants, or any commercial or industrial process that would require an enormous amount of CO_2 capture, is the stability of the adsorbent over hundreds to thousands of adsorption and desorption cycles. There are typically two different ways to regenerate solid amine adsorbents: one is using a sweep gas and increasing the temperature to remove the CO_2, while the other way is to use vacuum. [57] For initial studies of solid amine adsorbents most of the published studies used an inert sweep gas such as nitrogen, argon, or helium to regenerate the adsorbent. [29], [25] [50]

The use of an inert sweep gas is convenient to determine the possibility of regeneration at the lab scale, but it is not practical for commercial applications. This process is not practical in commercial applications because the desorbed CO_2 would be contaminated with the inert gas giving an exit stream that would not be much different from the inlet flue gas. The use of vacuum to regenerate the adsorbent is more practical than using an inert sweep gas, but, for sequestration, the CO_2 has to be pressurized and therefore the use of vacuum would result in an energy penalty. Two methods that seem to be the most practical ways to regenerate an amine solid sorbent are using low pressure "waste" steam, or using CO_2 at elevated temperatures as a sweep gas to regenerate the adsorbent.

There have only been a few studies that showed cycling ability over hundreds of cycles. A recent study that reported a significant amount of cycles using dry nitrogen and CO_2 and a humid nitrogen and CO_2 stream for cycling PEI impregnated adsorbents showed that there was slight degradation of the adsorbent over many cycles. Figure 2-6 is a graph of the CO_2

adsorption capacities over many cycles of a PEI impregnated adsorbent using isothermal adsorption and desorption at 75°C. [59]

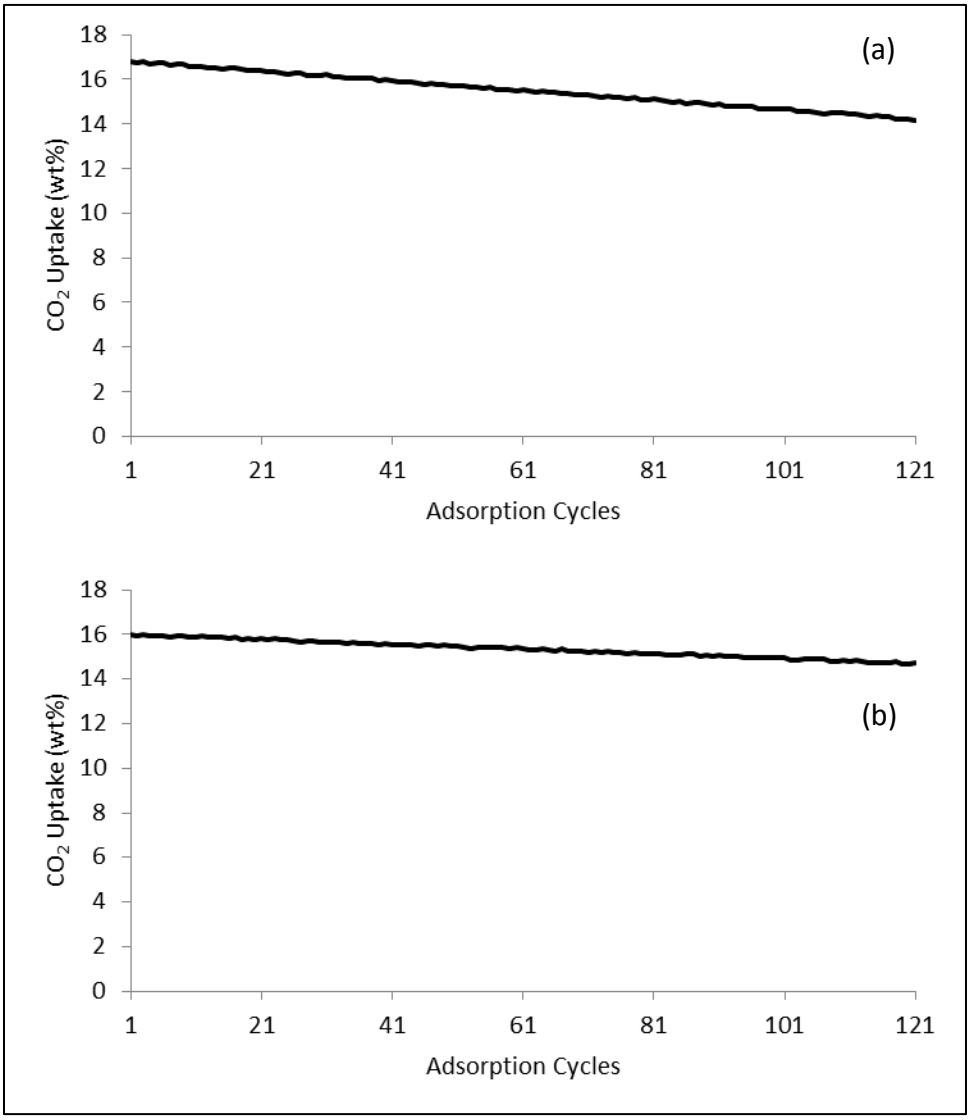

Figure 2-6: MCM-41 loaded with PEI cycles at 75°C; a) dry pure CO_2 and nitrogen, b) humid CO_2 and nitrogen (6% RH) [59]

In Figure 2-6 it is seen that when pure CO_2 is adsorbed onto PEI loaded support and desorbed using pure nitrogen, the stability is less than when using humid CO_2 and humid nitrogen to regenerate the adsorbent at 75°C. This is due to the slow formation of urea even at low temperatures when using pure CO_2 as the adsorption gas. Figure 2-7 is a graph of the

adsorption and desorption of a class two amine adsorbent using dry and humid gases at 70°C for adsorption and desorption.

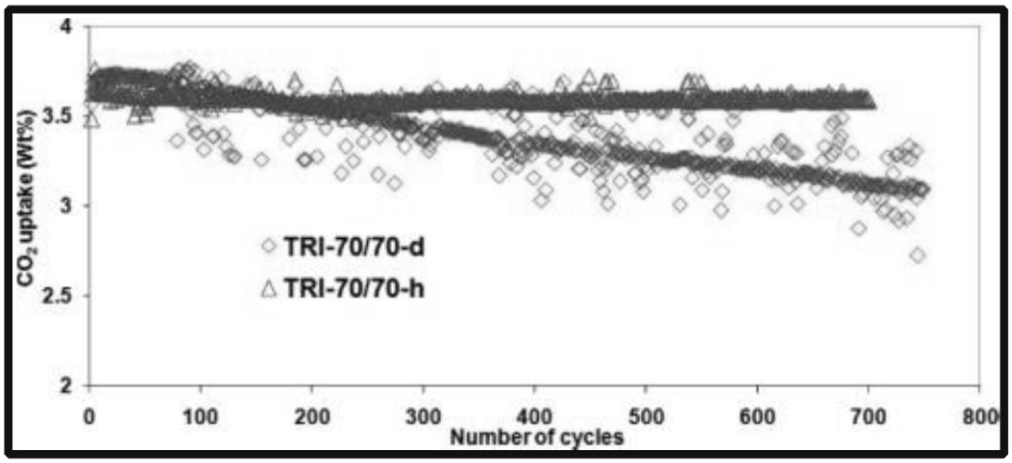

Figure 2-7: CO_2 adsorption and desorption at 70°C using TRI-PE-MCM-41 with dry gases (TRI-70/70-d) and humid gases (7% RH) (TRI-70/70-h) [60]

Again these studies showed that it was possible to regenerate an amine loaded support using dry and humid nitrogen over many cycles, but this is not applicable to commercial operations since they used humid nitrogen for regeneration.

Desorption using pure CO_2 at elevated temperatures is an interesting idea, but the concern is that PEI or other amines used will be evaporated or degraded at elevated temperatures. Another concern is the possible formation of stable urea onto the sorbent reducing the adsorption capacity of multiple cycles at elevated temperatures. A study that used an impregnated PEI support found that the adsorbent was not completely regenerated at temperatures under 140°C using pure CO_2 as a desorption sweep gas, indicating that desorption temperatures would have to be higher than 140°C. [61] The proposed scheme for the formation of urea compounds is shown in Figure 2-8, and this was determined using DRIFTS FTIR. [60]

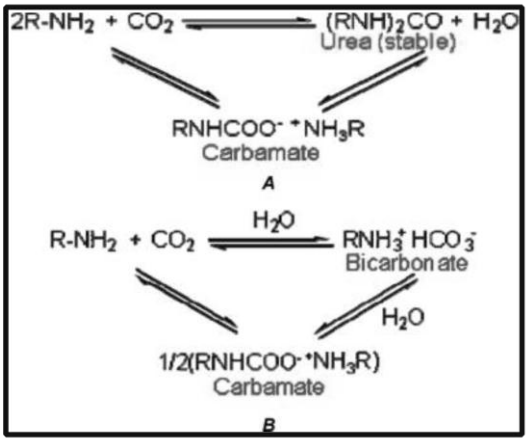

Figure 2-8: Proposed scheme of urea formation using amine sorbents [60]

The formation of urea compounds was shown to occur slowly even at relatively low temperatures (70°C), and this was attributed to the loss of CO_2 adsorption in Figure 2-7 over 700 cycles using pure CO_2. [60] The use of humid CO_2 is a regeneration method that could be used in commercial applications by recycling the CO_2 captured form the flue gas, adding water and using it as a sweep gas. The water could then be condensed out of the stream giving a pure CO_2 stream for sequestration. The possibility of this regeneration scheme has shown promise for solid amine sorbents in the literature.

Low pressure steam regeneration for solid amine adsorbents would seem as the most logical sweep gas for CO_2 regeneration because low pressure or waste steam is available at coal-fired power plants and water could easily be condensed out of CO_2. The regeneration and stability of amine solid sorbents using steam has been reported in only a few articles in the literature. [40], [54]For all three classes of solid amine adsorbents it was shown that steam at 105°C was able to fully regenerate the adsorbent over several cycles. [40] This showed promise for a commercially applicable regeneration scheme of solid amine adsorbents. A stability study

using steam at more extreme conditions used an autoclave to generate steam to test the three different classes of solid amine adsorbents using mesocellular foam MCF as a support. [54] In this study it was reported that all of the adsorbents were degraded after a 24 hour exposure to steam at temperatures from 106-180°C in an autoclave with air or nitrogen used as a purge gas.[54] The 24 hour exposure to steam was used to try to simulate hundreds to thousands of cycles using steam. The loss of CO_2 adsorption capacity was attributed to structural degradation of the MCF and degradation of the amine. Another interesting finding was that the class 2 adsorbent showed the most degradation upon long exposure to steam. [54] The use of low temperature and pressure steam to regenerate solid amine adsorbent has been shown to be a viable possibility, but the long term stability of solid amine adsorbents should be considered as a concern when using or developing solid amine sorbents.

2.9 Montmorillonite Clay

Montmorillonite (MMT) is a cationic smectite clay that consists of stacks of two tetrahedral silicate layers with a central alumina or magnesia octahedral layer. [62], [63], [64] This 2:1 ratio of tetrahedral to octahedral layers forms one layered sheet of clay with dimensions of about 1 nm thick by 30 nm to several microns in lateral dimensions. MMT has a surface area in the range of 750 m^2/g when the individual platelets are completely separated. [63], [64] Montmorillonite clay is typically used to make polymer nanocomposites and is the most widely used clay for clay polymer nanocomposites because of its ability to swell, its high surface area and its high surface reactivity. [63] Figure 2-9 is a representation of the structure of montmorillonite type clay.

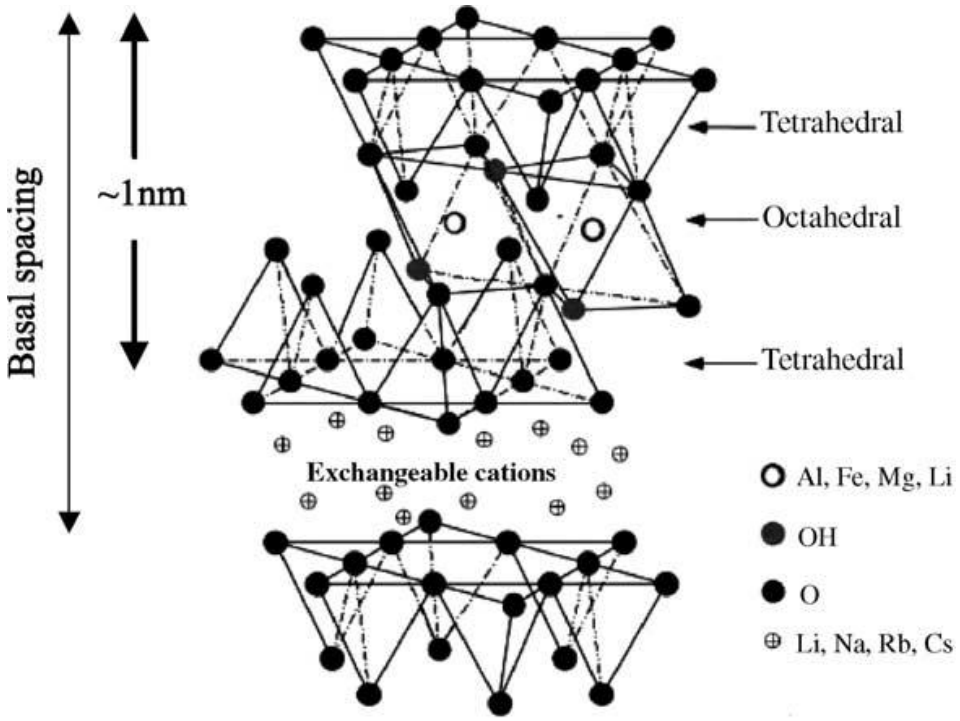

Figure 2-9: Schematic of 2:1 layered clay; d_{001} refers to basal plane spacing. [63]

The individual layers of clay tend to stack in several hundred layers, which are called tactoids, and are micro sized particles. The stacking of these layers leads to a regular van der Waals gap between the layers called the interlayer or gallery. [63] Pristine clay usually has Na^+ or Ca^+ in its interlayer gallery, and the amount that can be exchanged with another cation is usually characterized by cation exchange capacity (CEC), and this is generally expressed as mequiv/100 g. [63] The CEC depends on the crystal size, the pH and the type of exchangeable cation. [62], [63], [64] Separating the platelets into individual sheets will expose the edge hydroxyl groups and utilize the high surface area, but this can be difficult in practice.

2.10 Organically Modifying Montmorillonite Clay

While there are many different specific ways to modify MMT with an amine, the main steps are to swell the clay in a liquid and react the hydrophilic end of the amine compound to the edge OH groups leaving the hydrophobic amine on the outside end to better interact with

CO_2. Figure 2-10 is a representation of this mechanism where first the clay is swelled with water and then the clay is filtered and placed in an organic solvent, acetone, and then an amine, (3-aminopropyl) trimethoxysilane (APTMS), is reacted on the edge OH groups. Figure 2-10 illustrates how the clay platelets are swollen and then separated by the reaction with the amine. When producing a polymer nanocomposite the modified clay is then dispersed into the polymer by melt mixing or a solution process. The difference between the work conducted in the literature and the proposed research is that the work in the literature was conducted in polymers to improve their mechanical, thermal, and physical properties with concentrations of nanoclay around 5%. The proposed research uses this same idea, but uses the amine treated nanoclay for CO_2 adsorption experiments.

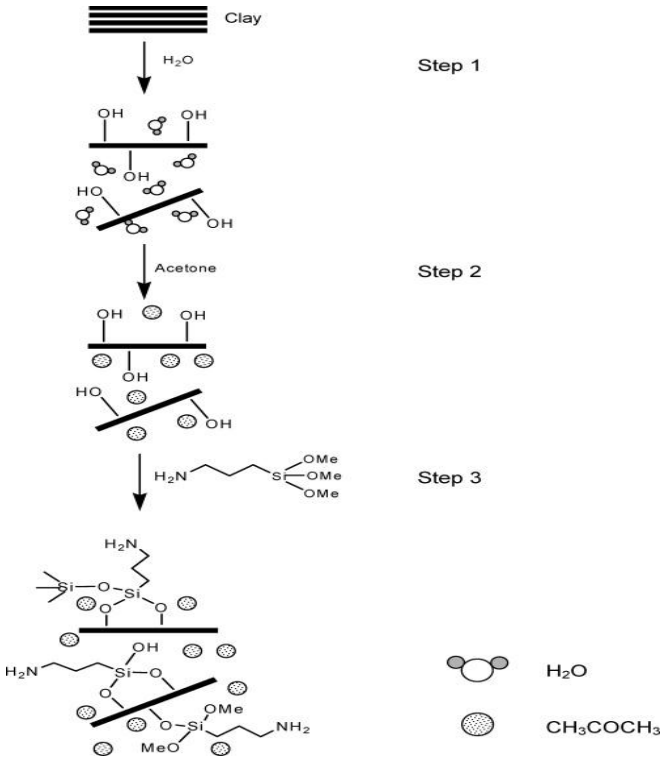

Figure 2-10: Schematic representation of amine reacted on clay [65]

Figure 2-10 shows a reaction with an aminosiliane. In this reaction, the water is replaced with an organic solvent after the swelling because the aminosiliane can agglomerate by a condensation reaction with the water. Replacing the water is therefore necessary in this reaction, but water is usually much better at swelling the clay than an organic solvent and would be preferred as the medium in the reaction. [65]

2.11 Methods for Attaching APTMS and PEI to Montmorillonite Clay

Cloisite® Na^+ is a montmorillonite clay that has Na^+ cations in-between its layers and was the clay used in this study. (3-aminopropyl) trimethoxysilane (APTMS) and Polyethylenimine (PEI) were used as the amines that are attached to the clay. To react APTMS with the clay, first the clay needs to be swelled in a solvent to separate the aggregated stacked layers into more separated layers of the clay. Then the APTMS is added and the trimethoxy silane group in APTMS reacts with the edge hydroxyl groups on the clay leaving the CO_2 adsorbing amine group available for the adsorption of CO_2 from the reaction stream. The expected reaction is shown in Figure 2-11. DMF was the solvent that was used extensively throughout the sample preparation experiments. Other solvents were initially used but preliminary results demonstrated that the greatest amount of APTMS grafted onto the clay was achieved using DMF as a solvent. Preliminary studies to determine the concentration of APTMS needed to ensure an excess for the grafting reaction were conducted and we determined that the ratio of clay to APTMS needed to be above 5:6 on mass basis. An excess amount of APTMS was then used for the majority of the experiments to ensure that the grafting reaction was not limited by the amount of APTMS. Water is very good at swelling clays, but it can agglomerate

APTMS through a condensation reaction. [65] A study with the swelling of the clay with water and then replacing it with an organic solvent to react the APTMS versus just using an organic solvent to swell the clay and react the APTMS was conducted. Figure 2-11 is the expected reaction between the clay and the aminosilane.

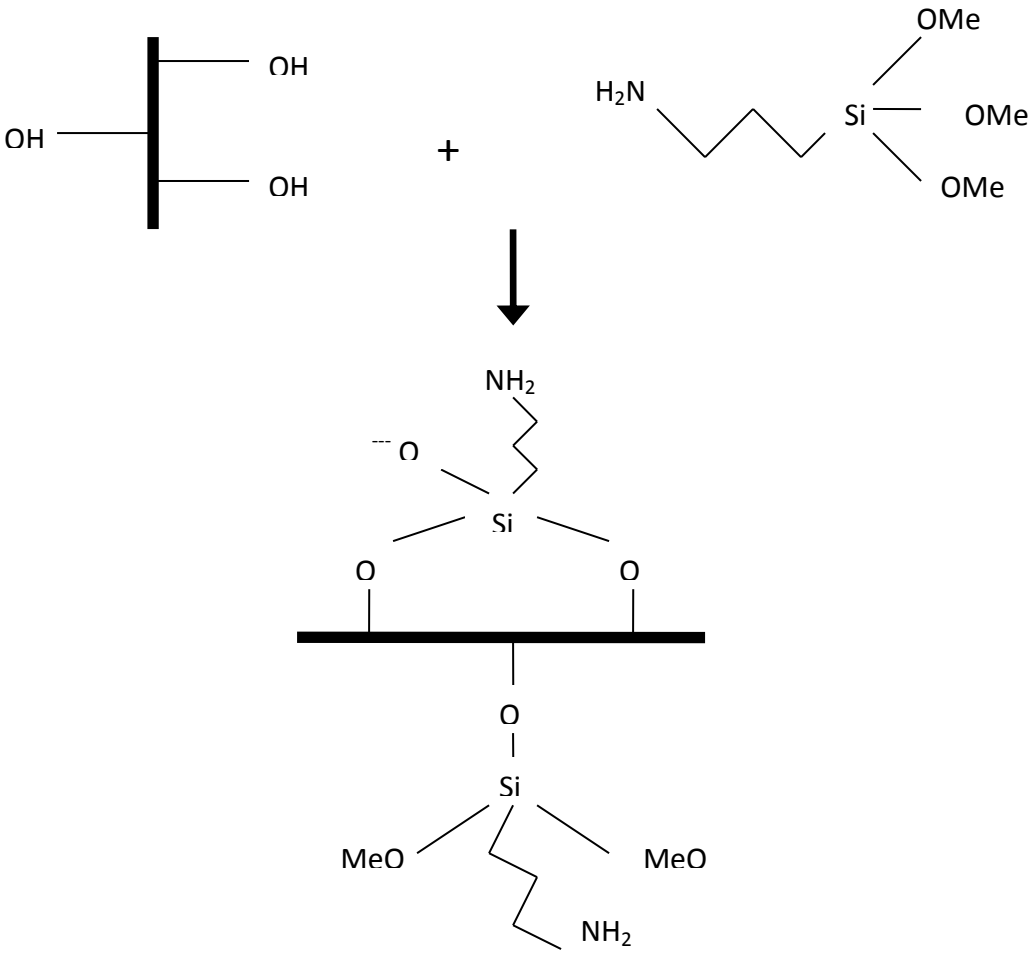

Figure 2-11: Expected reaction with APTMS and Cloisite® Na^+

PEI attached to silica supports has been shown to have high values of CO_2 adsorption. [30] PEI is attached to silica supports by a wet impregnation method, where PEI is dissolved in methanol, and then the support is added and mixed well with the PEI/methanol solution and then the methanol is evaporated in an oven. In this method the positively charged PEI is

attached to the negatively charged clay surface by electrostatic forces. The combination of reacting APTMS to the edge hydroxyl groups and then wet impregnating the PEI onto the surface of the clay was conducted to determine if the combination of the two amines would increase the amount of CO_2 adsorbed onto the sample.

Chapter 3

3. Experimental Materials and Procedures

Cloisite® Na^+ from Southern Clay products INC., a montmorillonite clay, was used as the support for the adsorbent developed. Ethylenimine, oligomer mixture (PEI) Mn 423 from Sigma Aldrich, and 3-Aminopropyltrimethoxy-silane, 97% (APTMS) from Sigma Aldrich were the amines used in the study. N,N-Dimethylformamide 99%, Methanol, and 99% Acetone ReagentPlus from Sigma Aldrich and deionized water were used for reaction solutions. Other PEIs that were used for comparison were Polyethylenimine 50 wt% solution in water Mn 60,000, and Polyethylenimine 50 wt% solution in water Mn 1,200 and were also purchased from Sigma Aldrich.

3.1 Grafting Amines to Clays

The grafting of APTMS onto the clay was performed by two methods. One was called the “dry method”. This method started by drying the clay in an oven overnight. Then 0.5 g of the nanoclay was dispersed in 80 ml of acetone, toluene or dimethylformamide (DMF), and a specified amount of APTMS was then added and the mixture was stirred at room temperature for 24 hours. After the mixture was stirred, the solution was sonicated for 30 seconds at an amplitude of 40% using a Cole Parmer 750 watt Ultrasonic Processor. The resulting mixture was then filtered using a vacuum filtration system and Fisher Scientific fine porosity P2 qualitative filter paper, washed multiple times with the solvent used, and dried in an oven at 60°C overnight. The second method, called the “slurry method”, used 15ml of deionized water to swell 0.5g of clay by stirring for 24 hours. 100 ml of DMF was then added to the clay/water suspension and stirred for 24 hours, sonicated for 30 seconds, filtered and washed. The filtered

clay was then added to 80 ml of DMF and was stirred for approximately 15 minutes to disperse the clay. APTMS was then added in different concentrations. The sample was then stirred for 24 hours, sonicated for 30 seconds, filtered and washed with copious amounts of DMF. The samples where then dried overnight in an oven at 60°C. After the sample was dried, it was crushed using a mortar and pestle to achieve a fine powder for testing.

For work with PEI, a wet impregnation method was used. This method involved dissolving PEI into methanol at a ratio of 8:1 methanol to PEI. The desired amount of support was added to achieve a specified percent loading of PEI onto the clay, and stir the sample for 24 hours. Samples were loaded with 33% PEI, 50% PEI and 66% PEI. An example of 50% loaded PEI onto the clay support would be adding 1 gram of clay to 1 gram of PEI dissolved in 8 grams of methanol. The solvent was then evaporated in a vacuum oven at 60°C overnight. These samples where easily broken into a powder without the use of a mortar and pestle.

For the samples treated with both APTMS and PEI, the sample was first treated with APTMS using the methods described earlier. The treated clay sample was then crushed using a mortar and pestle. PEI was dissolved into methanol in an 8:1 ratio using the same method as the wet impregnation with untreated clay. The treated clay was then added in a 1:1 ratio, based on the weight of the treated clay, with the PEI to achieve a 50% loading of PEI onto the treated clay.

3.2 Thermogravimetric Analysis for Amine Content on Clay

A TA Instruments TA-Q500 TGA was used to determine the amount of amine content that was grafted onto the samples. The samples were first heated at 20°C/minute to 900°C in nitrogen at a flow rate of 40ml/minute. The derivative of temperature weight loss was used to

determine different weight loss steps. The weight loss that occurred around 100°C was assumed to be adsorbed water or CO_2 that was reacted onto the sample. The weight loss after this step was used to calculate the amount of amine grafted onto the clay. Another method used to further investigate different weight loss steps was to heat the sample in nitrogen with a flow rate of 40ml/minute to 100°C and keep the sample at 100°C for 30 minutes to remove all of the water. The sample temperature was then ramped to 600°C at 20°C/minute, and kept at 600°C for 30 minutes to remove all of the grafted amine. The weight loss due to water was measured as the weight loss at 100°C. The weight loss due to the amine was calculated as the weight loss after the 100°C step.

3.3 High Pressure CO_2 Adsorption and Desorption Tests

High pressure CO_2 adsorption tests were conducted in a pressure vessel that was approximately 2 inches in diameter and 10 inches long. Up to eleven samples were run at one time. The pressure in the pressure vessel was determined using the secondary pressure gauge on the reaction gas cylinder. During the CO_2 adsorption experiments the valve on the gas cylinder was left open to insure that the pressure in the pressure vessel was maintained at the desired value. The temperature for the reaction of CO_2 was not altered and left at room temperature for the majority of the tests. The weight of CO_2 adsorbed in the high pressure tests was calculated by weighing the sample before it was placed into the reaction vessel. Then, once the sorbents had adsorbed CO_2 the sample was removed from the pressure vessel weighed to find the weight difference. After this, desorption and cycle tests were conducted using vacuum.

In order to determine the temperature effects of CO_2 adsorption at high pressures, the samples were loaded into the pressure vessel and CO_2 was introduced into the vessel. A valve

on the pressure vessel was then closed and the vessel was placed into a water bath at the desired reaction temperature in an oven at the same temperature for 24 hours. The initial pressure was determined by back calculating the pressure for a final pressure of 300 psi using the ideal gas law for the change in pressure due to the increase in temperature. The water bath was used to help limit any fluctuations in the oven temperature.

The vacuum desorption experiment for the samples exposed to high pressure CO_2 used the same procedure as the vacuum desorption for the samples in the TGA, as described in the next section. The procedure for vacuum desorption for the samples in the pressure vessel experiments was to weigh the sample after CO_2 adsorption, then place the sample into the vacuum oven at 85°C for 1 hour. The samples were then reweighed and the percentage weight loss was calculated and compared to the weight gained during the initial CO_2 adsorption experiment. The equation used for weight percent desorbed is given in Equation 3-1.

$$(1 - \frac{W_{vac}}{W_{CO_2}}) \cdot 100 = W_{des} \qquad 3\text{-}1$$

W_{vac} is the weight of the sample when it is removed from the vacuum oven, W_{CO_2} is the weight of the sample after it is removed from the pressurized CO_2 and W_{des} is the weight percentage regenerated from the vacuum oven experiment.

3.4 Thermogravimetric Analysis for CO_2 Adsorption and Desorption

Two TGAs were used in these experiments. These were a Thermo Cahn Thermax 500 and a TA Instruments TA-Q500. Samples in the Thermo Cahn were approximately 40-50mg, and this sample weight was used to minimize the noise in the results, but also to conserve the sample for multiple runs. With the TA-Q500, the noise was minimal so a sample size of around

10mg was used for all of the runs. The reaction gas for both TGAs was controlled by a flow controller. Since the sample size and the flow controller were larger in the Thermo Chan TGA, a flow rate of 100ml/min was used for all of the experiments. With the TA-Q500 a flow rate of 40ml/min for the reaction gas was used. Samples were run on both TGAs to compare results, and these were found to be comparable to each other.

The experimental procedure was the same for all of the samples and included an initial drying step in nitrogen at 100°C to remove any moisture or adsorbed CO_2 from the sample and to get a good baseline for the calculation of the CO_2 adsorbed. The sample was kept at 100°C for 30 minutes to achieve a stable weight before the CO_2 adsorption experiments. If the adsorption temperature was above 100°C, such as 125°C and 150°C, the initial drying step was completed using the CO_2 adsorption temperature instead of 100°C. For CO_2 adsorption at temperatures lower than 100°C, the sample was cooled in nitrogen and, once the reactor temperature reached the designated reaction temperature, the reaction gas was switched to CO_2.

The adsorption of CO_2 was tested at various temperatures to see which temperature would adsorb the most CO_2 in a reasonable amount of time. For the samples treated with APTMS, the adsorption of CO_2 reached equilibrium very quickly at temperatures above 75°C, but, for the clay treated with PEI, an adsorption time of 90 minutes was used. This was based on initial results that showed that, although the adsorption of CO_2 was still ongoing with increasing time, the increase in the amount of CO_2 adsorbed was minimal after 90 minutes. If equilibrium was not reached before 90 minutes, a 90 minute adsorption time was used as the

standard adsorption time for all of the samples at all of the different temperatures and conditions.

3.4.1 Multiple cycles in the TGA

For subjecting a sample to multiple cycles of adsorption and desorption in nitrogen, the reaction gas was switched to pure nitrogen and the sample was heated to 100°C and the temperature was kept constant for 30 minutes. Once the sample was regenerated, the TGA reactor was cooled back to the reaction temperature in nitrogen. When the reaction temperature was reached the desired value, the inlet gas stream was switched back to the initial reaction gas for CO_2 adsorption.

Cycling the samples in CO_2 was similar to cycling in nitrogen, except that the temperature for regeneration was 155°C for 30 minutes. The reaction gas was always pure CO_2 for all of the experiments during the cycling step. For example when the adsorption temperature of the sample was 85°C, the reaction gas was kept at pure CO_2 during the ramping of the temperature to 155°C and during the cooling of the temperature back to 85°C.

Humid carbon dioxide was also used to regenerate the samples. During this experiment, the reaction gas was bubbled through deionized water that was at room temperature before it went into the reactor. The regeneration temperature was 155°C which was the same temperature used during cycling using pure CO_2.

3.5 Vacuum Regeneration

To regenerate the samples using vacuum, carbon dioxide was reacted onto the sample in either the TGA or in the pressure vessel using the same adsorption methods already described. After CO_2 was reacted onto the sample, the sample was placed into the vacuum

oven at 85°C. The vacuum pump was then turned on to achieve a vacuum pressure of 93kPa as measured by a gauge on the vacuum oven. The samples were then removed after a designated period of time and the weight difference was measured. The samples were then placed back into the TGA or pressure vessel to measure the amount of CO_2 adsorbed after regeneration. The amount of CO_2 initially adsorbed was then compared with the amount adsorbed after the vacuum regeneration step.

3.6 Fourier Transform Infrared Spectroscopy (FTIR) Characterization

Fourier transform infrared spectroscopy (FTIR) was used to determine if any amine was attached to the clay support. A Thermo Scientific Nicolet iS10 FTIR with the Attenuated Total Reflectance (ATR) attachment and a diamond crystal was used with a resolution of $1cm^{-1}$ and 40 scans per sample. The procedure was to take a background spectrum before every sample with no sample on crystal surface. If the background spectrum had no unexpected peaks, a small amount of sample was placed onto the crystal surface and the spectrum was then collected.

3.7 Surface Area Analysis

To determine the surface area of unmodified Cloisite® Na^+, a ASAP 2020 surface analysis machine was used to determine the BET surface area. A sample of fumed silica with a surface area of 250 +/- 30 m^2/g was tested in the BET ASAP 2020 surface analysis machine to determine the accuracy of the method. First a sample was placed into the sample tube with an auxiliary sample rod also placed into the tube. A vacuum was place onto the tube and the sample was heated to 120°C to remove any moisture in the sample. The vacuum was held for at least 30 minutes or until 100mTorr was observed on the vacuum gauge. Once this was achieved, the vacuum was turned off and nitrogen was allowed to flow into the sample tube. The lid was then

quickly placed onto the sample tube and the sample was connected to the surface analysis machine for sample analysis. The ASAP 2020 used liquid nitrogen to cool the sample and the BET surface area was calculated using nitrogen adsorption at 77K.

3.8 Scanning Electron Microscopy (SEM)

SEM images were taken using a Hitachi S-4700 FE-SEM. The samples were attached to a sample holder using double sided carbon tape. The samples were coated with gold before the images were taken because the samples were not conductive enough for SEM imaging. The procedure for coating the samples was to place the samples into a SPI-MODULE™ sputter coater. The samples were then evacuated to 400-600mTorr. The chamber was then flushed with argon, the vacuum was then restored to 80mTorr, and approximately 3nm of gold was sputtered onto the samples. The samples were then placed into the SEM for imaging. SEM images were taken using various magnifications, with a general working distance of 12.1-13.1mm and a voltage of 5.0kV.

3.9 Activation Energy Analysis

The stability of amines on solid supports is a big concern for the applicability of the amine solid adsorbents in commercial applications. Therefore the activation energy of the degradation of APTMS and PEI on montmorillonite was studied using TGA as described in a paper by Friedman [66] and similar to other papers on TGA activation energy. [67], [68] The procedure was very similar to the procedure for determining the amount of amine grafted to the sample. A sample of approximately 10mg was placed into the TGA and the temperature was ramped from 5-20°C to 900°C in nitrogen. The difference in the degradation curves were then used to estimate an activation energy using equations described in the literature.

Chapter 4

4. Results of Grafting APTMS and PEI onto Montmorillonite Clay

Samples of treated clay were produced using the steps described in the experimental sections for grafting amines to clay. Once these samples were created, the samples were characterized using TGA, FTIR and SEM techniques to determine if an amine was successfully attached to the clay, the amount of amine loaded, and the morphology of the treated samples.

4.1 TGA analysis

Samples using Cloisite® Na^+ and DMF as a solvent were first grafted with APTMS using the "dry method" described in the experimental section. After the sample was filtered washed and dried, the sample was crushed using a mortar and pestle to a fine powder. To determine the amount of amine attached to the sample TGA analysis was conducted. Using methods similar to those described in the literature, the temperature was ramped at 20°C/minute to 600°C and kept at 600°C for 60 minutes. Figure 4-1 is a TGA graph of Cloisite® Na^+ treated with 0.4g APTMS/g clay using the "dry method". In Figure 4-1 it can be seen that there are multiple weight loss steps when heating the sample to 600°C in nitrogen. The first weight loss step that is clearly seen in the derivative weight loss curve in Figure 4-1 is at a temperature of 25-140°C, and this is attributed to the loss of water. The remaining weight loss is attributed to the loss of the amine.

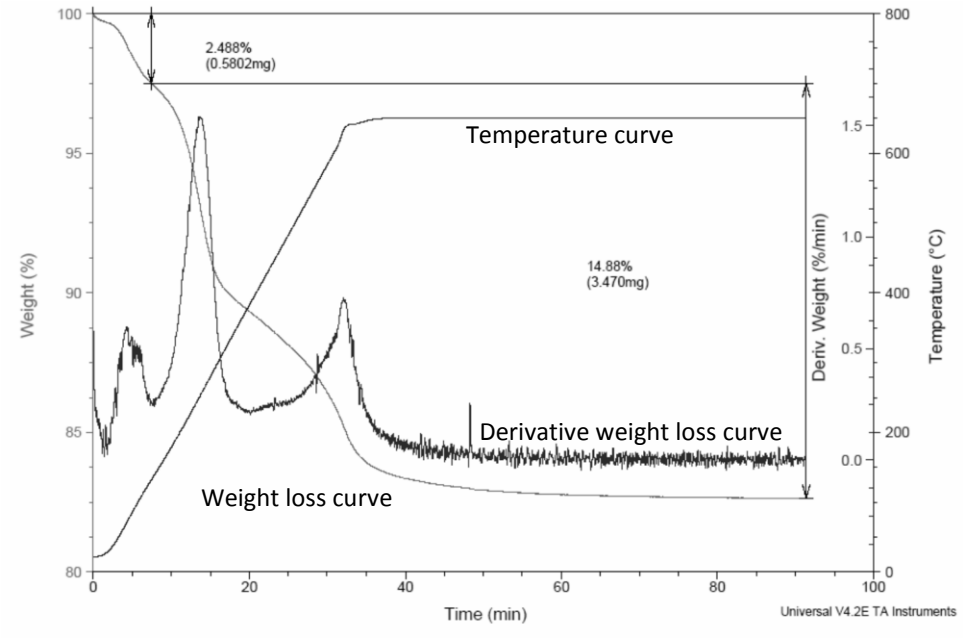

Figure 4-1: TGA Curve of clay treated with 0.4g APTMS/g Clay in nitrogen

This procedure and procedures similarly used in the literature assumed, that after the weight loss due to water and unattached molecules, the remaining weight loss is due to the removal of the attached organic amine from the inorganic support. In order to test this theory the untreated clay was run using the same procedure as a control. The TGA curve for untreated clay ramped to 600°C is shown in Figure 4-2. In this figure it can be seen that there is an initial weight loss step that is attributed to water, similar to the weight loss step seen in the APTMS treated sample. Then there is another weight loss step, in which there is approximately 5.7 wt% lost. This weight loss is possibly due to the degradation of the clay and possibly weight loss of water entrapped in the intergalleries of the clay. It is obvious that some sort of degradation is happening at high temperatures to the clay since the color of the clay changes from white to dark gray after exposure to high temperatures in nitrogen.

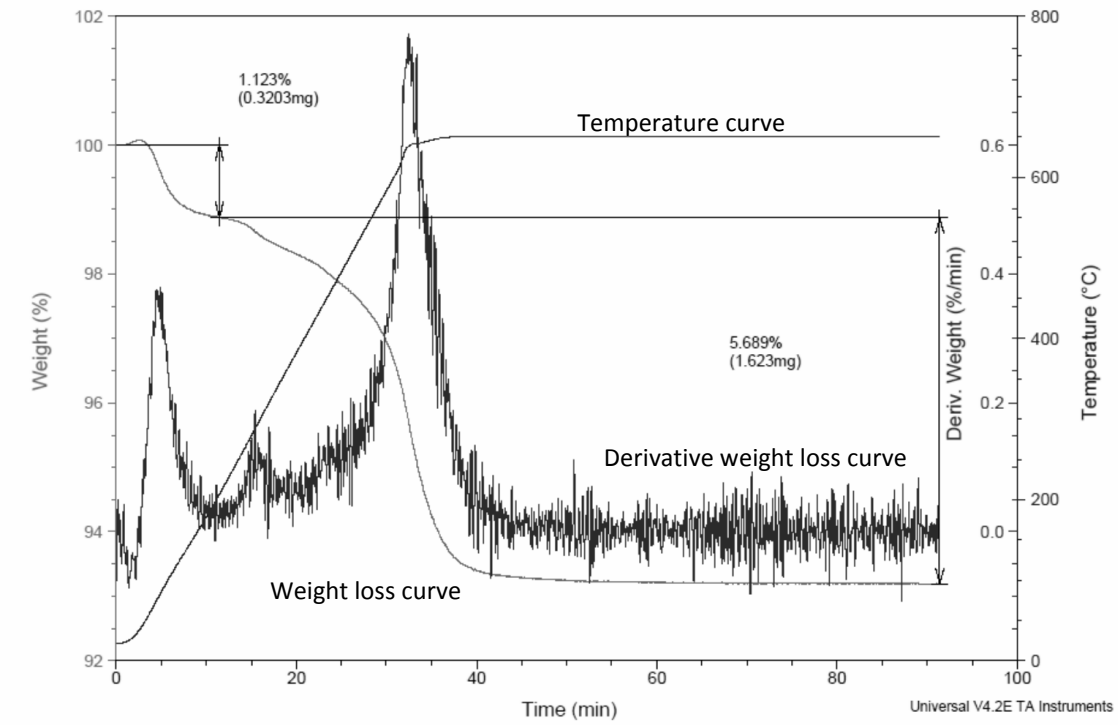

Figure 4-2: TGA curve of untreated Cloisite® Na^+ in nitrogen.

In order to determine the stability of the clay used in this study, the untreated clay was heated progressively to 900°C to determine if there was any more degradation weight loss. Figure 4-3 is a TGA curve of untreated Cloisite® Na^+ heated to 900°C at 20°C/minute in nitrogen. In Figure 4-3 the weight loss is graphed versus temperature and it can be clearly seen that there are two main weight loss steps, one due to the loss of water and the other due to some degradation to the untreated clay. The weight loss due to water is more in Figure 4-3 than in Figure 4-2 using the 600°C method. This is due to the amount of moisture that the sample was able to adsorb during that particular day and while the sample was stored. This weight loss is expected to change depending on the humidity during that day and the difference in the two runs is not a concern. The more important weight loss is the weight loss after the desorption of water. This weight loss step is approximately the same using the two different ending

temperatures. Both procedures were repeated multiple times using untreated clay and showed similar results indicating that the weight loss is the same due to the degradation of clay using an ending temperature of 600°C and 900°C. The average weight loss after desorption of water from the untreated clay was calculated as 5.6±0.7. This weight loss should be taken into account when calculating the amount of amine grafted onto the sample.

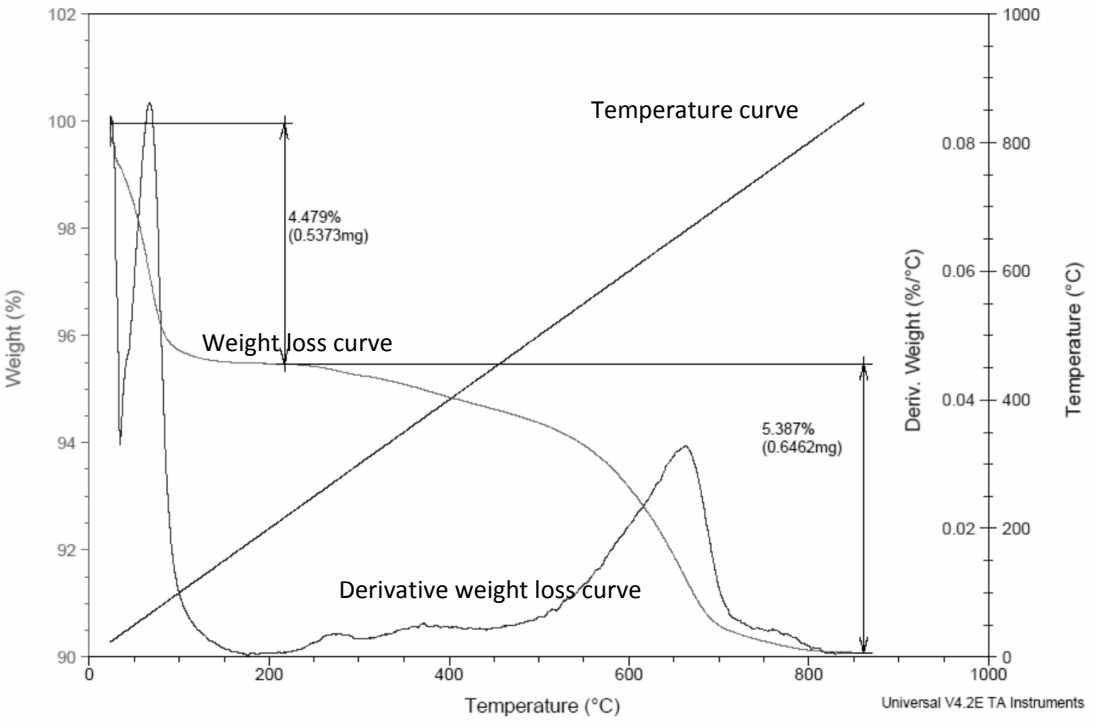

Figure 4-3: TGA curve of untreated Cloisite® Na^+ ramped to 900°C in nitrogen

Experiments were performed to see the effect of various solvents and APTMS concentration on amine grafting. Solvents such as acetone, toluene and DMF vary in their polarity which can affect the nanoclay dispersion. A short study using different solvents and the "dry method" described in the experimental chapter was conducted to quickly determine which solvent allowed the most amine to graft to the clay. Shown in Figure 4-4 are the results of the

average amount of amine grafted to Cloisite® Na^+ using the dry method with different liquid media. Although this was a quick study and not enough runs were performed to prove that the differences between the solvents were significant, there was some indication that DMF had the highest amount of amine grafted and therefore was the solvent used in producing all of the additional samples treated with APTMS.

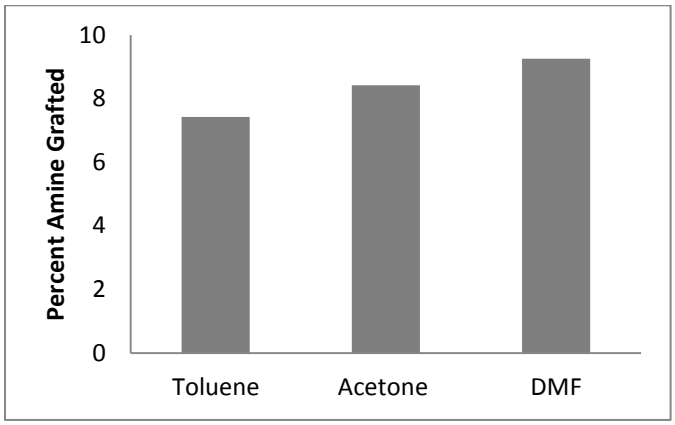

Figure 4-4: Average amount of amine grafted using different solvents "dry method"

Montmorillonite is easily swollen by water which separates the clay platelets and exposes more surface area of the clay for APTMS to react to the edge hydroxyl groups. Therefore, experiments were conducted by first swelling the clay in water and then adding DMF using the procedure called the "slurry method" which is described in detail in Chapter 4. A comparison of the two methods and the amount of amine grafted to them are shown in Figure 4-5 with two different concentrations of APTMS used. The error bars in Figure 4-5 represent the standard deviation of the repeated runs, for the dry method using a concentration of 0.4g APTMS/g clay the standard deviation is 0.1 and is difficult to see in the figure. The data that is shown in Figure 4-5 indicates that on average the slurry method did increase the amount of

amine grafted onto the sample. Therefore the remaining samples created were produced using the slurry method.

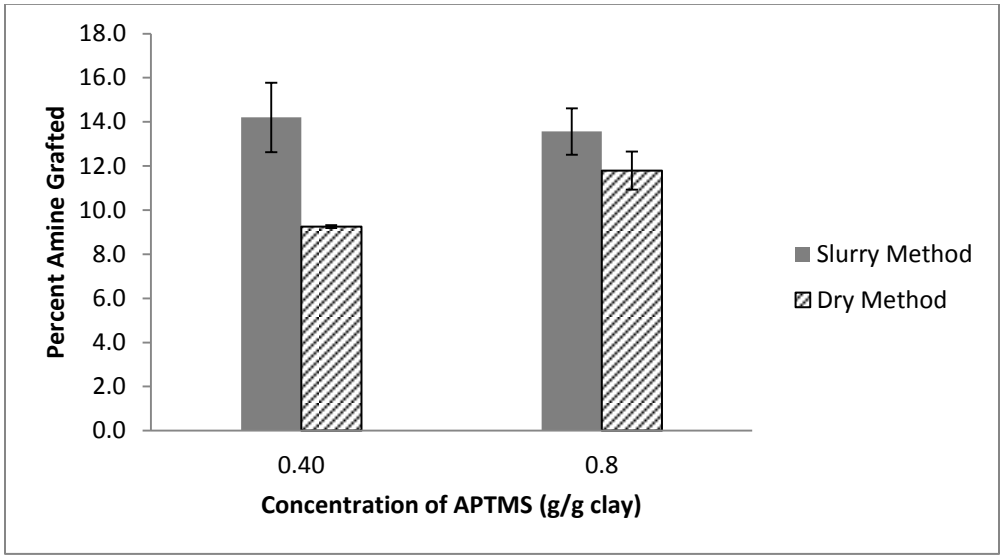

Figure 4-5: Comparison of the dry method versus the slurry method using DMF

The next study was on the concentration of APTMS added compared to the amount of amine that is attached to the clay. Again the slurry method was used since the slurry method showed a greater amount of amine grafted onto the sample. Figure 4-6 shows the effect of the concentration of APTMS on the amount of APTMS grafted to the sample.

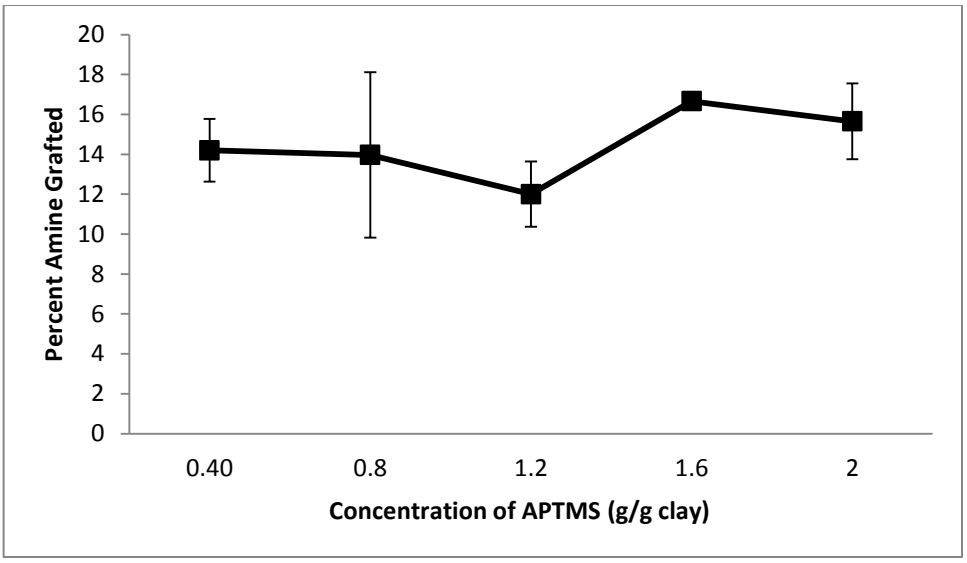

Figure 4-6: Percent amine grafted versus the concentration of APTMS "slurry method"

As the concentration of APTMS is increased, there is no significant change in the amount of amine grafted over the concentrations tested. This would indicate that the concentration of APTMS used is not the limiting step in the amount of APTMS reacted to the clay. In order to ensure that the concentration of APTMS was not the limiting step in the reaction, the highest concentration of 2g APTMS/g clay was used for all of the future tests. Samples treated with this concentration of APTMS are labeled C-APTMS-1-2 indicating the ratio of clay to APTMS used in the grafting procedure.

Cloisite® Na^+ treated with PEI was also studied using the TGA for the amount of amine immobilized. A representative TGA graph for a sample treated with 50% PEI is shown in the Figure 4-7. In Figure 4-7 it can be seen that there are a few different weight loss steps.

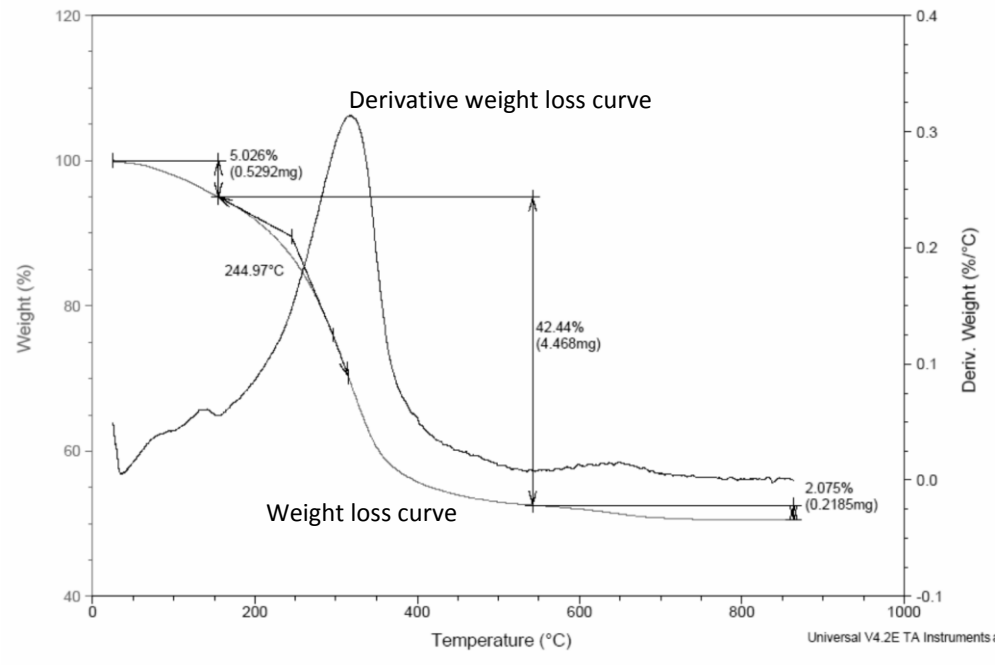

Figure 4-7: TGA graph of Cloisite® Na^+ treated with 50% PEI

The initial weight loss step is contributed by the loss of water and is measured at the point where the derivative weight loss is at a minimum around 160°C. The next weight loss step is clearly seen and is attributed to the loss of PEI from the clay surface. The final weight loss step is contributed by the degradation of the clay which is seen around 600°C for the untreated clay samples as well. The amount of amine attached is calculated by taking into account the weight loss after the removal of water and subtracting the average weight loss seen due to the degradation of the untreated clay. The average weight loss attributed to the amount of amine attached to the samples loaded with 50% PEI using this calculation was 37.4±1.5 percent.

Samples were also treated with both APTMS and PEI. The samples were first treated with APTMS using the slurry method and then loaded with 50% PEI using the same wet impregnation method described in the experimental sections. The same TGA procedures and calculations were used to determine the amount of amine loaded onto the clay. Figure 4-8

shows the amount of amine grafted for each treatment used. In Figure 4-8 it can be seen that there is only a slight increase in the amount of amine measured on the clay for samples treated with both APTMS and PEI. This was not necessarily expected, but one reason for this is that the APTMS prevents the PEI from attaching to the ends of the clay platelets.

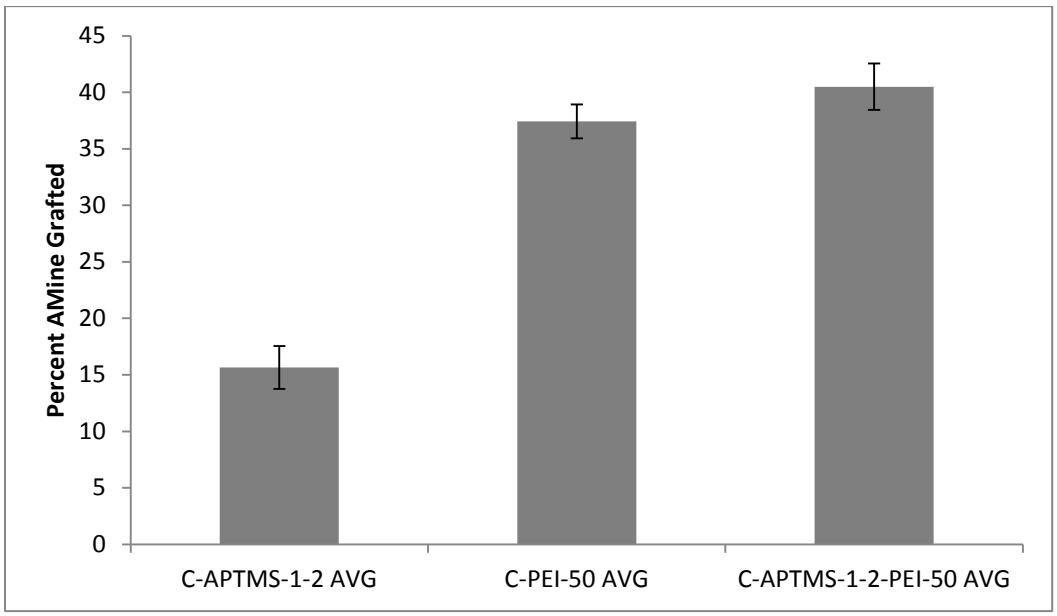

Figure 4-8: Comparison of the amount of amine grafted versus treatment

Additionally the amount of PEI loaded was measured using the weight of the APTMS treated sample and not the theoretical weight of the clay in the treated sample. Using the amount of amine grafted onto the samples treated with only APTMS and only PEI the theoretical amount of amine loaded onto the samples treated with both APTMS and PEI can be calculated based on Equation 4-1.

$$C_o P_A + (C_o - C_o P_A) P_p = C_{A+P} \qquad 4\text{-}1$$

In Equation 4-1 P_A is the weight percent of APTMS grafted onto untreated clay (15.7%), C_o is the weight of the untreated clay, $P_p$is the weight percentage of PEI grafted onto untreated

clay (37.4%), and C_{A+P} is the weight of amine grafted onto the clay for the combination of APTMS and PEI. Using Equation 4-1 and assuming 1 gram for C_o the theoretical weight of amine loaded onto the samples treated with both APTMS and PEI is 0.47 grams or 47 weight percent. However, the amount measured using the TGA is 40.5±2.05 weight percent. The difference in the theoretical percentage of the amount of amine attached to the sample and the actual amount measured using the TGA is the result of APTMS blocking some of the surface of the clay for the PEI to attach. Additionally, the treated clay may not disperse as well in methanol as the untreated clay resulting in less area for the PEI to attach to the clay. The ability of the treated clay to disperse into the methanol and PEI solution is a concern based on the consistency of the samples. Some of the APTMS treated samples did not seem to mix as well with the PEI based on visual observations of the samples.

4.2 FTIR Analysis

Fourier transform infrared spectroscopy (FTIR) was used to determine if any amine was attached to the clay support. A Thermo Scientific Nicolet iS10 FTIR with the Attenuated Total Reflectance (ATR) attachment was used using a resolution of 1cm^{-1} and 40 scans per sample. The untreated Cloisite® Na^+ was first characterized to determine the peaks of the untreated clay. The untreated clay spectrum was then compared with a sample of Cloisite® Na^+ treated with APTMS, with PEI, and with APTMS and PEI. Figure 4-9 is a spectrum of Cloisite® Na^+

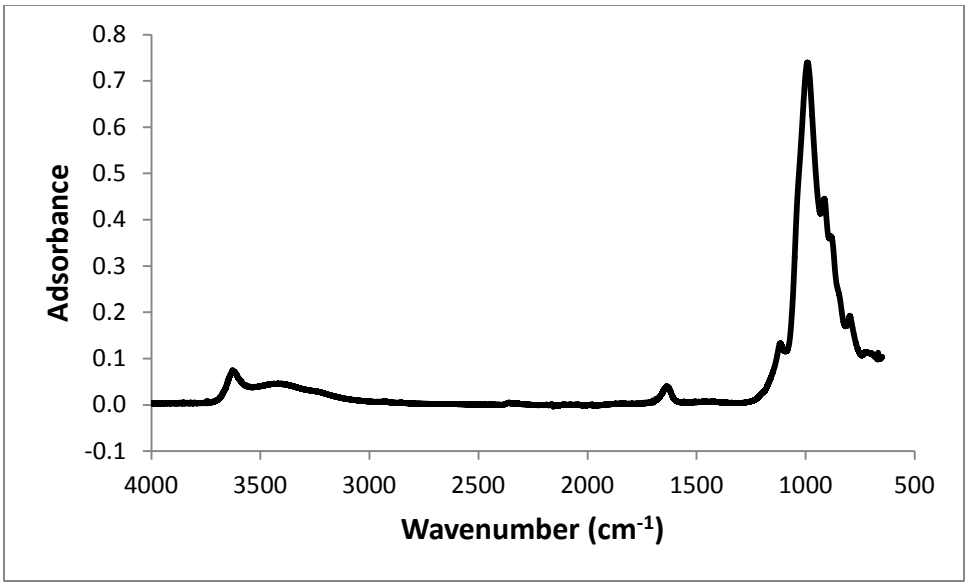

Figure 4-9: FTIR spectrum of Cloisite® Na^+

This spectrum was taken at room temperature and compares well with spectra of Cloisite® Na^+ seen in the literature. [69] Figure 4-10 shows spectra of Cloisite® Na^+ seen in the literature taken at different temperatures.

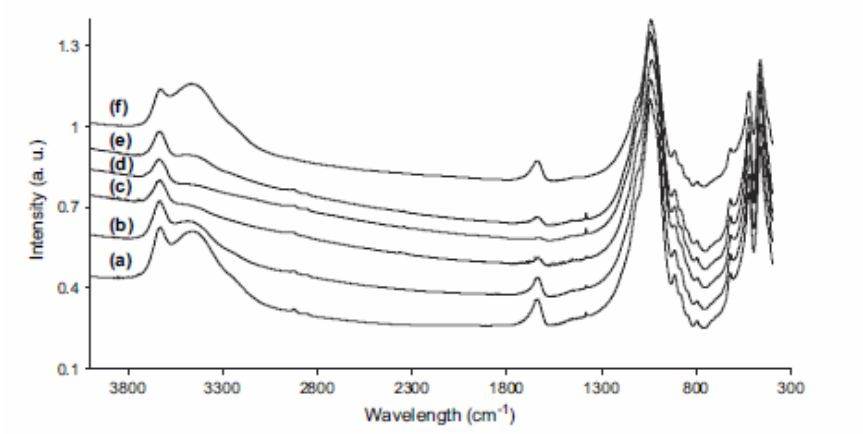

Figure 4-10: FTIR spectra of Cloisite Na®: (a) spectrum of the initial sample at room temperature, (b) spectrum of the sample at 100°C, (c) spectrum of the sample at 200°C, (d) spectrum of the sample at room temperature immediately after cooling, (e) spectrum of the sample at room temperature after 70h, and (f) spectrum of the sample at room temperature after thermal treatment at 250°C for 4h. [69]

The Large peak at 985 cm^{-1} indicates a Si-O in plane stretching which is similar to results in the literature. The broad peak around 3440 cm^{-1} that is not seen with much intensity in our spectrum is associated with O-H stretching from water that is not bound, but adsorbed on the surface. [69], [70] This would indicate that the clay was dry during the test. The peak around 1659 cm^{-1} is also associated with O-H stretching in water. [69] The peak around 3630 cm^{-1} is assigned to an asymmetric H_2O stretching for bound water in the clay. [70] When the untreated clay was heated to 900°C there were two weight steps observed. One weight loss step was attributed to the loss of adsorbed water. The weight loss step at high temperatures was attributed to some other degradation to the clay. Figure 4-11 shows the FTIR comparison between untreated clay and untreated clay heated to 900°C in nitrogen.

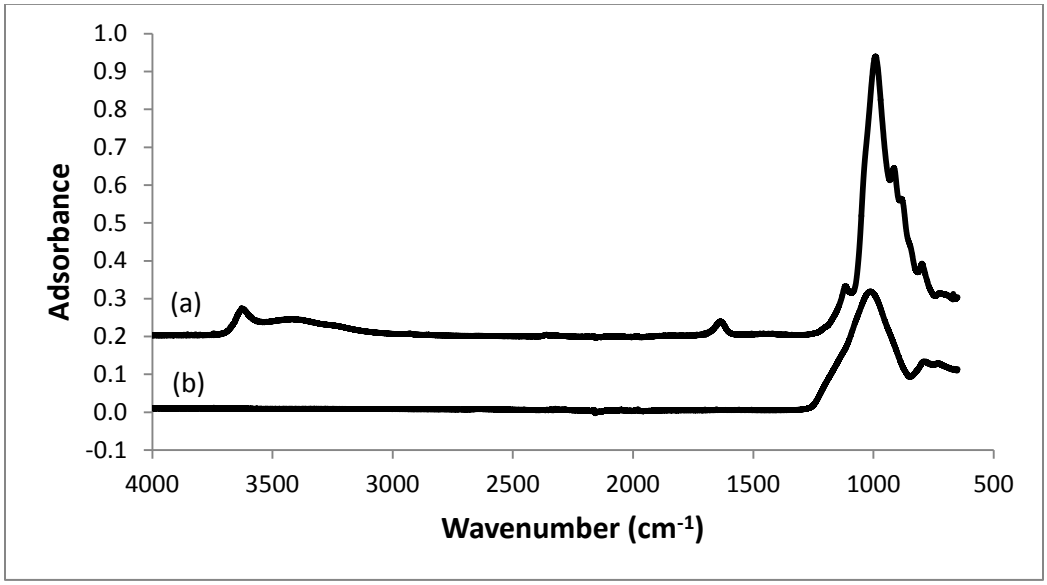

Figure 4-11: FTIR spectrum: (a) untreated clay, (b) untreated clay heated to 900°C in N_2

In Figure 4-11 it can be clearly seen that the peaks attributed to adsorbed water and bound water are removed when the untreated clay is heated to 900°C. The only peak that remains for the untreated clay that was heated to 900°C is the one attributed to Si-O stretching.

This is expected since any organic impurities or bound water is expected to be removed at such a high temperature. Comparisons using FTIR untreated clay and the amine treated clay were also conducted. Figure 4-12 is a spectrum of clay treated with APTMS.

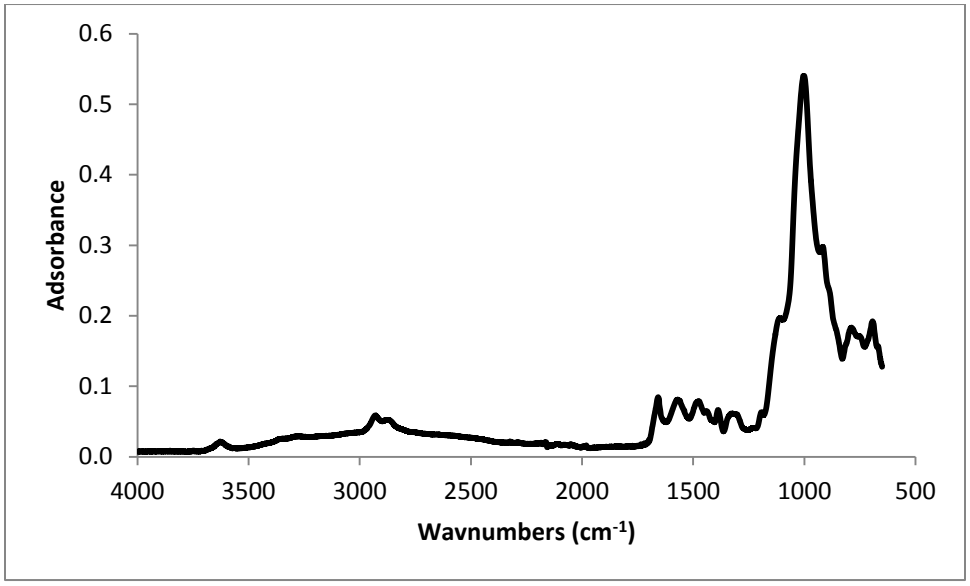

Figure 4-12: FTIR spectrum of Cloisite® Na^+ treated with APTMS

Figure 4-12 shows that the O-H peak at 3630 cm^{-1} is still seen, and is the contribution of the bound water in the clay. The peaks around 2870 cm^{-1} and 2930 represent C-H asymmetric and symmetric vibration of the methylene groups on APTMS. [47], [65], [71] The broad peak at 3300 cm^{-1} is observed with N-H stretching from the amine in APTMS. [50] To compare the treatments of APTMS and PEI a spectrum of Cloisite® Na^+ treated with PEI is shown in Figure 4-13. Additionally, a spectrum of clay treated with the combination of APTMS and PEI are shown in Figure 4-14.

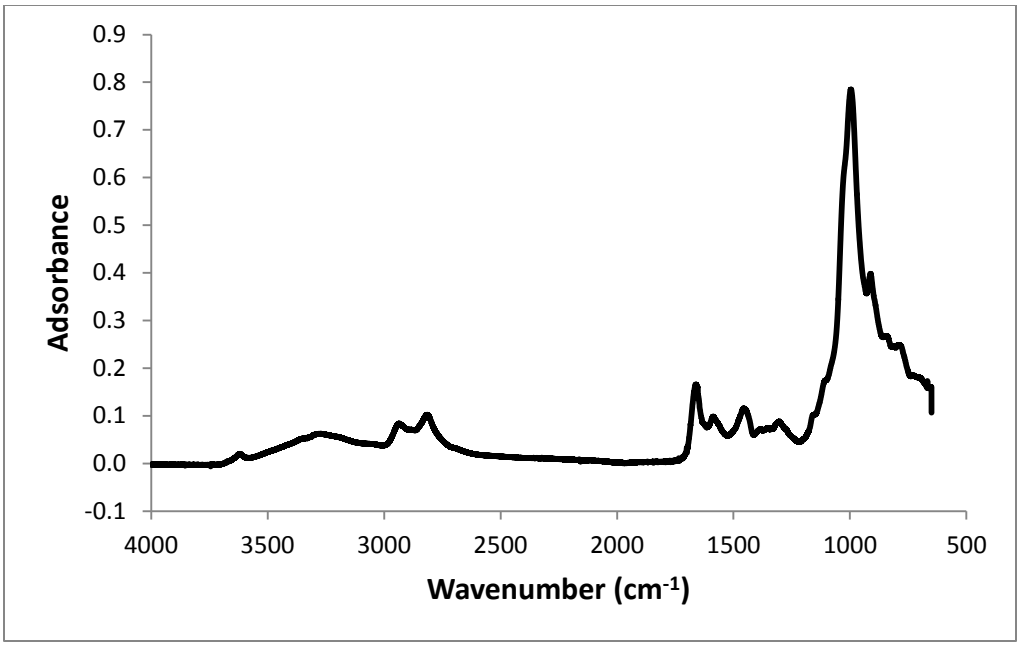

Figure 4-13: FTIR spectrum of Cloisite® Na^+ loaded with 50% PEI

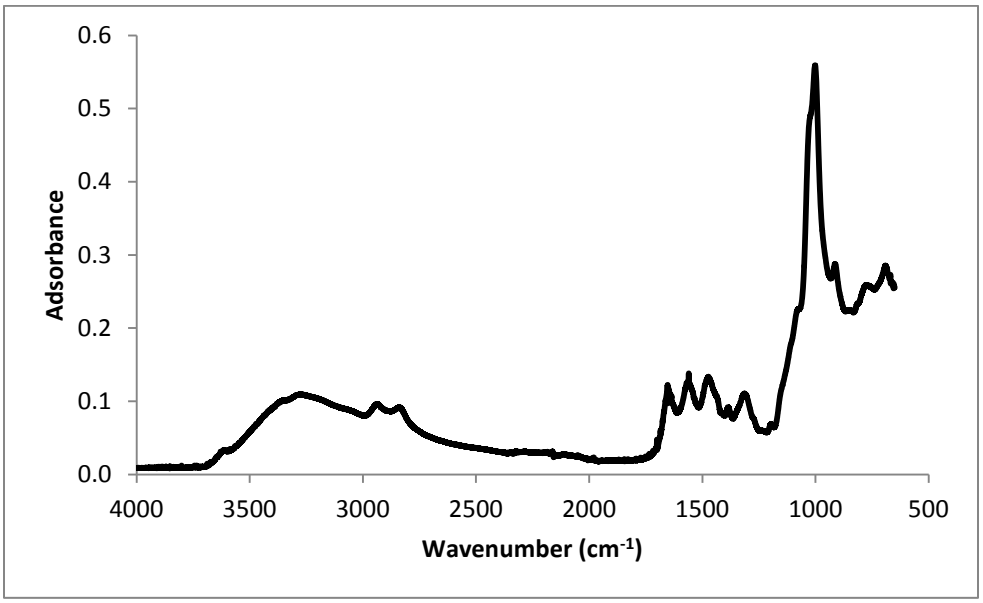

Figure 4-14: FTIR spectrum of Cloisite® Na^+ treated with APTMS and PEI

In Figures 4-13 and 4-14 the 3275 cm^{-1} (Broad Peak) is attributed to symmetric NH_2 stretching. [50] It can be seen that the samples treated with PEI have a much more intense peak around 3275cm^{-1}, and this indicates that there are more NH bonds due to the presence of more

amine groups. The 2940, 2812 cm^{-1} peak is also more intense with the PEI treated samples indicating that there is more CH stretching due to the increase in loading of PEI. The peak at 1590 cm^{-1} for samples treated with only PEI is contributed to NH scissoring vibration similar to the peak at 1560 cm^{-1} for the APTMS sample. [52], [72] The sample treated with both APTMS and PEI had a more intense peak around 1560 cm^{-1}, and this is attributed to NH scissoring vibration overlap of APTMS and PEI. [72] The peaks in the 1400cm^{-1} region are attributed to CH_3 and CH_2 deformation. [71] Figure 4-15 is a comparison of the amine treatments compared to the untreated clay.

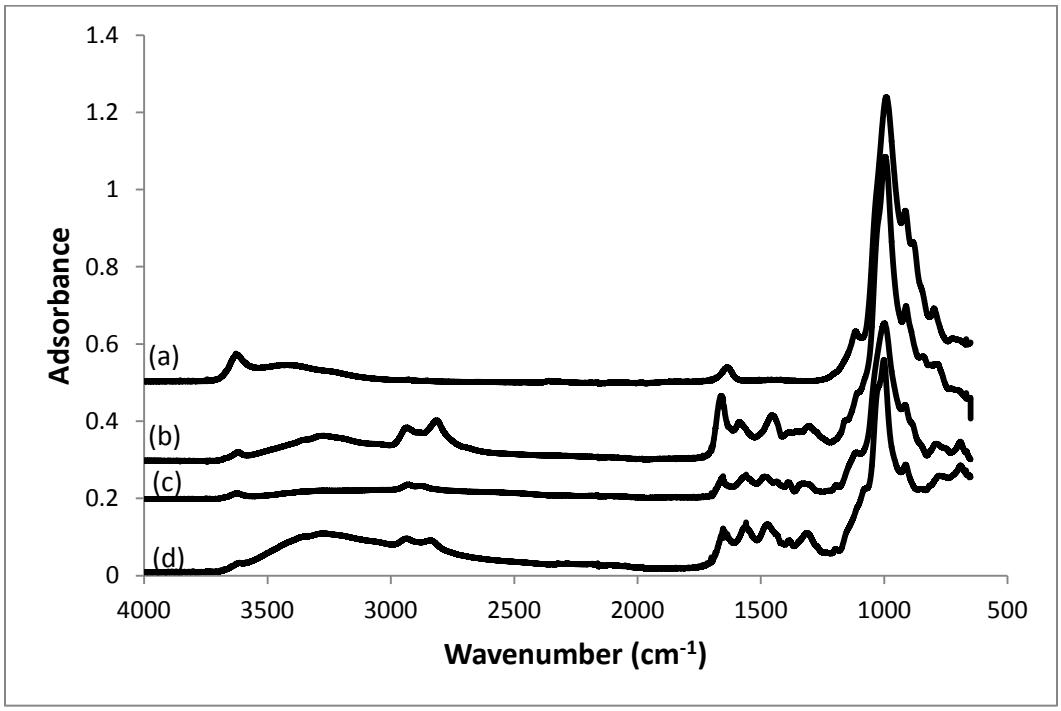

Figure 4-15: FTIR Spectra comparing the differences in amine treatments: (a) untreated clay, (b) clay treated with PEI, (c) clay treated with APTMS, (d) clay treated with APTMS+PEI

From Figure 4-15, it can be easily seen that there are amine and carbon chain vibrations associated with APTMS and PEI attached to the clay. Additionally it is evident that the clay

treated with both APTMS and PEI has all of the representative peaks of each treatment. This indicates that PEI and APTMS were both attached to the clay.

FTIR spectra were taken of treated samples that had been reacted with CO_2 to see if the formation of carbamates could be seen using this method of FTIR. Other researchers have used diffuse reflectance infrared spectroscopy (DRIFTS) to study the adsorption of CO_2 on their amine treated supports in real time. [71], [72], [73] One advantage of taking a spectrum while exposing a sample to CO_2 is that a spectrum can be taken of the exact same sample immediately before exposure to CO_2. This enables one to subtract the spectra to find very minute differences in the spectra of the same sample reacted with CO_2. Figure 4-16 is a comparison of Cloisite® Na^+, Cloisite® Na^+ treated with APTMS and Cloisite® Na^+ treated with APTMS and reacted with CO_2 in the TGA at 85°C. The sample that was reacted with CO_2 was stored in a sample bottle at room temperature until FTIR was conducted. This experiment was studied to see if there was any difference in the sample exposed to CO_2 compared to the sample not exposed to CO_2.

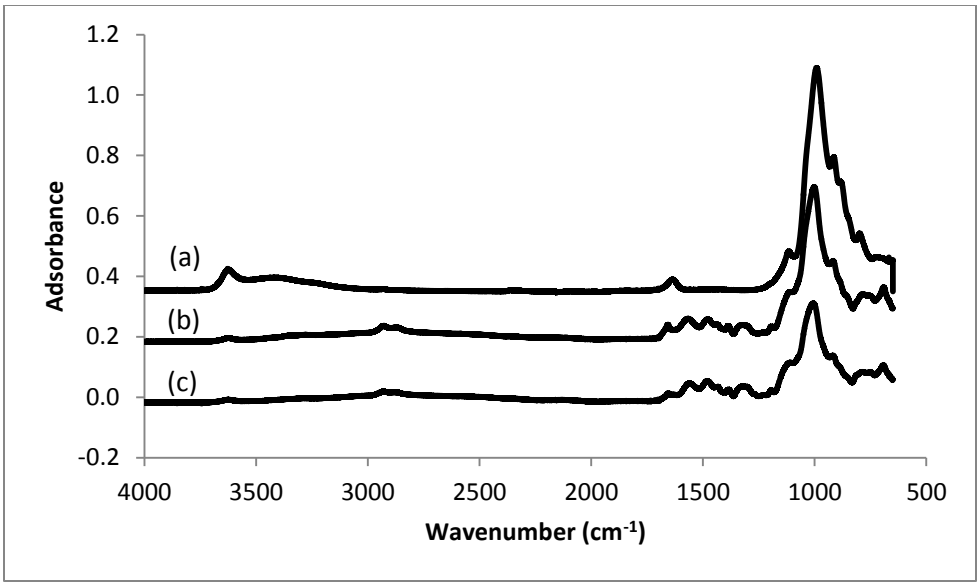

Figure 4-16: FTIR Spectra: (a) untreated clay, (b) clay treated with APTMS and, (c) clay treated with APTMS after CO_2 adsorption in TGA at 85°C in pure CO_2

The spectra in Figure 4-16 are consistent with the previous spectrum taken in Figures 4-9 and 4-12. The treated clay and the treated clay exposed to the CO_2 are very similar indicating that either the reacted CO_2 is no longer attached to the amine or the reaction product of CO_2 with the amine is difficult to see using this method. Figure 4-17 is a magnified spectrum of Figure 4-16 from 1800 cm^{-1} to 800cm^{-1} to better see the similarities in the spectra.

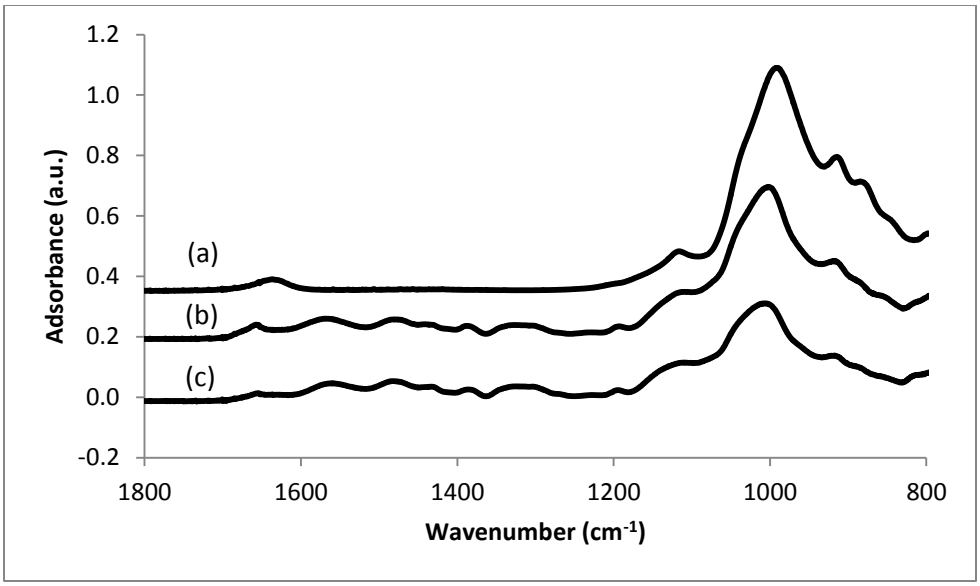

Figure 4-17: FTIR Spectra from 1800 cm^{-1}-800cm^{-1}: (a) untreated clay, (b) clay treated with APTMS, and (c) clay treated with APTMS after CO_2 adsorption in TGA at 85°C in pure CO_2

In Figure 4-17 there are slight shifts in peaks from 1660-1300cm^{-1} which might be due to reacted CO_2, but the shifts are slight and might be due to other factors since the sample had to be moved from the TGA where the sample was reacted with CO_2 to a different building were the FTIR tests was conducted. Similar observations were made with CO_2 reacted PEI samples.

FTIR tests concluded that there is a clear difference between the amine treated samples and the untreated clay. This is contributed to the peaks associated with the amines attached to the clay. FTIR experiments were conducted to try to see the difference between samples exposed to CO_2, but the differences in the spectra were slight and could not be conclusively attributed to reacted CO_2.

4.3 Surface Area Results

If montmorillonite clay could be separated into individual sheets the surface area is expected to be 750m^2/g. This is according to the material data supplied by the Southern Clay

Products for Cloisite® Na^+. To determine the surface area of unmodified Cloisite® Na^+, a ASAP 2020 surface analysis machine was used to determine the BET surface area. A sample of fumed silica with a surface area of 250 +/- 30 m^2/g was tested in the BET ASAP 2020 surface analysis machine to determine the accuracy of the method. First, a sample was placed into the sample tube with an auxiliary sample rod also placed into the tube. A vacuum was placed onto the tube and the sample was heated to 120°C to remove any moisture in the sample. The vacuum was held for at least 30 minutes or until 100 mtorr was observed on the vacuum gauge. Once this was achieved, the vacuum was turned off and nitrogen was allowed to flow into the sample tube. The lid was then quickly placed onto the sample tube and the sample was connected to the surface analysis machine.

Two consecutive runs were conducted using the same sample without removing the sample from the machine to test the repeatability of the results. The results were 218.9879 m^2/g +/- 1.9554 m^2/g and 222.9788 m^2/g +/- 2.7113 m^2/g, which when averaged fit between the parameters of the surface area reported for the fumed silica. A standard was run before these tests were conducted and the results were satisfactory. This result led us to believe that the numbers obtained from this machine were accurate. The BET surface area results are reported in Table 4-1.

Table 4-1: BET surface area results using ASAP 2020

	Untreated Clay	C-APTMS-1-2	C-PEI-50	C-APTMS-PEI-50	Fumed Silica (250 m^2/g +/- 30 m^2/g)
BET Surface Area m^2/g	11.66	7.26	0.10	0.35	220.98
error +/-	0.17	0.10	0.02	0.02	2.33

The results showed that the untreated Cloisite® Na^+ had the highest surface area, followed by Cloisite® Na^+ treated with APTMS, Cloisite® Na^+ treated with APTMS and PEI, and Cloisite® Na^+ treated with PEI. The reduction in the surface area when the clay is treated with PEI is expected since the PEI coats the surface and seems to promote agglomeration of the particles. Also when other researchers coated their molecular baskets and other solid supports (SBA-15, MCM-41) with PEI, the surface area went down. This is also assumed to be the reason why the surface area went down with clay treated with APTMS and PEI. The reduction in surface area when the clay was treated with only APTMS is not necessarily expected since it was thought that the APTMS would react with the edge hydroxyl groups and even further separate the clay platelets, resulting in less stacking of the individual platelets and therefore more surface area. The increase in surface area was expected since the surface area for Cloisite® Na^+ is reported by Southern Clay Products as being 750 m^2/g when the platelets are fully exfoliated. One possible reason that the surface area did decrease is when the sample is filtered and dried it forms into a hard solid that needs to be crushed back into a powered. This is done by mortar and pestle, and the resulting powder might have to be crushed more finely to achieve a greater surface area.

4.4 Scanning Electron Microscopy (SEM)

SEM pictures were taken of the treated and untreated clay to determine the particle size and the general composition of the sorbents. The use of a particle size analyzer was initially attempted, but the particles had to be dispersed in a liquid medium (water). Since water swells the clay, it breaks apart the layers, and this significantly alters the clay particle size. This technique was assumed to give results not representative of the dry powder samples.

Particle size can be determined using dry powders, but this instrument was not available for use, and since the samples treated with PEI tended to be sticky, the results from this technique would also be questionable.

The samples were placed onto a sample holder using double sided carbon tape. Multiple images were taken of all of the samples in different areas to determine that the images taken were representative of the sample. The images shown in this section were representative of the samples tested, based on all of the images that were taken.

The untreated clay was first imaged at a low magnification to determine the general particle size of the powder. In Figure 4-18 it can be seen that there are a large number of particles with various sizes throughout the image. The large aggregates are indicative of many layers of clay stacked together in large clusters. The smaller particles are not individual platelets, but just smaller stacks of platelets. Other images at this magnification were taken to make sure that this was representative of the sample. An image of the smallest and largest particle of the untreated clay was taken to get a general particle size range for the material, and to see more of the features of the sample at a higher magnification. Figure 4-19 and 4-20 are images of the smallest and largest representative particle in the sample of untreated clay.

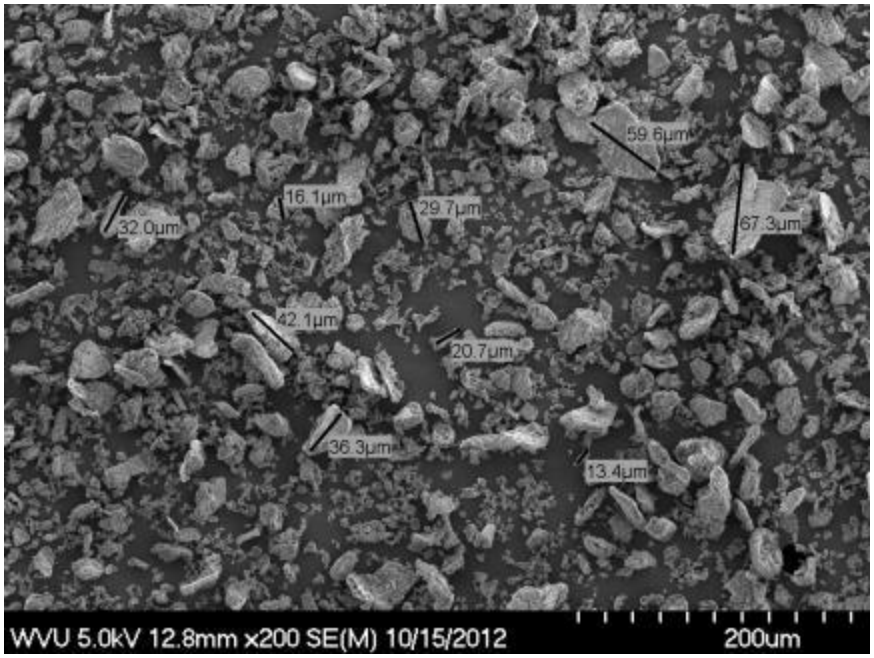

Figure 4-18: SEM image of untreated clay magnified 200 times, with a working distance of 12.8mm, using 5.0kV and both detectors

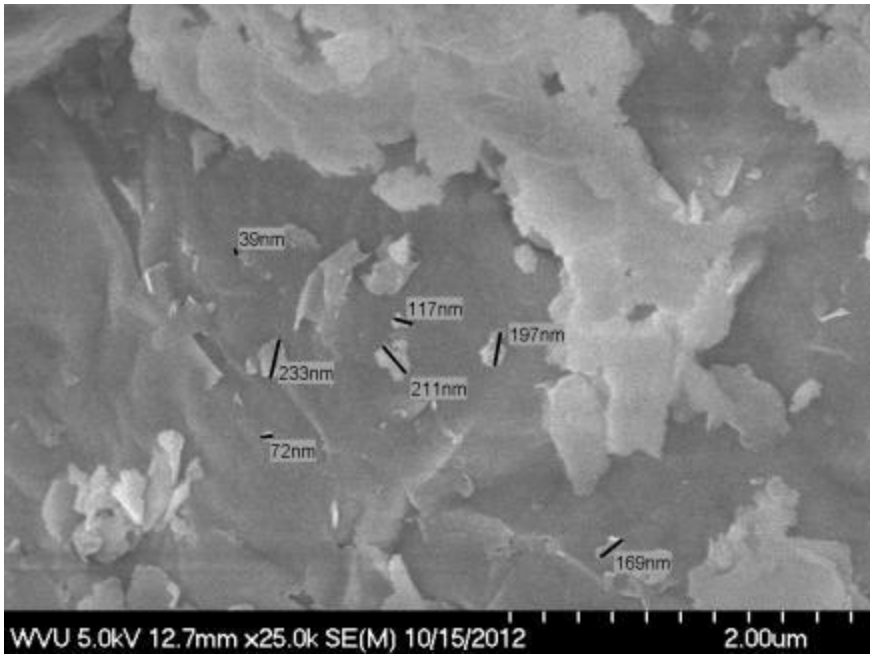

Figure 4-19: SEM image of untreated clay magnified 25,000 times, with a working distance of 12.7mm, using 5.0kV and both detectors

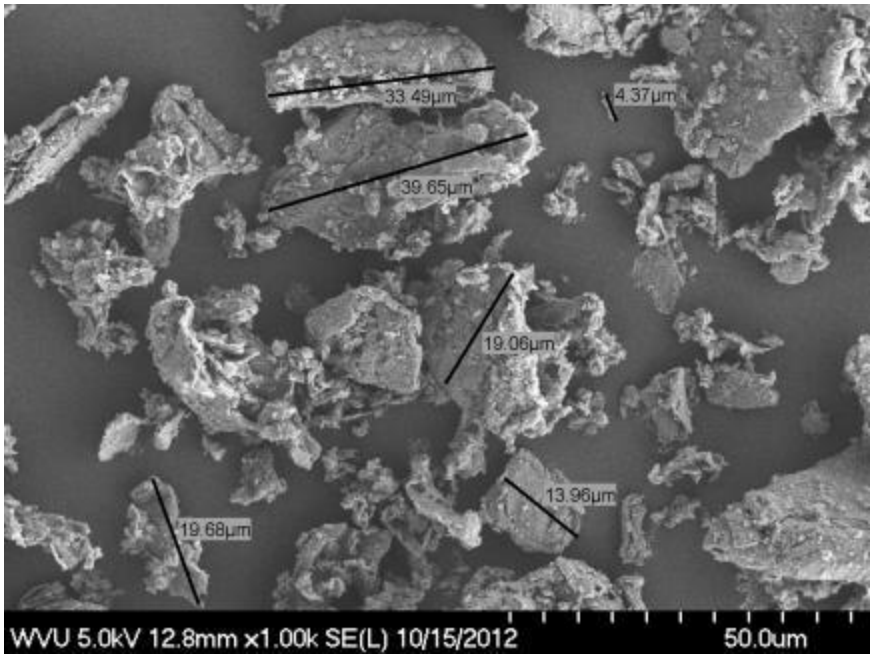

Figure 4-20: SEM image of untreated clay magnified 1,000 times, with a working distance of 12.8mm, using 5.0kV and the lower detector

From Figures 4-18-20 it can be seen that the smallest particle that can be imaged using the SEM and untreated clay is 39nm and the largest particle is 67.3µm. This indicates a wide size range of the untreated clay particles. The smallest particle seen of 39nm is close to the expected lateral dimensions of a single clay particle. The majority of the particles are larger than this, which is expected since the clay platelets stack together to form large aggregates.

Clay treated with APTMS using the slurry method was imaged to determine the difference in the treated and untreated clay. The sample was crushed in a mortar and pestle to form a fine powder. Figure 4-21 is an image at low magnification to get a general representation of the sample. In Figure 4-21 it can be seen that there are larger particles in the clay sample treated with APTMS than with the untreated clay. Similarly to the untreated clay sample there is a wide range of particle sizes. This indicates that the clay is still stacked in large clusters of individual sheets.

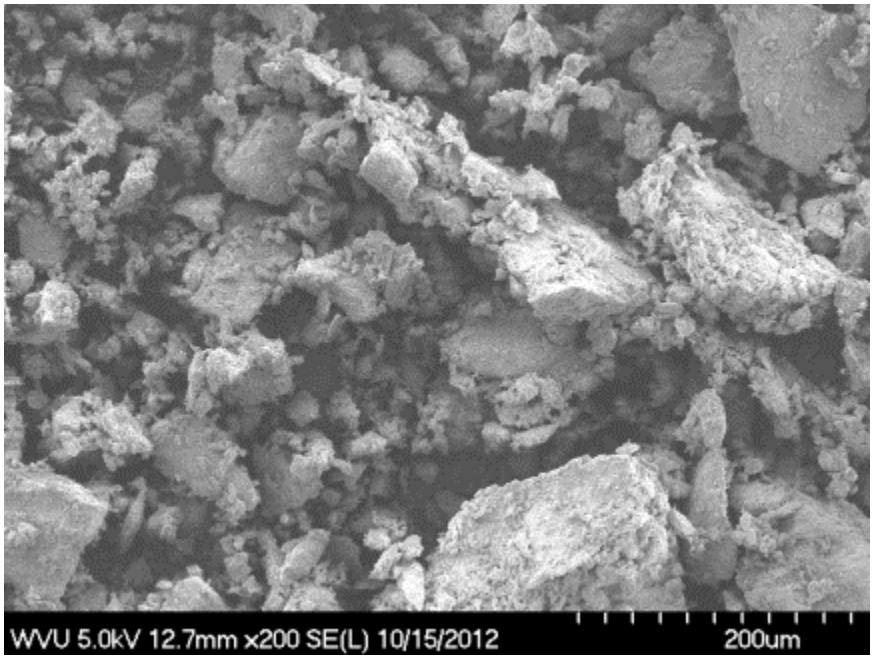

Figure 4-21: SEM image of treated clay with APTMS magnified 200 times, with a working distance of 12.7mm, using 5.0kV and the lower detector

Figures 4-22-23 are representative images of the treated clay particles at higher magnifications. In Figure 4-22 the smallest particle that could be imaged and measured was 177nm. This indicates that treatment with APTMS did not separate the clay platelets when dried, crushed in a mortar and pestle and imaged in the SEM. It was difficult to determine individual particles at low magnification. The largest particle seen in the SEM with a magnification of 350 times was 86.7μm. The smallest and largest particles seen while imaging the clay treated with APTMS tend to be larger than the untreated clay.

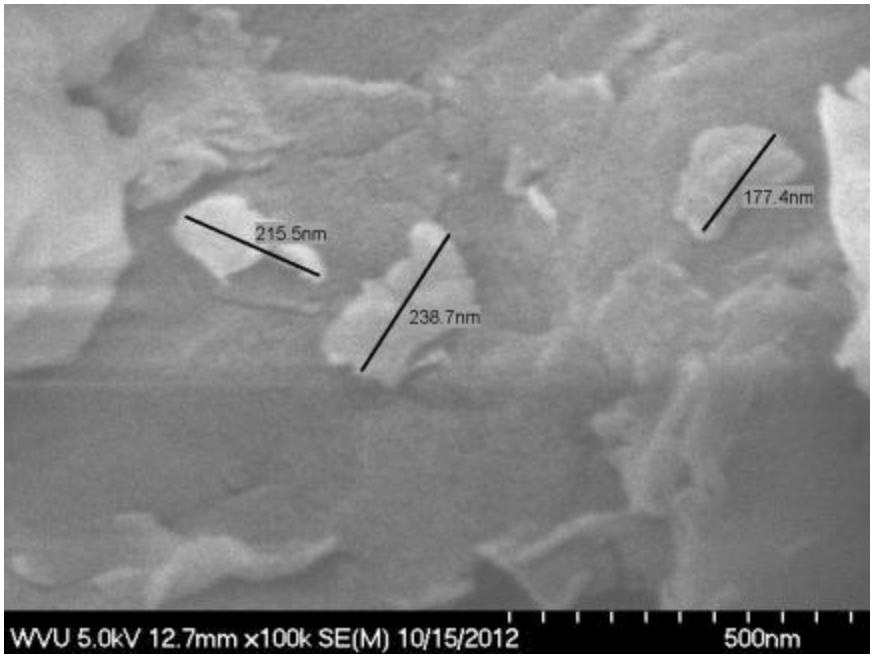

Figure 4-22: SEM image of treated clay with APTMS magnified 100,000 times, with a working distance of 12.7mm, using 5.0kV and the both detectors

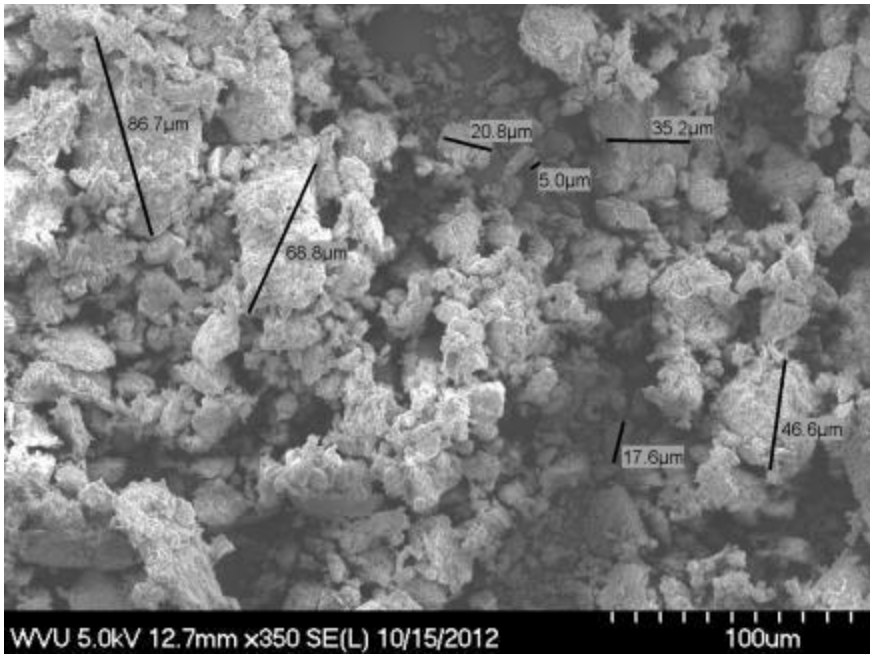

Figure 4-23: SEM image of treated clay with APTMS magnified 350 times, with a working distance of 12.7mm, using 5.0kV and the lower detector

The clay samples treated with APTMS appear to have a rough layer covering the surface of the material that is probably due to the APTMS on the surface. The particles are also in general larger than the particles in the untreated clay. Other than those differences, the particles generally look the same when treated with APTMS. When looking at them with the naked eye this is also the case. The particles appear to be slightly larger than the untreated particles, but are of the same color and consistency.

The clay samples loaded with 50% PEI are still a powder but tend to stick together. There is a noticeable difference in appearance and consistency when looking at samples treated with PEI. A low magnification of nanoclay treated with 50% PEI is shown in Figure 4-24.

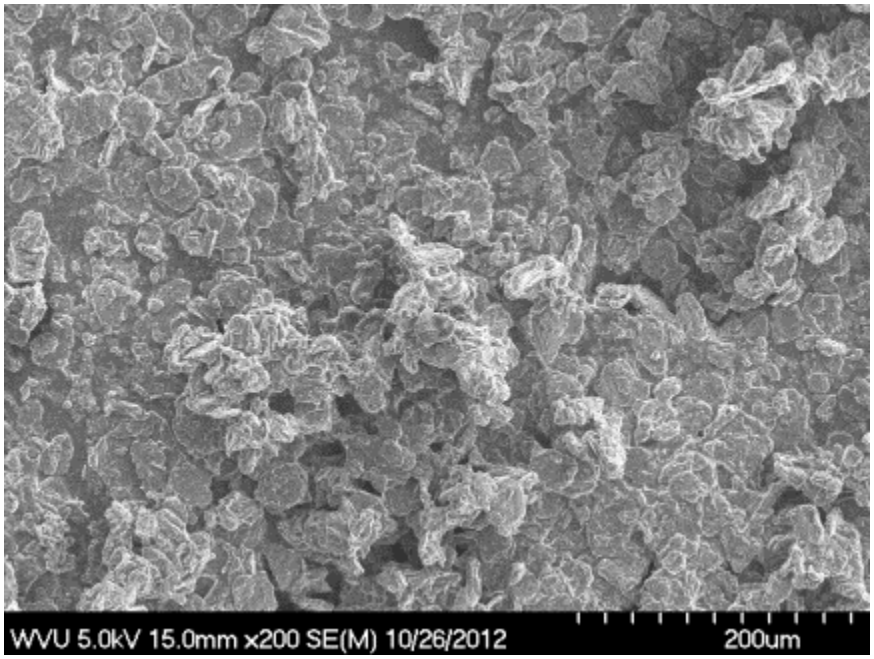

Figure 4-24: SEM image of treated clay with 50% PEI magnified 200 times, with a working distance of 15.0mm, using 5.0kV and both detectors

In Figure 4-24 it can be seen that the general morphology of the nanoclay treated with PEI is completely different from that of the nanoclay treated with APTMS. In Figure 4-24 the

particles are apparently coated with a layer of PEI and seem to form an almost continuous matrix of PEI with the nanoclay underneath. The clay particles can be seen in Figure 4-24 and appear to be completely covered with PEI. This indicates that the PEI is completely covering the clay surface. A higher magnification image of the clay treated with PEI is shown in Figure 4-25. Since the PEI was completely covering the surface, it was difficult to get dimensions of the clay particles. Using a higher magnification used in Figure 4-25, some of the particles could be measured. The particle size range in Figure 4-25 is 1-32µm. This is just a very general representation of the size of the particles since generally the separate particles could not be distinguished from each other, which is seen in Figure 4-24.

Figure 4-25: SEM image of treated clay with 50% PEI magnified 1,800 times, with a working distance of 12.7mm, using 5.0kV and the lower detector

The consistency of the samples treated with APTMS and PEI in general had more of a paste like consistency than a powder, but varied apparently on how well they mixed together.

Figure 4-26 is a low magnification image of a sample treated with both APTMS and PEI, in which the consistency was more paste like.

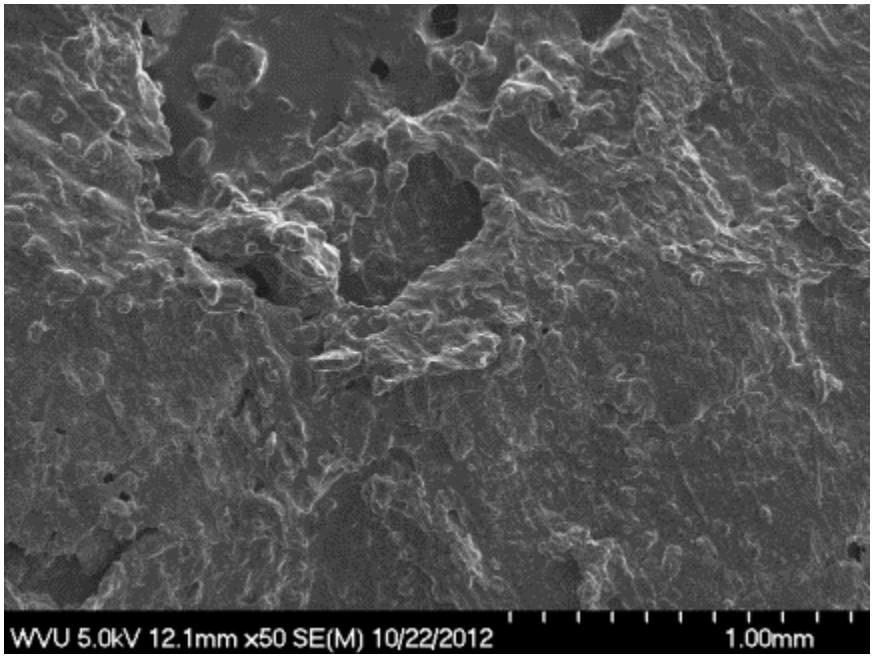

Figure 4-26: SEM image of 20 treated clay with APTMS and 50% PEI magnified 50 times, with a working distance of 12.1mm, using 5.0kV and both detectors.

In Figure 4-26 the clay particles cannot be seen clearly indicating that with the combination of APTMS and PEI, the clay is completely covered with amines and forms a more paste like consistency. In Figures 4-27 and 4-28 a different sample, 2L, of clay treated with APTMS and PEI was imaged. This sample was less paste like than the earlier sample, and very large particles can be seen.

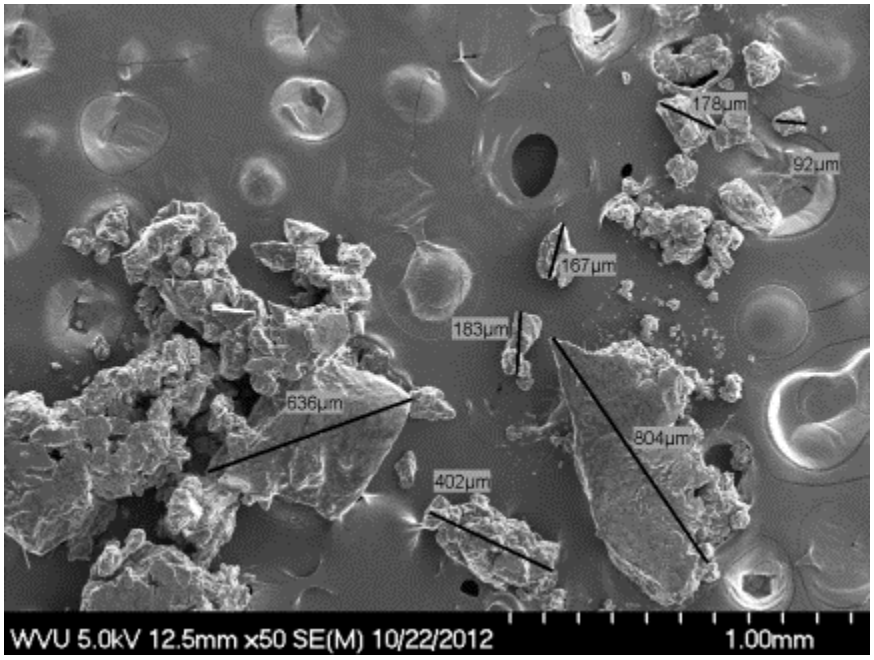

Figure 4-27: SEM image of 2L treated clay with APTMS and 50% PEI magnified 50 times, with a working distance of 12.5mm, using 5.0kV and both detectors. The blisters and holes are due to the carbon tape not the sample

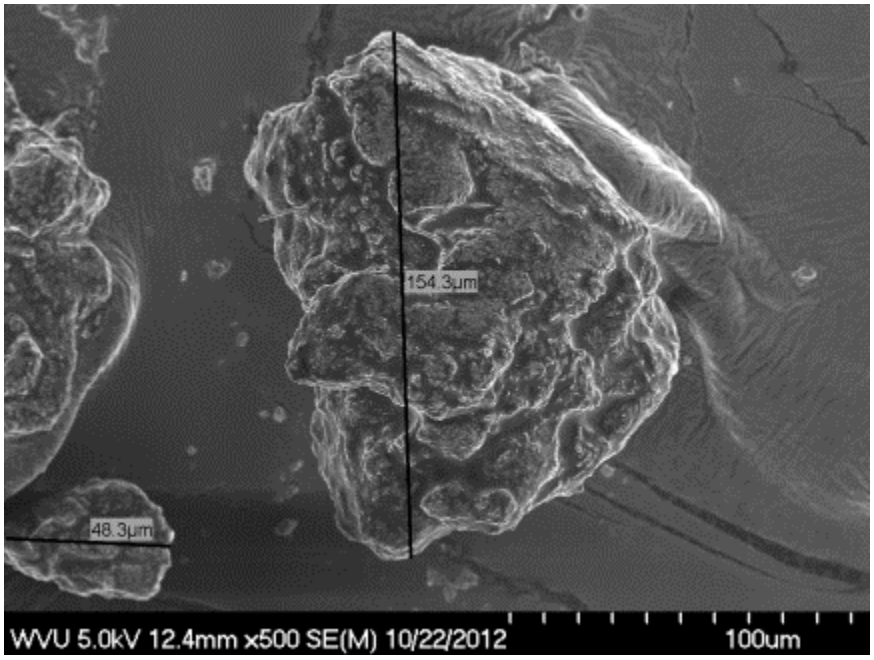

Figure 4-28: SEM image of 2L treated clay with APTMS and 50% PEI magnified 500 times, with a working distance of 12.4mm, using 5.0kV and both detectors

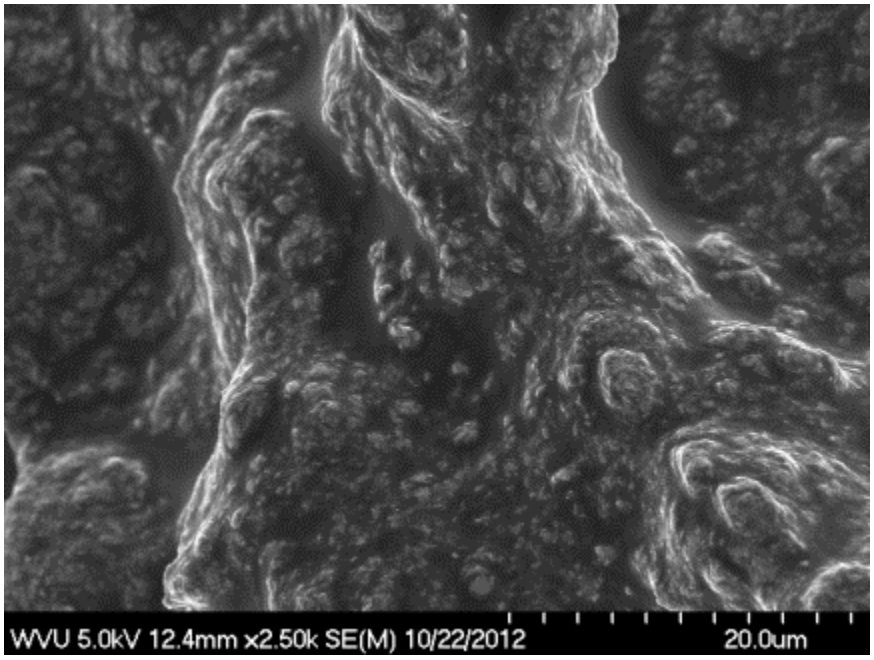

Figure 4-29: SEM image of 2O treated clay with APTMS and 50% PEI magnified 2,500 times, with a working distance of 12.4mm, using 5.0kV and both detectors

Figure 4-29 is a high magnification image of sample 20, clay treated with APTMS and 50% PEI. In Figure 4-29 the clay particles cannot be easily distinguished, but there is obviously a surface roughness that is most likely caused by the clay particles underneath the PEI.

Using the SEM it can be clearly seen that the amine treatments change the size and morphology of the untreated clay. The samples treated with only APTMS looked similar and had similar consistency to the untreated clay with the naked eye and at low magnification in the SEM, but generally formed larger particle sizes. The samples treated with PEI, and the combination of PEI and APTMS had a more paste like consistency than the untreated clay and the PEI seemed to be completely covering the surface of the clay.

Chapter 5

5. CO_2 Adsorption and Desorption

In order to determine the adsorption capacity of the sorbents at different temperatures and at atmospheric conditions, a series of experiments using a TGA was conducted. The initial experiments used pure CO_2 and nitrogen to determine the CO_2 adsorption capacity and the ability of the sorbent to desorb CO_2. Experiments using a mixed gas of 10% CO_2 and nitrogen were also used to determine the ability of the adsorbent to adsorb CO_2 from mixed gases. Desorption experiments were also conducted and included using sweep gases of pure nitrogen, pure CO_2 and CO_2 containing water. CO_2 adsorption at high pressure was conducted using a pressure vessel and pure CO_2. Pressure Tests for CO_2 adsorption were conducted to determine the effect of pressure and possible applications to pre-combustion adsorption. Regeneration using vacuum and water vapor test were also conducted.

5.1 Pure CO_2 Adsorption using TGA

Pure CO_2 was used to determine if the sorbents would adsorb any CO_2. In order to establish a baseline for each sorbent, the procedure was to heat the sample to 100°C in pure nitrogen for 30 minutes and then cool the reactor to the desired CO_2 reaction temperature. Initial experiments used 60 minutes of nitrogen at 100°C, but after a few experiments it was determined that 30 minutes was sufficient to achieve a stable sample weight for the carbon dioxide weight gain experiments. A representative TGA graph from the Thermo Cahn Thermax 500 apparatus is shown in Figure 5-1 for untreated clay. In Figure 5-1 it can be seen that the weight is reduced to about 94% of the starting value during the drying step in nitrogen. This decrease in weight is attributed to the loss of water from the sample. After the sample weight

becomes stabile, the reaction temperature is reduced to 85°C for the adsorption of CO_2 onto the sample. Once the reaction gas is switched to CO_2, there is a dip in the weight which is due to buoyancy effects. The percent carbon dioxide adsorbed is measured by taking the weight difference at the point when the reaction gas is switched to CO_2 and the weight gained during the adsorption time. An adsorption time of approximately 90 minutes was used to compare the sample treatments.

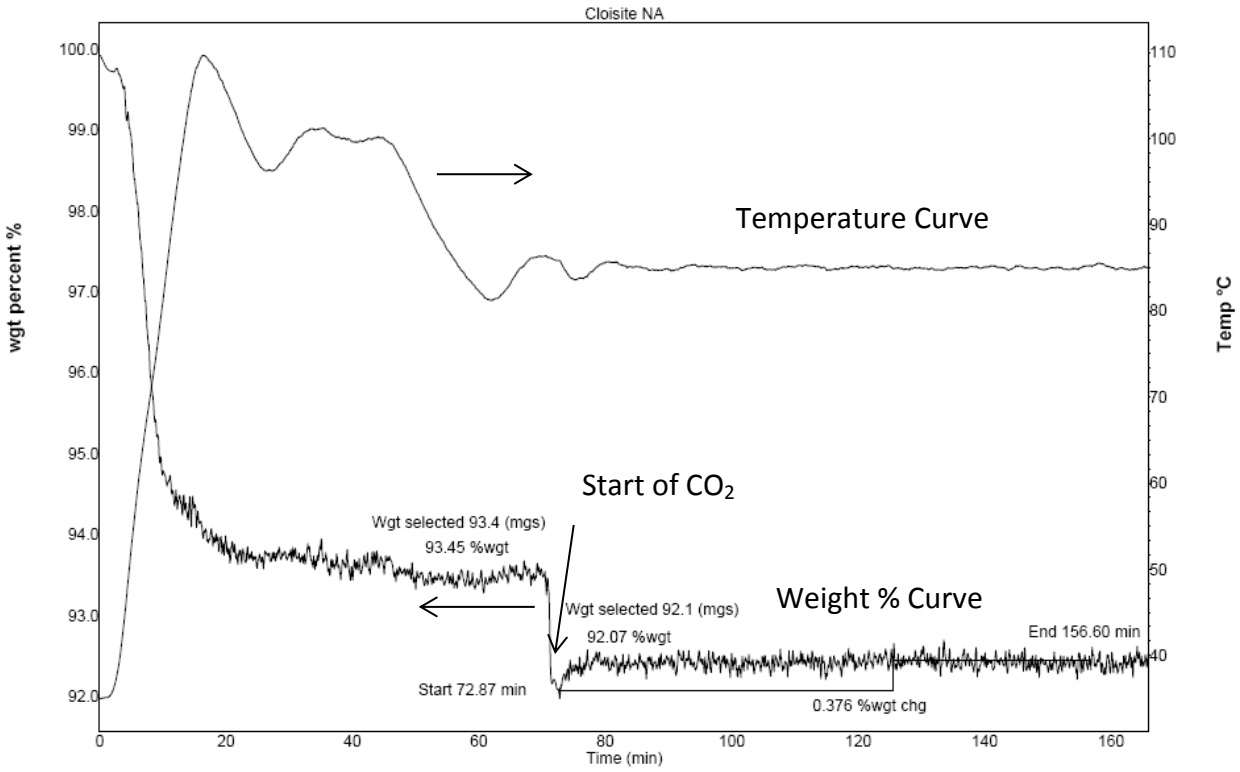

Figure 5-1: TGA graph of untreated clay for CO_2 adsorption at 85°C in pure CO_2

Figure 5-1 shows that there is very little CO_2 adsorbed on the untreated clay. Additionally, the noise in the weight percent curve can clearly be seen. After the reaction gas is switched to CO_2 the weight is quickly stabilized, indicating that there is no CO_2 being adsorbed or diffused into the untreated clay.

Figure 5-2 shows a TGA curve using the TA-Q500 TGA for clay treated with PEI. Using this TGA, it can be seen that there is significantly less noise in the weight percent curve. With the loading of PEI onto the clay, it can be clearly seen in Figure 5-2 that CO_2 is adsorbed onto the sorbent. The CO_2 adsorption is rapid when the reaction gas is first switched to CO_2; this is followed by a slow adsorption step as time continues.

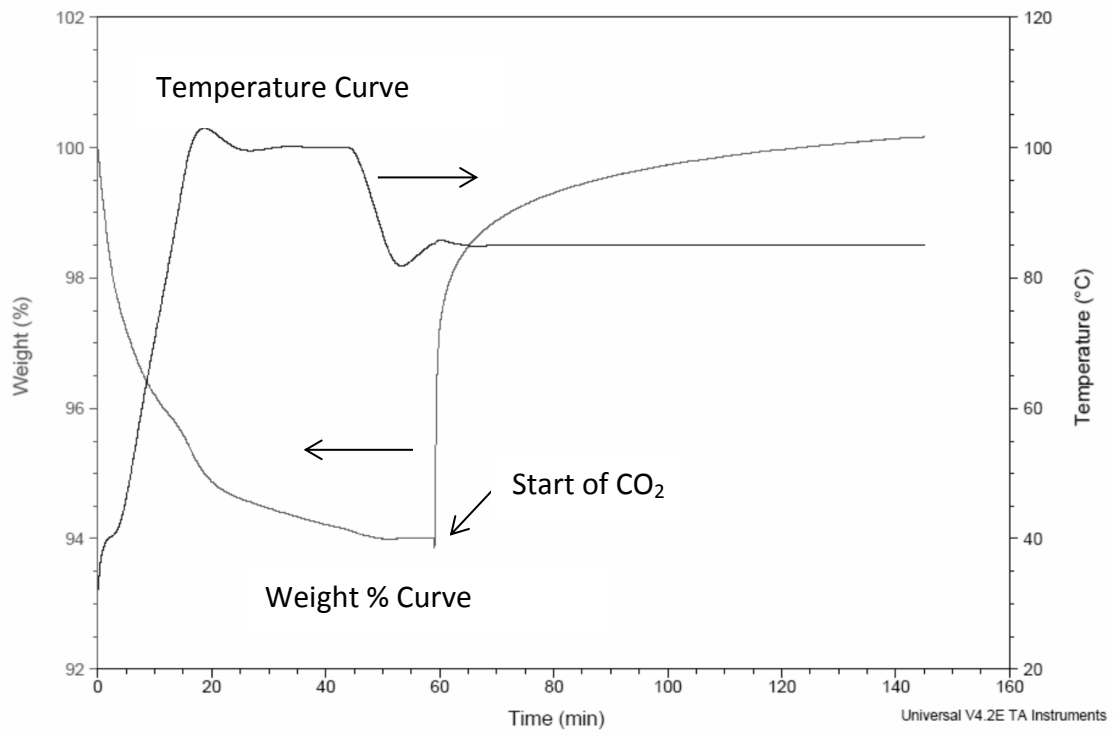

Figure 5-2: TGA graph of clay treated with PEI, pure CO_2 adsorption at 85°C

A TGA graph with clay treated with APTMS is shown in Figure 5-3. Again it can be seen that there is a significant amount of CO_2 adsorption compared to the untreated clay. The adsorption profile for the clay treated with APTMS has a rapid adsorption step followed by little to no weight gain. This is attributed to CO_2 reacting with the APTMS and having very little diffusion limitations.

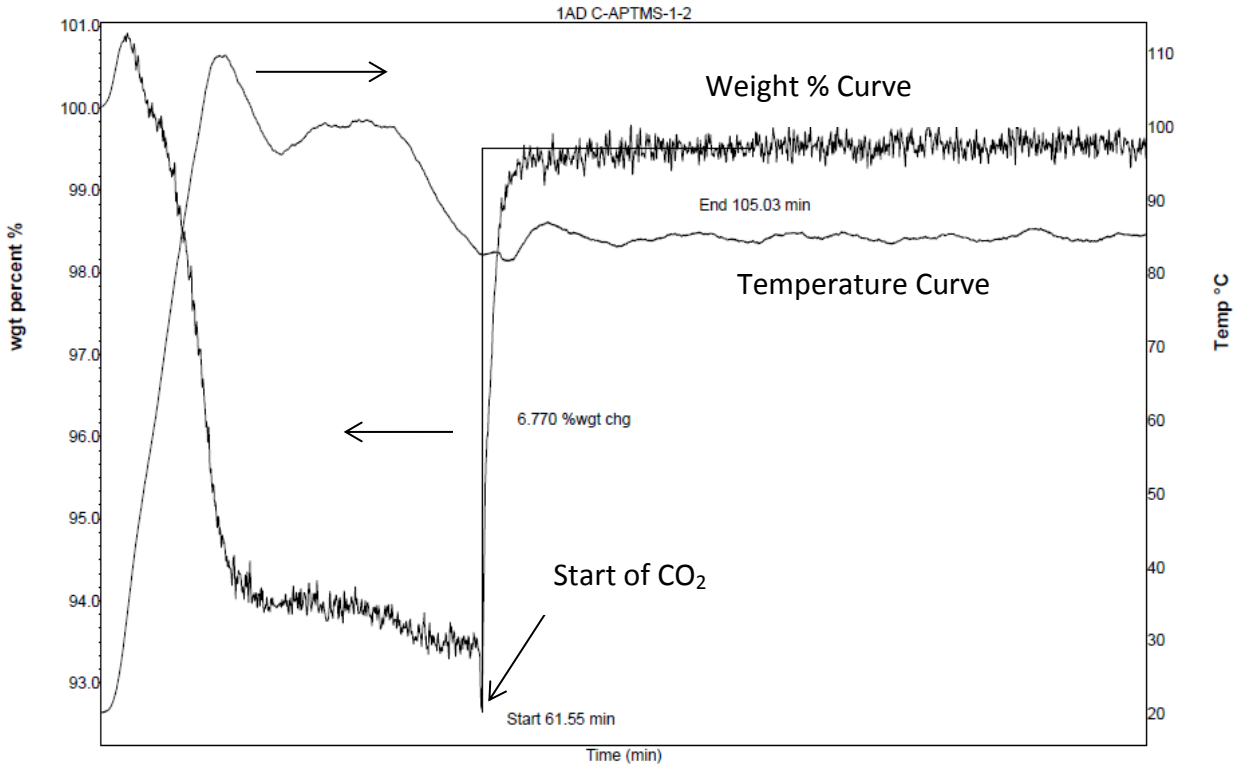

Figure 5-3: TGA graph of clay treated with APTMS, CO_2 adsorption at 85°C

Figure 5-4 is a TGA graph of clay treated with the combination of APTMS and PEI. The CO_2 adsorption profile in Figure 5-4 appears to follow the same adsorption profile as the clay treated with only PEI. This is expected since the PEI is covering the majority of the clay surface, and this would cause the same diffusion limitations in the adsorption profile. To determine the temperature dependence of the carbon dioxide adsorption capacity of the adsorbent, experiments were conducted at multiple adsorption temperatures. Results are shown in Figure 5-5.

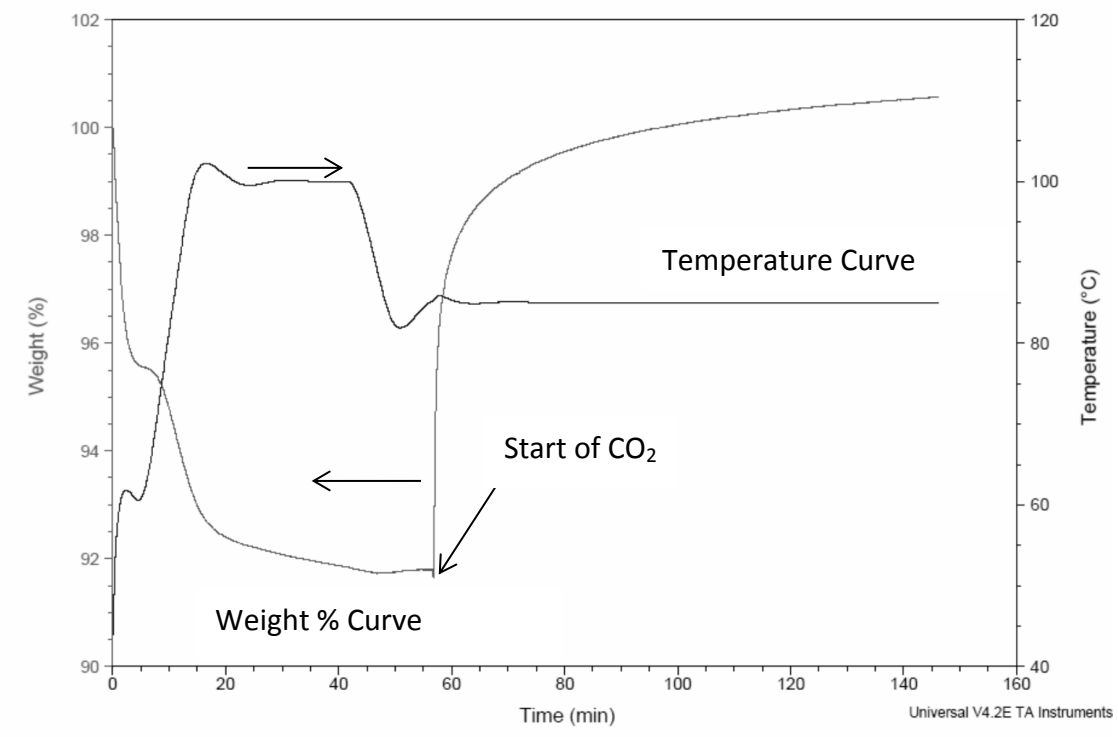

Figure 5-4: TGA graph of clay treated with APTMS and PEI, CO_2 adsorption at 85°C

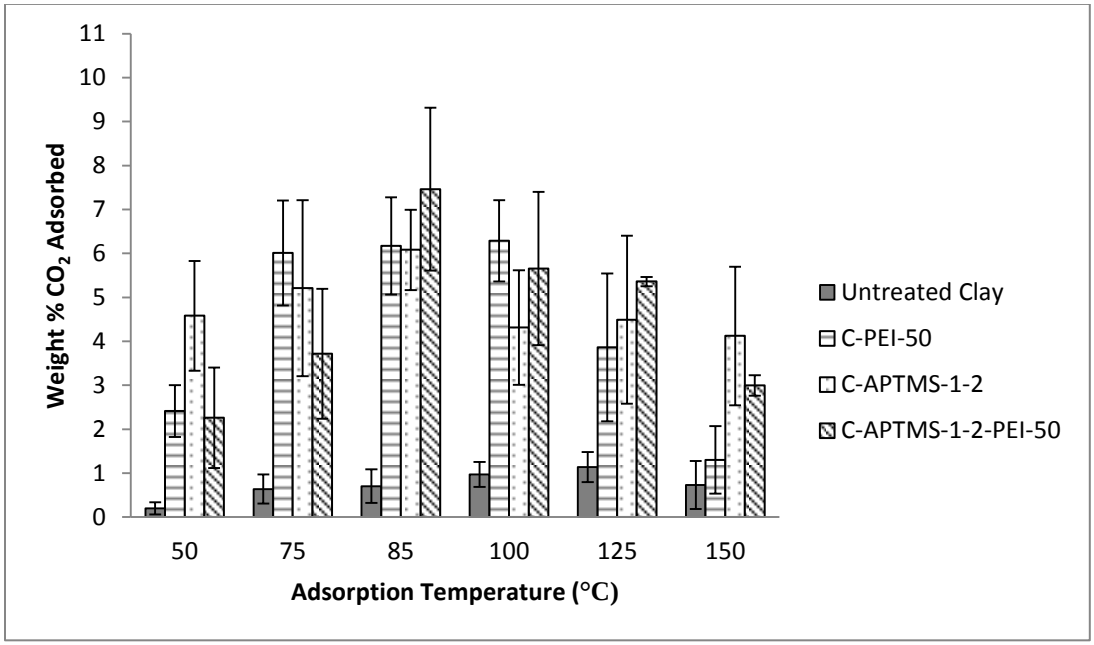

Figure 5-5: Carbon dioxide adsorption capacity as a function of adsorption temperature at atmospheric pressure in the TGA

Figure 5-5 is a comparison of the CO_2 adsorption capacities of untreated clay, clay treated with APTMS, PEI, and APTMS+PEI. Unless it is otherwise stated, the PEI used in the experiments was Mn 423. From Figure 5-5 it can be seen that the adsorption capacity for the treated samples increases from 50°C to 75°C. The temperature range with the highest adsorption was 75°C-100°C, with the highest adsorption rate being at 85°C for clay treated with APTMS+PEI. Therefore, the majority of the other experiments conducted used an adsorption temperature of 85°C.

Additionally, Figure 5-5 shows that, as the temperature is increased above 100°C, the adsorption of carbon dioxide is reduced for the samples treated with PEI. The CO_2 adsorption capacity for clay treated with APTMS decreased when the temperature was above 85°C. The untreated clay adsorption capacity does not change significantly with increasing temperature. This is attributed to the reaction of CO_2 with amines being exothermic; therefore, as the temperature rises, the equilibrium of the reaction will tend to go towards the reactant side of the equation according to LeChâtelier's principle. One reason for the increase in adsorption capacity from 50°C to 85°C for the clay samples treated with PEI is that, with the higher temperature, the PEI molecule can expand giving more access to the amine reaction sites for the CO_2. At lower temperatures, the CO_2 reacts with surface PEI molecules, and the CO_2 adsorption is limited due to diffusion. Other researchers have also seen this phenomenon using PEI and other supports. [44]

When the reaction temperature is 150°C, the adsorption with APTMS+PEI is less than the adsorption with APTMS alone. This is due to the fact that there is more PEI attached to the

clay as compared to APTMS and since the PEI adsorbs very little CO_2 at this elevated temperature the adsorption capacity of APTMS+PEI is also reduced.

The rate at which the adsorbent can adsorb CO_2 is very important when doing calculations for reactor design, and other future design calculations. It was qualitatively observed that clay treated with APTMS alone exhibited rapid adsorption of CO_2 and reached near equilibrium very quickly. The clay treated with PEI and the combination of PEI and APTMS showed a quick adsorption followed by a slow adsorption profile. Samples reacted at 85°C, and these had the highest adsorption capacities, were used in calculating the adsorption times. The times were measured by assuming 100 percent adsorption at 90 minutes, and then measuring the time at 50, 75, 90, and 95 percent CO_2 adsorption. At least four runs were used to measure the adsorption times at each percent adsorption. The results are shown in Figure 5-6.

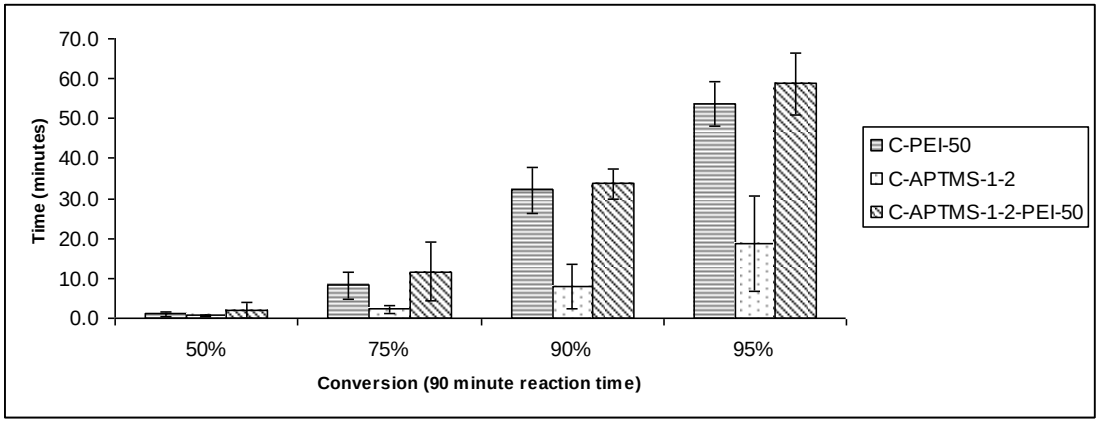

Figure 5-6: Time versus percent CO_2 adsorbed based on a 90 minute adsorption run

In Figure 5-6 it can be seen that the adsorption rate of clay treated with only PEI closely follows the adsorption rate for clay treated with the combination of APTMS and PEI. This confirms the observation that the reaction rates appeared to be similar when studying the TGA curves qualitatively. Additionally it can be seen that the clay treated with APTMS achieves 90 percent

of its adsorption capacity under 10 minutes and 95 percent adsorption capacity around 20 minutes. The data can also be viewed in Table 5- 1

Table 5-1: Time to reach different CO_2 adsorption percentages based on a 90 minute adsorption time

Percent Adsorption	50%	75%	90%	95%
Clay+PEI (minutes)	1.1	8.2	32.2	53.8
Clay+APTMS (minutes)	0.7	2.2	8.1	18.7
Clay+APTMS+PEI (minutes)	2.0	11.7	33.8	58.8

The results shown in Figure 5-6 and Table 5-1 confirm that the CO_2 adsorption rate for samples treated with only PEI and the combination of APTMS and PEI have very similar adsorption profiles. This is to be expected since the PEI is covering the surface of the untreated clay and the clay treated with APTMS. The samples treated with only APTMS showed quick CO_2 uptake, which is also expected when looking at the TGA graphs. This also may indicate that although the adsorption capacity for the samples treated with PEI and the combination of APTMS and PEI have a slightly higher adsorption capacity than the samples treated with only APTMS, the clay treated with APTMS might be a better adsorbent because of it fast adsorption kinetics.

To compare the behavior of different molecular weight PEI on the adsorption of CO_2, a loading of 50 weight percent PEI onto the surface of clay was employed using the same wet impregnation that is described in the experimental section. The appearance and consistency of the sample using PEI Mn 1200 closely resembled the samples made using PEI Mn 423. The sample made with PEI Mn 60,000, however, formed clumps of material instead of a powder; this is probably due to the large increase in the molecular weight as compared to either Mn 423

or Mn 1200. Figure 5-7 and Figure 5-8 are representative TGA graphs for CO_2 adsorption on samples made with clay treated with PEI Mn 1200 and Mn 60,000.

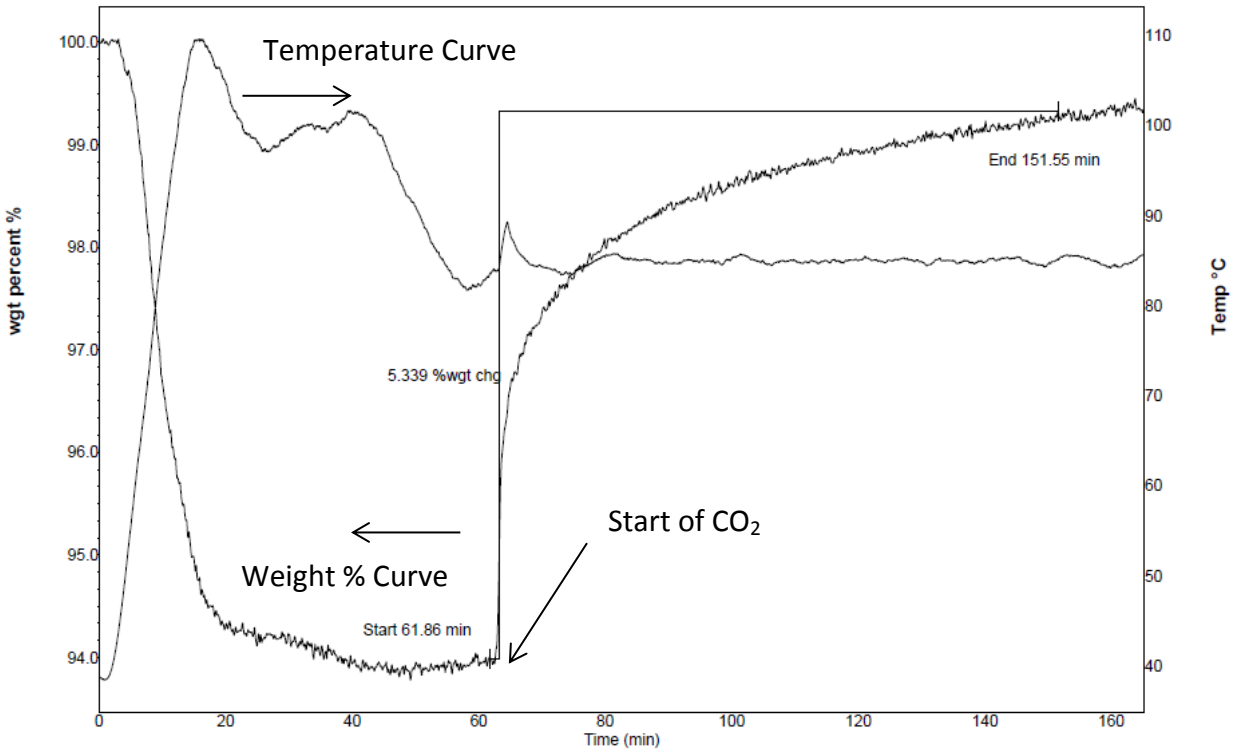

Figure 5-7: TGA CO_2 adsorption graph at 85°C of clay loaded with 50% PEI Mn 1200

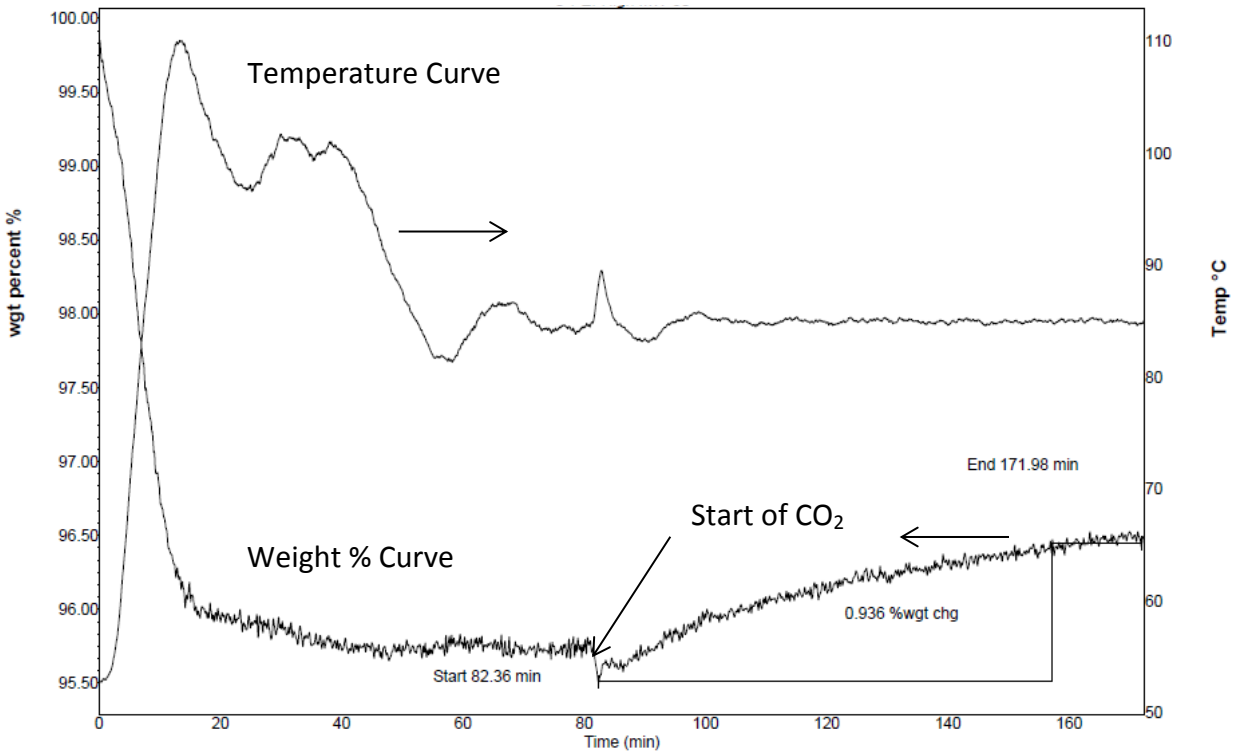

Figure 5-8: TGA CO_2 adsorption graph at 85°C for clay loaded with 50% PEI Mn 60,000

The adsorption capacity and profile for CO_2 adsorption on clay treated with PEI Mn 1200 was very similar to the adsorption capacity of PEI Mn 423. The adsorption capacity and profile for CO_2 adsorption using high molecular weight PEI had a greatly reduced adsorption capacity and seemed to show a more diffusion-controlled mechanism. This indicates that the amine sites on the high molecular weight PEI are not easily accessed at 85°C. Figure 5-9 is a graph of the comparison of the adsorption capacity of three different molecular weight PEIs when 50 percent PEI was loaded onto the clay support.

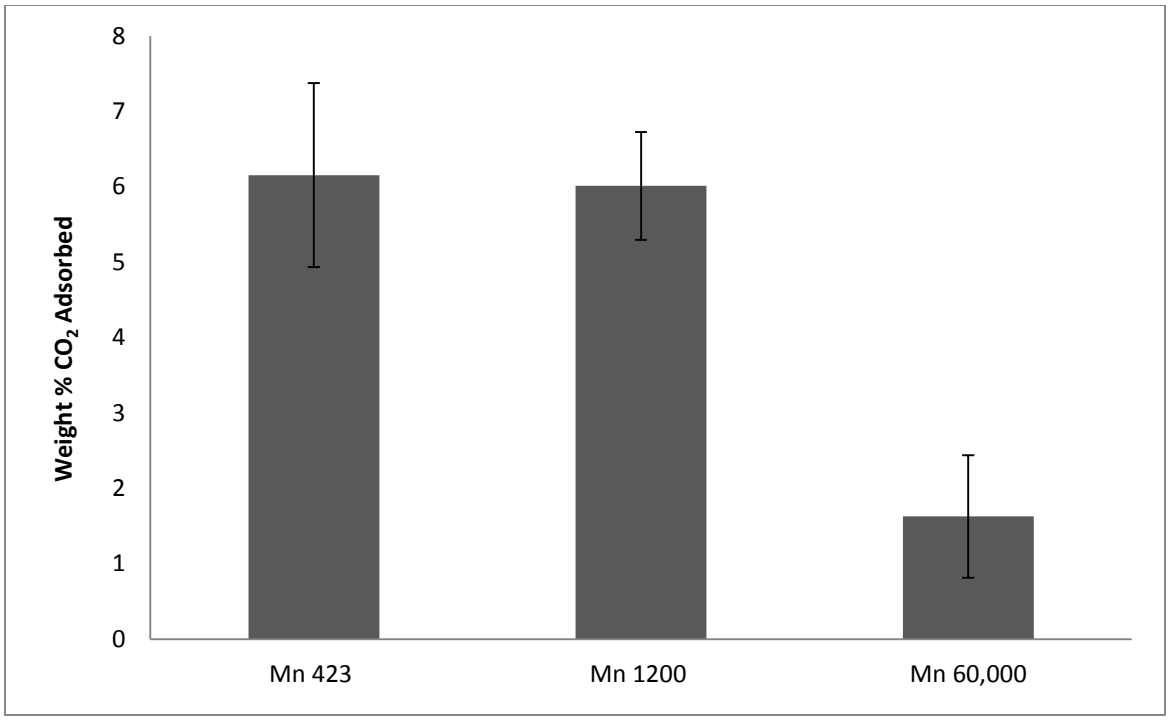

Figure 5-9: CO_2 adsorption for clay loaded with PEI at 85°C

Supports treated with PEI in the literature for CO_2 adsorption were typically prepared using a 50% loading. This was because this loading value showed the best overall CO_2 adsorption per gram of PEI. [44] A study using a loading of 33%, 50% and 66% loading based on the concentrations used in the wet impregnation method was studied for the CO_2 adsorption capacity at 85°C in a TGA. The results are presented in Figure 5-10 and these show that, with the increased loading of PEI from 50% to 66%, the adsorption capacity did not change. The adsorption capacity did increase when the loading was increased from 33% to 50%. Additionally, with the higher loadings, the sample turned into a more paste like consistency. This observation would indicate that a loading of more than 50% PEI does not significantly increase the amount of CO_2 adsorbed onto the adsorbent.

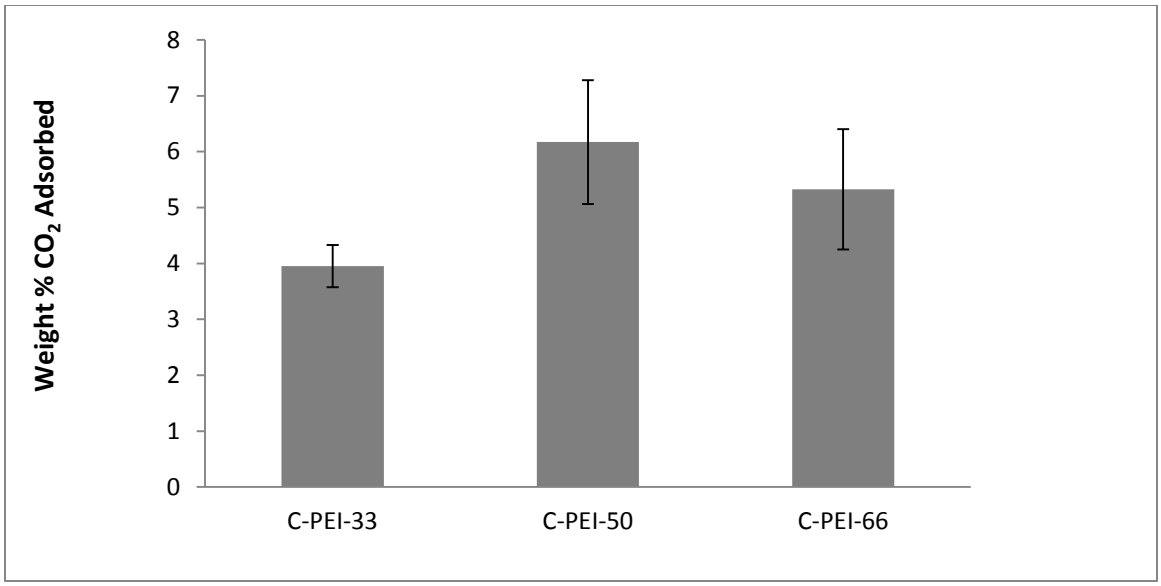

Figure 5-10: Comparison of PEI loading on CO_2 adsorption capacity at 85°C

The data collected during these experiments using pure CO_2 at atmospheric conditions showed that the best adsorption temperatures were in the range of 75°C-100°C for all of the treated adsorbents. The untreated clay did not adsorb significant CO_2 at any temperature. An adsorption temperature of 85° is in the middle of this range, and it showed the best adsorption results and was, therefore, used for the majority of the other experiments. A study using different molecular weight PEI showed that the best PEI for adsorption at 85°C using pure CO_2 in a TGA was the lowest molecular weight studied, PEI Mn 423. Studying the different loadings of PEI showed that a loading of 50% appeared to be enough to achieve the maximum amount of CO_2 adsorption at 85°C using pure CO_2.

5.2 Adsorption from a Mixed Gas Containing 10% CO_2

In order to test the adsorbents in a more realistic flue gas stream, a gas cylinder containing 10% CO_2 with the balance being nitrogen was ordered from Airgas and used in the TGA experiments at 85°C for CO_2 adsorption. The adsorption temperature of 85°C was used because previous results using pure CO_2 showed that the highest CO_2 adsorption capacity was

attained at 85°C. Figure 5-11 is a representative graph of the adsorption of CO_2 in this mixed gas stream using a sample of clay treated with APTMS. In Figure 5-11 it can be seen that the adsorption of CO_2 followed the same profile as the adsorption in pure CO_2 with comparable adsorption capacities. Additionally, there is a cycle step using pure nitrogen at 100°C to insure cycling was still possible when using 10% CO_2 reaction stream. The same adsorption profile that occurred in pure CO_2 was also evident with the samples of clay treated with PEI and APTMS+PEI. This indicated that CO_2 can be adsorbed in a reaction stream that has a significantly lower percentage of CO_2.

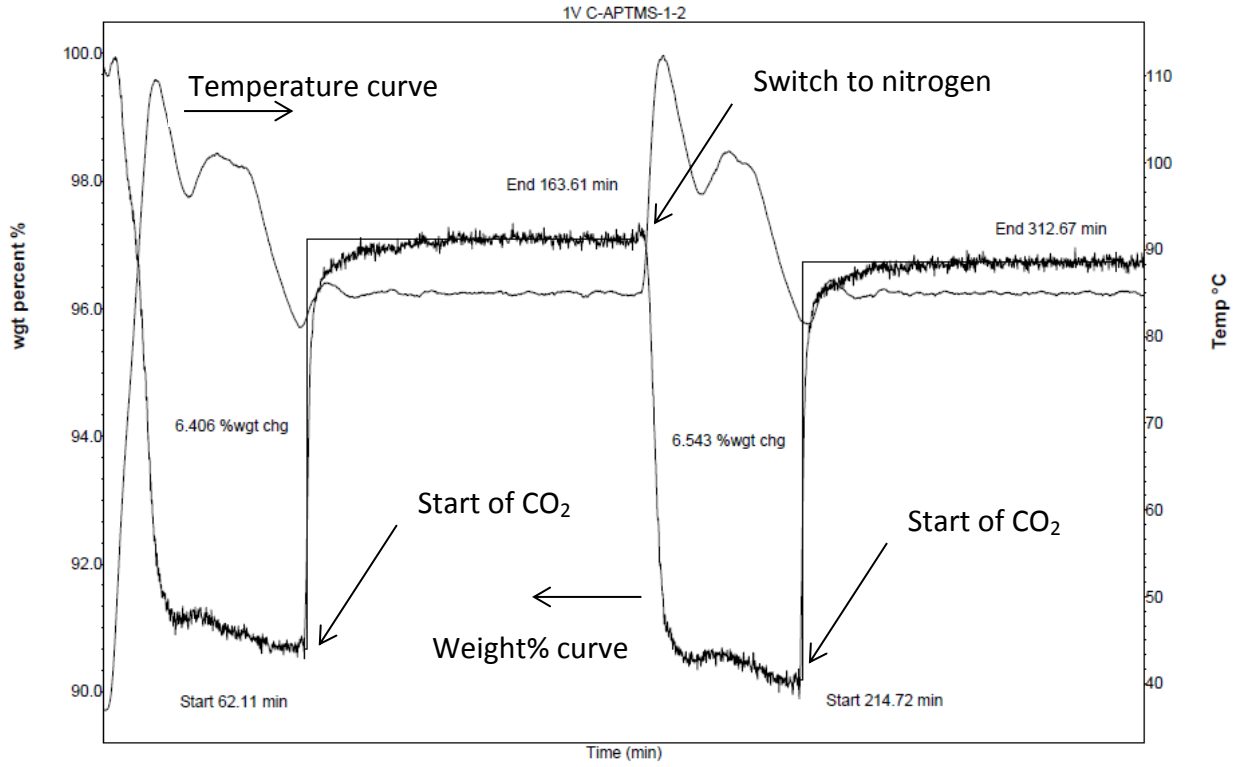

Figure 5-11: CO_2 adsorption using 10% CO_2 and 90% N_2, clay treated with APTMS

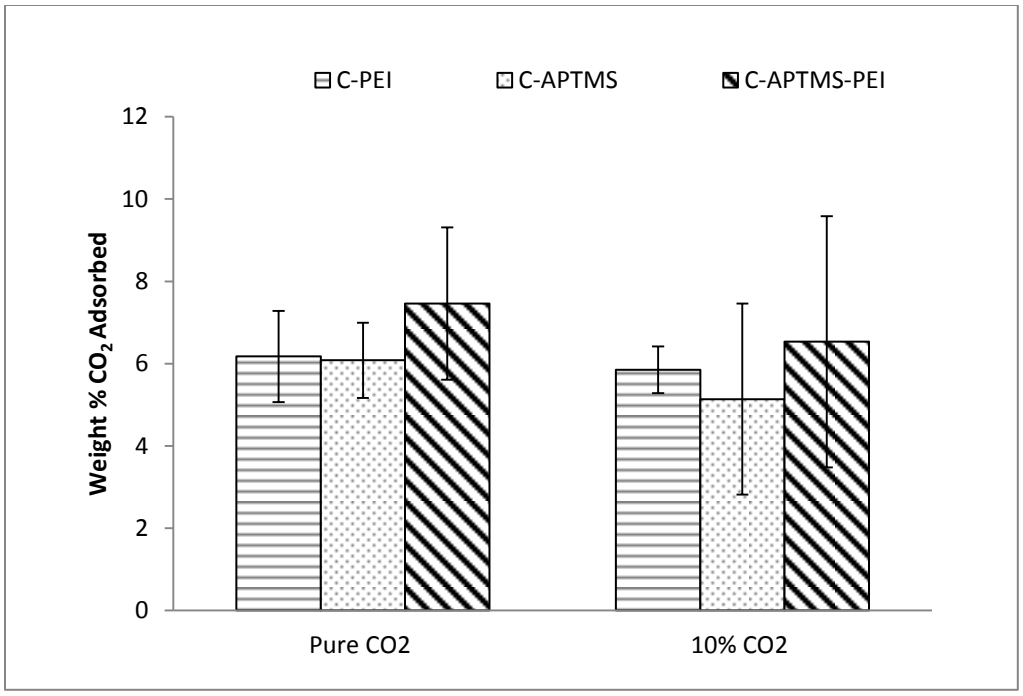

Figure 5-12: CO_2 adsorption capacity in pure CO_2 and 10% CO_2 balanced with nitrogen

Comparison of the results for all of the amine treatments for a pure CO_2 reaction stream and a reaction stream containing 10% CO_2 and 90% N_2 can be seen in Figure 5-12. From this it is evident that the adsorption capacity for all of the amine treatments was approximately the same for CO_2 adsorption in 10% CO_2 as it was with CO_2 adsorption in pure carbon dioxide. This indicates that the adsorption of CO_2 is not hindered by the presence of nitrogen. Additionally, this indicates that the adsorption of CO_2 in more realistic flue gases is possible. The ability to adsorb CO_2 in a mostly nitrogen stream is a basic requirement for all solid sorbents for post-combustion capture. The adsorbents produced in this research showed that this is possible with approximately the same adsorption capacity as in pure CO_2 stream.

5.3 Regeneration of Adsorbents using Pure Nitrogen

Regeneration of the adsorbents using nitrogen is one of the easiest ways to determine if CO_2 can be desorbed using a TGA and is one of the most widely used techniques in the

literature. Regeneration using nitrogen was carried out by heating the sample after CO_2 adsorption to 100°C for 30 minutes. Table 5-2 portrays the data for 1 cycle using nitrogen as the sweep gas. From the data in this table, it is concluded that cycling is possible with samples of clay treated with APTMS using nitrogen at 100°C, but the regeneration of clay treated with PEI and clay treated with the combination of APTMS and PEI lost some of its original CO_2 adsorption capacity on average when the samples were regenerated with nitrogen at 100°C.

Table 5-2: Regeneration using nitrogen at 100°C in a TGA

	Initial CO_2 adsorption	First cycle adsorption	Percent regeneration
C-PEI-50 Average	5.8	5.5	94%
C-PEI-50 Standard deviation	0.9	0.7	4.3%
C-APTMS-1-2 Average	6.0	6.0	101%
C-APTMS-1-2 Standard deviation	1.1	1.0	2.4%
C-APTMS-1-2-PEI-50 Average	7.6	7.3	97%
C-APTMS-1-2-PEI-50 Standard deviation	2.0	1.9	3.9%

Figure 5-13 shows the same data in Table 5-2 in a graph for a better comparison of the results. In Figure 5-13 it can clearly be seen that some of the samples had a near 100 percent regeneration in nitrogen, but on average the sample treated with PEI and APTMS+PEI had a decrease in its carbon dioxide adsorption capacity when regenerated with nitrogen.

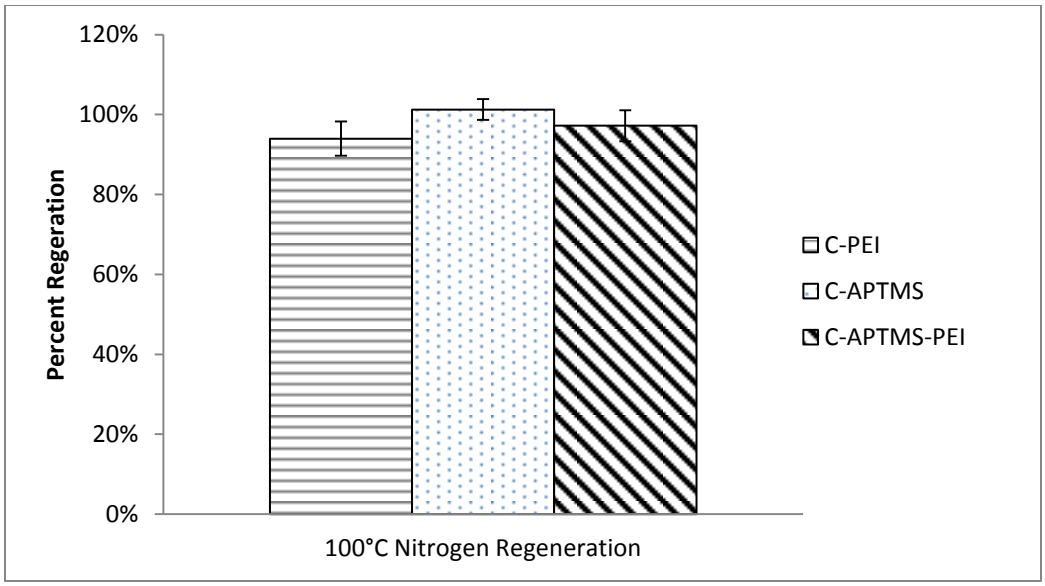

Figure 5-13: Percent regeneration using pure nitrogen at 100°C in a TGA

The regeneration of the adsorbents using pure nitrogen at 100°C showed that regeneration of the adsorbents was possible. Samples treated with only APTMS showed the best cycling capabilities with the use of pure nitrogen at 100°C. The loss in adsorption capacity of the samples treated with PEI could be from loss of PEI due to evaporation of the amine, or the slow formation of stable urea onto the adsorbent.

In order to determine the effects of multiple cycles using nitrogen as the sweep gas, an experiment with 10 cycles was conducted for each treatment. Three runs using samples with high CO_2 adsorption capacities were conducted. Figure 5-14 shows the CO_2 adsorption capacity for each treatment over 10 cycles using nitrogen at 100°C for regeneration.

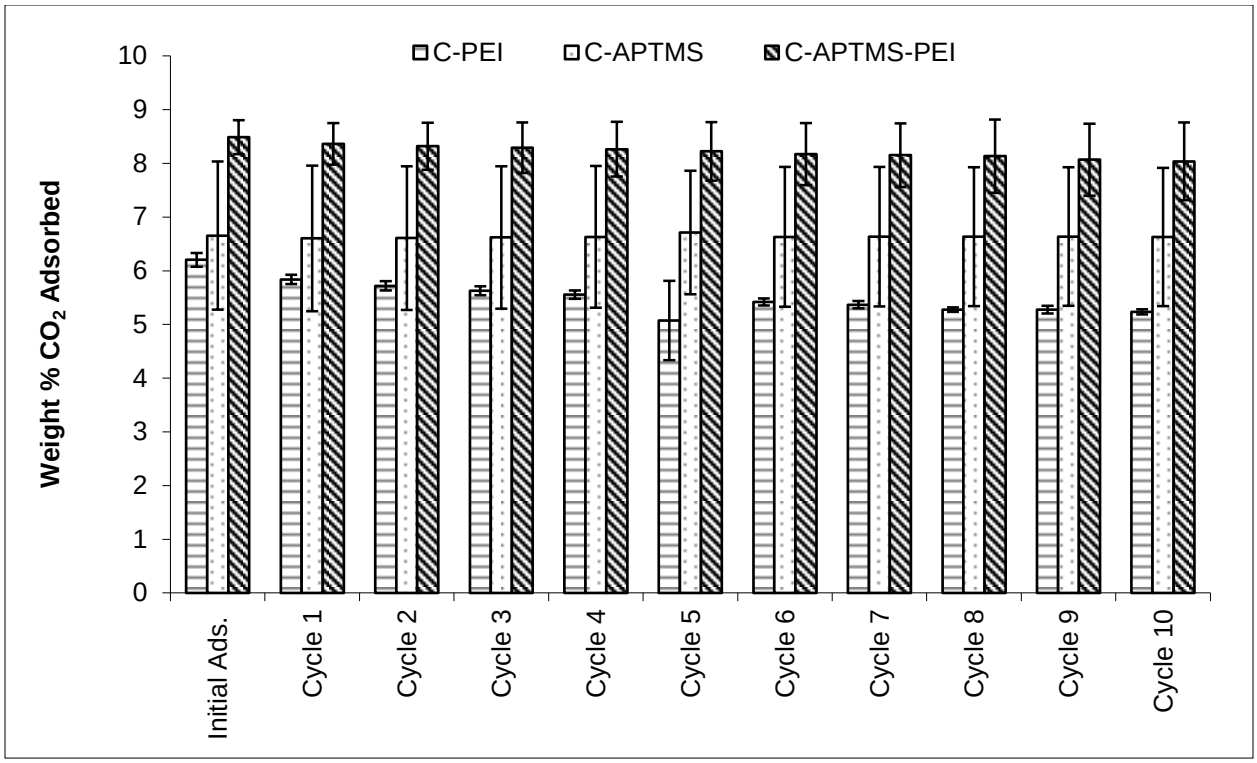

Figure 5-14: CO_2 adsorption capacity over 10 cycles

Figure 5-14 shows that there is a slight loss in the average CO_2 adsorption capacity for each treatment after the initial adsorption. The adsorption capacity for each treatment over ten cycles is reasonably constant. This would indicate that cycling of the amine treated adsorbents with little loss of CO_2 adsorption capacity is possible.

5.4 Regeneration of Adsorbents using CO_2 and Humid CO_2

One of the problems with using nitrogen as a sweep gas during regeneration is that it is not very realistic in an actual commercial setting. This is because the flue gas for a coal-fired power plant consists of a large amount of nitrogen and CO_2. Regeneration using nitrogen basically leaves one with the same composition as the initial flue stream. If a different sweep gas is to be used, one possibility is low pressure steam, which can be easily removed from the CO_2 by condensing out the water. Another possibility would be using pure CO_2 as the sweep

gas. Using CO_2 as a sweep gas would require heating the sorbent to a temperature were CO_2 is released from the sorbent. The problem with using dry CO_2 to regenerate the sorbent is that it has been reported that dry CO_2 can react with amines at high temperature to produce urea, which is difficult to remove. [60] This would reduce the amount of CO_2 adsorbed in subsequent cycles. The first experiment conducted was a temperature test on a clay sample treated with APTMS. In this test the sample was heated in pure nitrogen to 100°C for 30 minutes and then cooled to 30°C. The reaction gas was then switched to CO_2 and the temperature was increased at 2°C/minute until 350°C. Figure 5-15 is a TGA graph of this procedure.

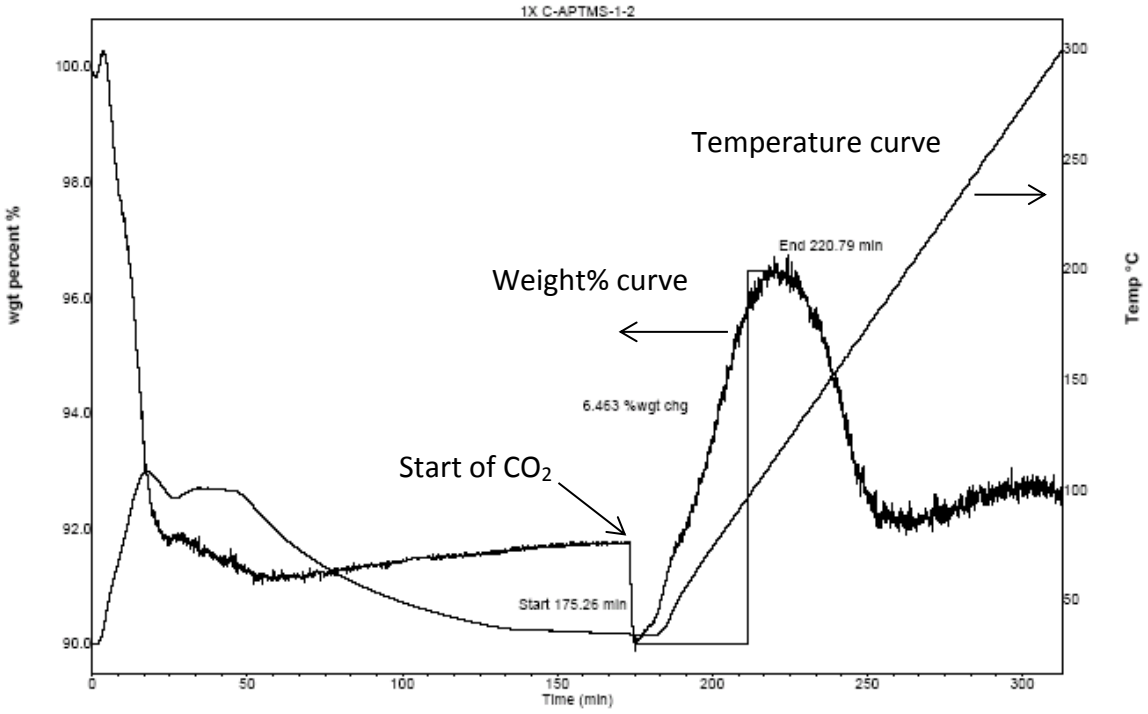

Figure 5-15: TGA graph clay treated with APTMS pure CO_2 temperature study

In Figure 5-15 the CO_2 adsorbed increased with temperature until about 100°C and then started to decrease, but eventually leveled out before returning back to the starting CO_2 adsorption weight. This would indicate that there is an irreversible reaction taking place where

some of the CO_2 that was reacted did not desorb. This phenomenon has been reported by other researchers using amines on solid sorbents. [60] This test was also conducted on a sample of clay treated with PEI, and the results are shown in the TGA curve in Figure 5-16.

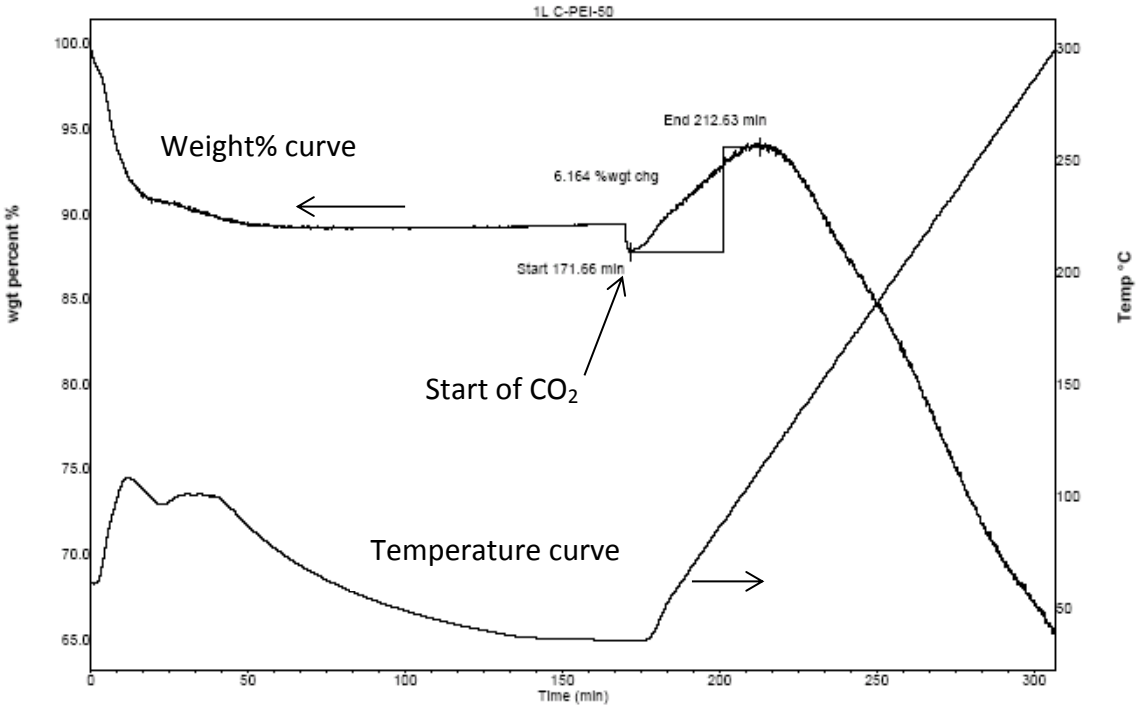

Figure 5-16: Clay treated with PEI pure CO_2 temperature study

It can be seen that the graph in Figure 5-16 differs from the graph generated with clay treated with APTMS. Once the weight begins to decrease, indicating the removal of CO_2, the weight continues to decrease with increasing temperature, without leveling. This is probably due to the loss of PEI from the sample as the temperature increases. In Figure 5-16 the temperature at which the weight loss is greater than the CO_2 adsorbed is about 155°C. Therefore, for the regeneration study in CO_2 the regeneration temperature used was 155°C.

The procedure to test the regeneration of the sorbents in pure CO_2 involved heating the sample in nitrogen to 100°C and, keeping the temperature isothermal for 30 minutes to get a

good baseline for CO_2 adsorption. The reactor was then cooled to 85°C, and the reaction gas was switched to CO_2. After the adsorption of CO_2, the reactor was heated to 155°C for 30 minutes under pure CO_2 to regenerate the adsorbent. The reactor was then cooled to 85°C for the first cycle of CO_2 adsorption. The amount of CO_2 adsorbed initially was then compared to the amount adsorbed at the end of the first cycle. Figure 5-17 is a TGA graph of sample 1AT, clay treated with PEI, using this procedure. In Figure 5-17, the initial CO_2 adsorption is 6.8 weight percent, but the amount desorbed is only 5.3 weight percent. When the temperature was reduced back to 85°C, the weight increased by 5.6%. This reduction in carbon dioxide adsorption indicates that all of the CO_2 was not removed from the sample.

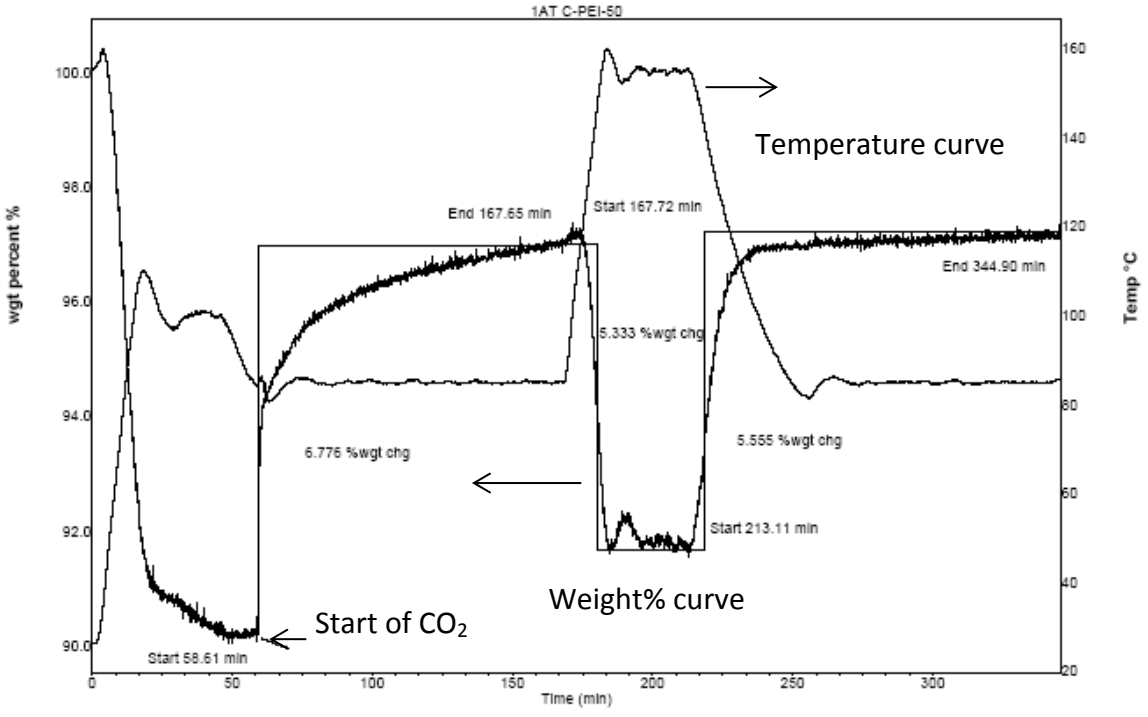

Figure 5-17: Clay treated with PEI, initially in pure nitrogen at 100°C then switched to pure CO_2 for adsorption at 85°C and desorption at 155°C

Cycling in pure CO_2 for all three treatments was conducted using a temperature of 155°C for 30 minutes, with an adsorption temperature of 85°C. The same initial step of ramping the sample to 100°C in nitrogen was still performed. The results of this experiment are given in Figure 5-18. For all three treatments, the CO_2 adsorption capacity went down with the second cycling. If this trend continued and did not stabilize after a couple cycles, which has been shown to happen in the literature with solid amine adsorbents, [59], [57] this technique would not be recommended if hundreds or thousands of regenerations were needed.

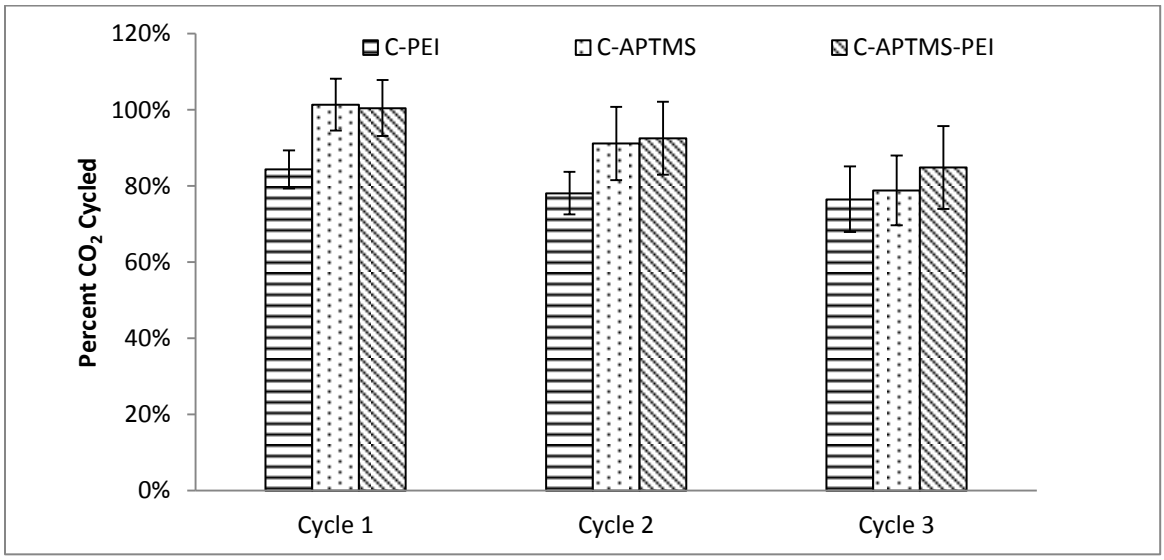

Figure 5-18: Percent carbon dioxide cycled at 85°C in the TGA using pure CO_2 at 155°C for 30 minutes for regeneration

The results in Figure 5-18 show that there is a reduction in the CO_2 adsorption capacity when cycling in pure CO_2. This would indicate that cycling in pure CO_2 is not the most ideal way to regenerate the adsorbent.

The regeneration using humid CO_2 was conducted by bubbling the reaction gas through a beaker of deionized water. The amount of water in the reaction gas was assumed by

calculating the vapor pressure at room temperature using the Antoine equation shown in Equation 5-1.

$$\log_{10}(P) = A - \frac{B}{C+T} \qquad 5\text{-}1$$

The pressure *P* is in mmHg and the temperature *T* is in degrees Celsius. *A*, *B*, and *C* are constants for water, which are 8.07131, 1730.63, and 233.426 respectively. Using this equation, the vapor pressure for water at an average room temperature of 22°C can be calculated to be 2.63 kPa, assuming atmospheric pressure and pure CO_2, the amount of water added to the reaction stream is 2.6% with the balance being CO_2. Figure 5-19 is a schematic of the setup for the addition of water to the reaction stream.

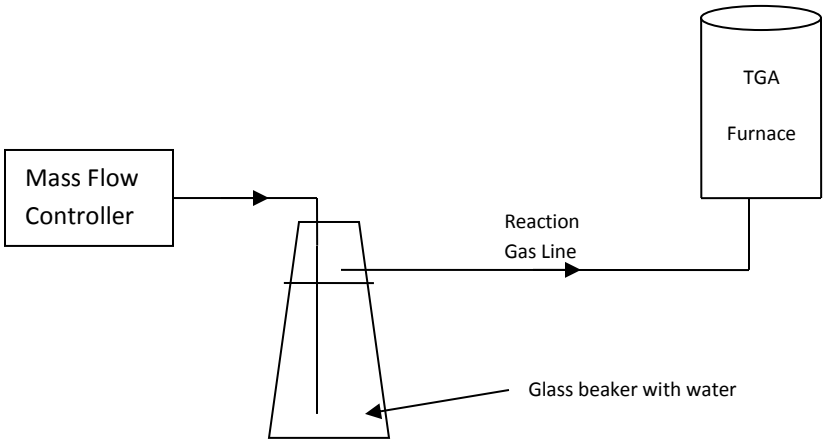

Figure 5-19: Schematic of the addition of water to the reaction gas

The regeneration of the adsorbent using humid CO_2 employed humid CO_2 over the entire run, and it was conducted at the same conditions as the regeneration using pure CO_2, which is desorption at 155°C for 30 minutes. The results for the regeneration of clay treated with APTMS, PEI, and APTMS+PEI are shown in Figure 5-20. The regeneration for clay treated

with APTMS averaged 95% regeneration over two cycles. The regeneration for clay treated with PEI also showed good results with a cycling of 95% and 92% for the first and second cycle respectively. The regeneration of samples treated with both APTMS+PEI went down to 92% over two cycles.

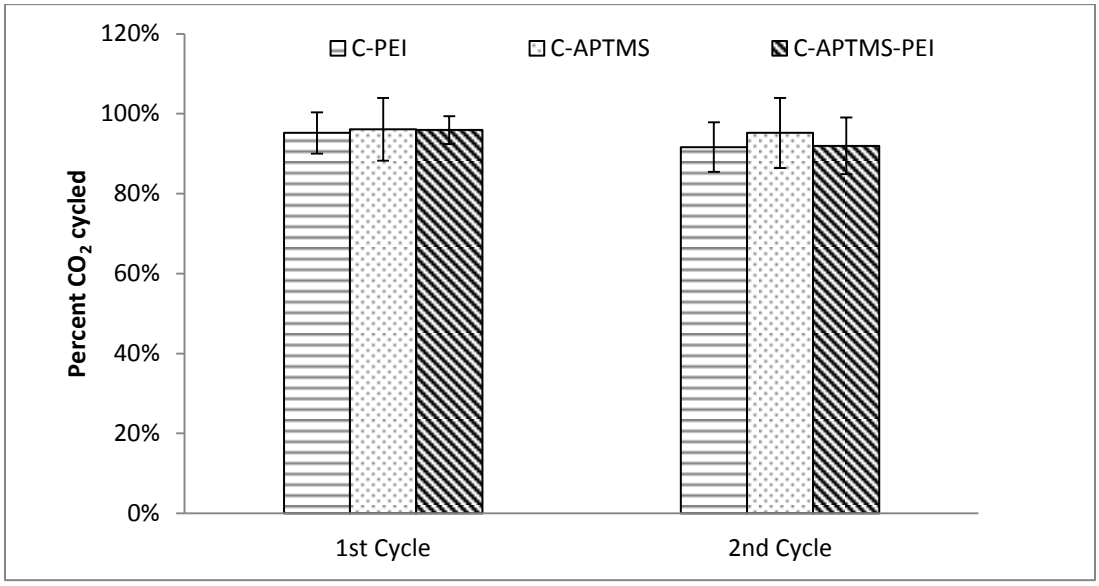

Figure 5-20: Percent CO_2 cycled using humid CO_2 at 155°C for 30 minutes

The regeneration using humid CO_2 showed some promising results. Although there was still some degradation to the adsorption capacity, the amount of water in the reaction stream was very low and increasing the percentage of water in the reaction gas might show better results similar to the literature. [57] The use of humid CO_2 showed results that are apparently better than cycling with pure CO_2, although there is some degradation to the CO_2 adsorption capacity with samples treated with PEI. This degradation could be attributed to the loss of PEI on the sample from the regeneration temperature being too close to the temperature were PEI starts to be removed from the sample.

5.5 Regeneration of Adsorbents using Vacuum

Vacuum desorption is one conceivable way to desorb a solid adsorbent in real world applications. Therefore, experiments were done to test to see if vacuum, at the same temperature as the CO_2 adsorption temperature (85°C), could remove all of the CO_2 that was adsorbed onto the adsorbent.

The first test of this hypothesis was conducted using Thermo Cahn Thermax 500 in pure CO_2 and N_2 streams. A sample of clay treated with APTMS, 1AK, was placed into the TGA, and the regular CO_2 adsorption test at 85°C was conducted. This entails a drying step in pure N_2 at 100°C for 30 minutes, then reducing the temperature to 85°C and switching the gas to CO_2. The weight gained during the adsorption step is used to calculate the weight percent CO_2 gained.

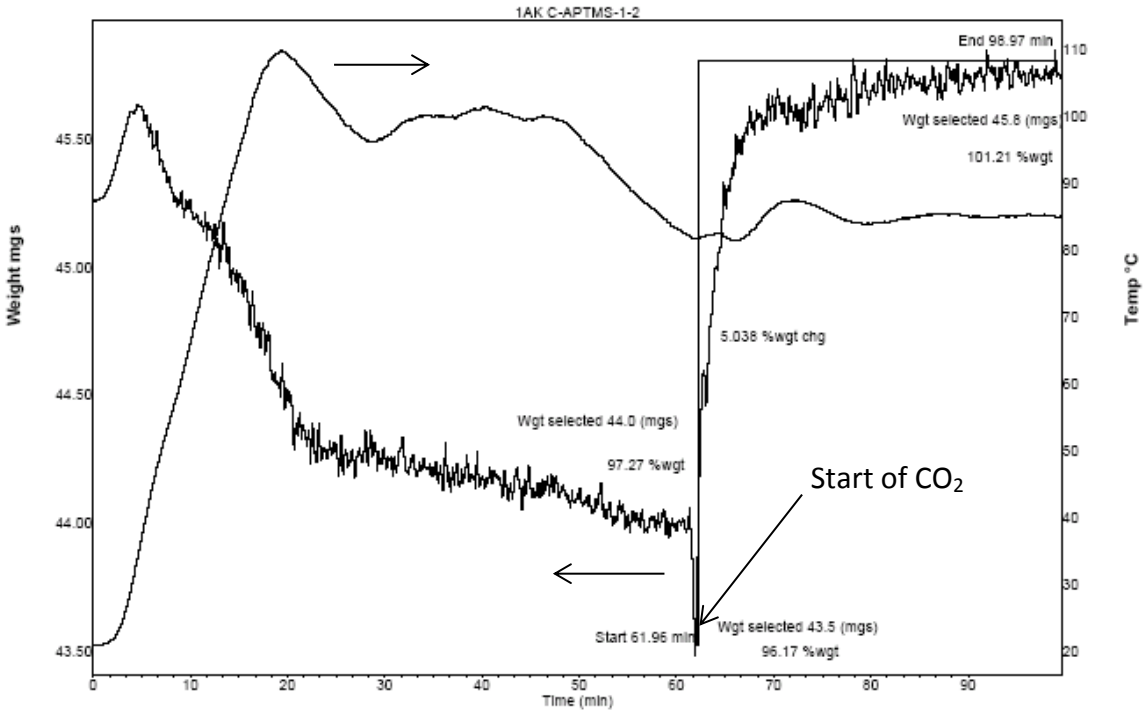

Figure 5-21: Clay treated with APTMS initial CO_2 adsorption run for vacuum study

In Figure 5-21, there is a 5.0wt% gain of CO_2 which is in the standard deviation range of samples of clay treated with APTMS at 85°C. The run was stopped because an apparent equilibrium had been reached. The sample was then removed and weighed in the balance to confirm the weight after the TGA run. The sample was then placed into the vacuum oven at 85°C for 1 hour under vacuum with a gauge reading of 93kPa. Table 5-3 shows the results of the weight of the sample before and after the TGA run and after vacuum at 85°C for 1 hour. The weight after the drying step in N_2 is assumed to be the weight of the adsorbent that has no CO_2 adsorbed onto it. Therefore, the target weight after removing the sample from the vacuum oven was 44.0mg. The weight after removing the sample from the vacuum oven was 43.27mg. The weight of the sample after removing from the vacuum oven however was rising very quickly and the weight after only 1 minute was 43.84. This rapid increase in the weight is thought to come from water condensing onto the sample or the pan as it cools to room temperature. The sample was then placed into the TGA for adsorption of CO_2 to determine the CO_2 adsorption capacity after vacuum desorption of the sample.

Table 5-3: Weight of clay treated with APTMS during different steps of the vacuum study

	Weight (mg)
Initial Sample Weight	45.256
Sample weight after N_2 drying step in TGA	44.0
Sa. Wt. after gas switch to CO_2 in TGA	43.5
Sa. Wt. after CO_2 adsorption reached Eq.	45.8
Sa. Wt. 1 min after 1st vacuum desorption	43.84
Weight after gas switched to CO_2 2nd TGA run	43.7
Weight after CO_2 adsorption 2nd TGA run	45.35

After the sample was run in the TGA it was then weighed again in the balance to confirm the weight in the TGA. Again the weight was increasing quickly on the balance. After 10 minutes

the sample was weighed again and placed back into the vacuum oven at 85°C and 93 kPa overnight for 17 hours. The sample was then weighed in the balance to compare and measure the decrease in weight during the vacuum regeneration step. This long desorption time was conducted for more than one reason. First to simulate the effects of many regenerations of the sample using vacuum regeneration, and second to see if the longer desorption time removed any more CO_2 or H_2O that could have reduced the CO_2 capacity of the sample after the first vacuum run of 1 hour. To determine if any desorption was taking place in the TGA not attributed to the desorption in the vacuum, the weights of sample when it was initially placed into the TGA were compared to the weight just before the reaction gas was switched to CO_2. Figure 5-22 is a TGA graph of a sample of clay treated with APTMS, 1AK, after the second vacuum desorption step of 17 hours at 85°C.

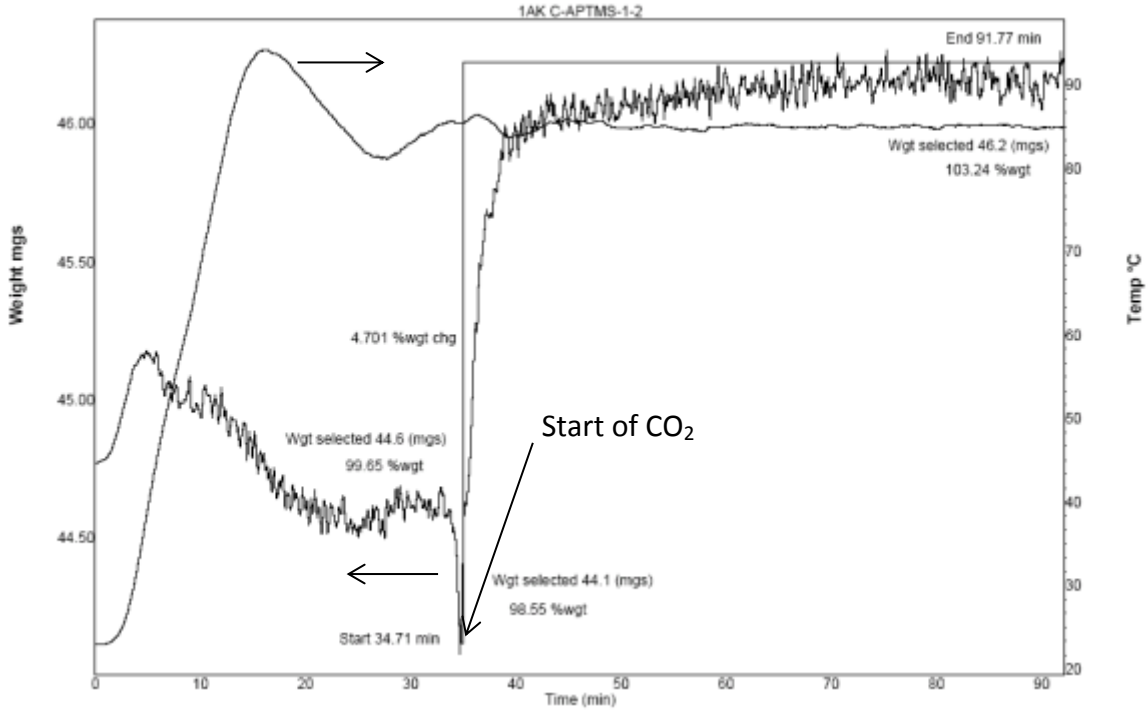

Figure 5-22: TGA graph of clay treated with APTMS after the 2nd vacuum desorption step

In Figure 5-22 it can be seen that there is very little weight loss during the ramping step to the reaction temperature of 85°C. This indicates that all of the CO_2 desorption occurred during the vacuum desorption step and not in the TGA.

The second sample that was studied was clay treated with PEI. The same procedure was performed on this sample. There was an initial TGA run conducted with a drying step in N_2 at 100°C, then the temperature was reduced to 85°C and the reaction gas was switched to CO_2 to calculate the amount of CO_2 adsorbed onto the sample. The sample was then weighed and placed into the vacuum oven at 85°C and 93kPa for 1hour. The sample weight was recorded and the sample was placed into the TGA with a N_2 purge.

The TGA procedure after the first and second vacuum was the same for this sample and consisted of ramping the sample in N_2 to 85°C then switching the reaction gas to CO_2. Table 5-4 is a comparison of the weight of the sample at the beginning of the run compared to the weight of the sample right before the reaction gas was switched to CO_2.

Table 5-4: Comparison of the beginning TGA weight with the TGA weight right before the reaction gas was switched to CO_2

C-PEI-50	Beginning TGA weight (mg)	TGA weight (mg) before switching to CO_2
1st TGA run base run	39.4	36.5 (93% of beginning TGA wt)
2nd TGA run after 1st vac 1hr	34.6	34.6 (100% of beginning TGA wt)
3rd TGA run after 2nd vac 17hr	33.2	33.2 (100% of beginning TGA wt)

In Table 5-4, the weight in the 1st TGA run is reduced by 7% before the reaction gas is switched to CO_2 this is expected because it is assumed that water and or CO_2 is adsorbed onto the sample while it is stored before the TGA run. Also, in the base run the sample is

intentionally dried at 100°C in N_2 for 30 minutes to establish a baseline for CO_2 adsorption. In the TGA runs after the vacuum desorption studies, one would not want any drying or desorption occurring while the TGA is ramping to the reaction temperature of 85°C, because the effect of desorption due to vacuum is being studied. Therefore, since there is no overall reduction or gain in weight during the ramping to 85°C in N_2, one can assume that the TGA procedure is a relatively good one to study the effects of vacuum desorption. Table 5-5 is a comparison of the CO_2 adsorption capacities of a sample of clay treated with PEI during the vacuum study.

Table 5-5: Sample of clay loaded with 50% PEI comparison of CO_2 adsorption capacities

C-PEI-50	CO_2 adsorption capacity (wt %)
1st TGA run base run	5.2
2nd TGA run after 1st vac 1hr	5.4 (104% of initial)
3rd TGA run after 2nd vac 17hr	4.7 (90% of initial)

The CO_2 adsorption capacity after the first vacuum run compares very well with the initial value indicating that the vacuum completely desorbs all of the CO_2 from the sample. The CO_2 adsorption capacity after 17 hour vacuum treatment is reduce to 90% of the initial capacity indicating there might be some degradation to the sample, probably due to loss of amine or some other mechanism. Figures 5-23 and 5-24 are the TGA graphs for sample clay treated with PEI during the vacuum study. Figure 5-23 shows then initial CO_2 adsorption at 85°C for clay treated with PEI. Figure 5-24 shows the CO_2 adsorption of clay treated with PEI after one hour vacuum desorption at 85°C. Figure 5-24 shows very little weight difference of the sample during the heating to 85°C in nitrogen. This indicates that all of the desorption was due to the vacuum desorption step.

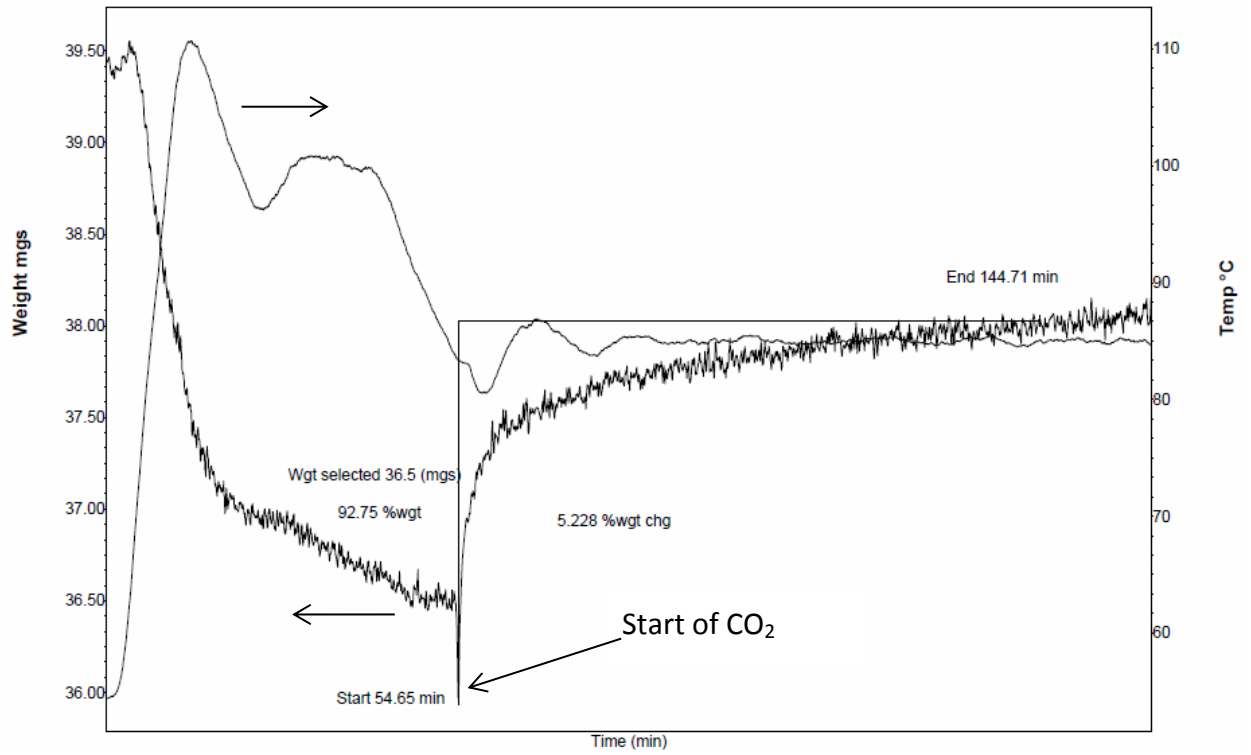

Figure 5-23: TGA graph of clay treated with PEI initial CO_2 adsorption at 85°C

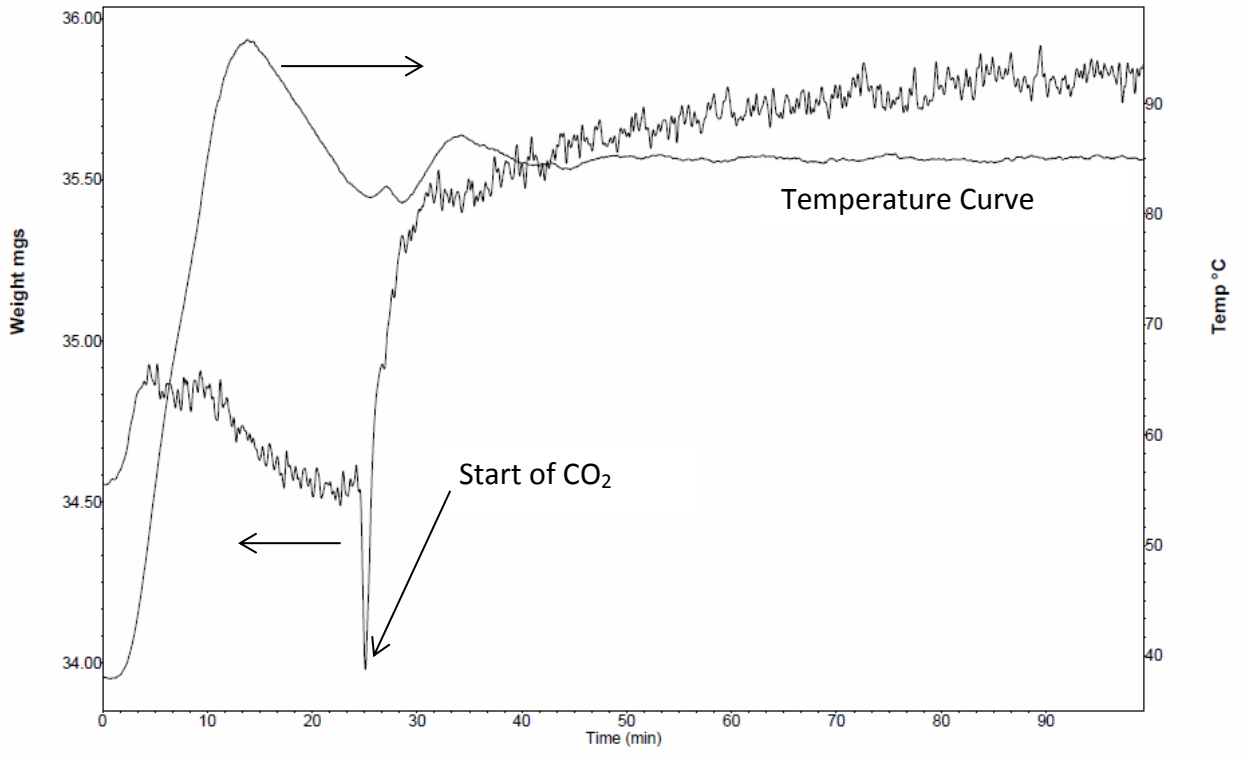

Figure 5-24: TGA graph of clay treated with PEI after first vacuum desorption step

This procedure was utilized on all of the treated samples to confirm the data. Figure 5-25 is a graphical representation of the regeneration using vacuum desorption with CO_2 adsorption at 85°C in the TGA. It shows that regeneration with vacuum at 85°C and 93kPa is possible for cycling the treated adsorbents. After the first regeneration using vacuum at 1 hour, it can be seen that there is apparently very little degradation for the treated samples. The CO_2 adsorption capacity for the samples treated with APTMS decreased the most. Two reasons for this are that the desorption time in the vacuum was not long enough to desorbed all of the CO_2 or the samples are being degraded. After the 17 hour vacuum desorption step the CO_2 adsorption capacity for the samples treated with APTMS went up. This indicates that the desorption time might need to be increased above 1 hour for samples treated with APTMS to achieve the best cycling CO_2 adsorption capacity. Additionally, this indicates that samples treated with APTMS are possibly stable to vacuum desorption for potentially 17 cycles. The samples treated with PEI and the combination of APTMS and PEI had a decrease in the CO_2 adsorption capacity after the 17 hour vacuum desorption step. This means there is probably some degradation to the samples probably caused by the loss of amines from the support. For clay treated with only PEI the sample showed very little degradation during the first one hour vacuum cycle, but after 17 hours the regeneration was only 86.6% indicating that the sample does not return to its original CO_2 adsorption capacity over 17 hours vacuum at 85°C. This is not completely unexpected since the PEI is not covalently attached to the clay as APTMS is.

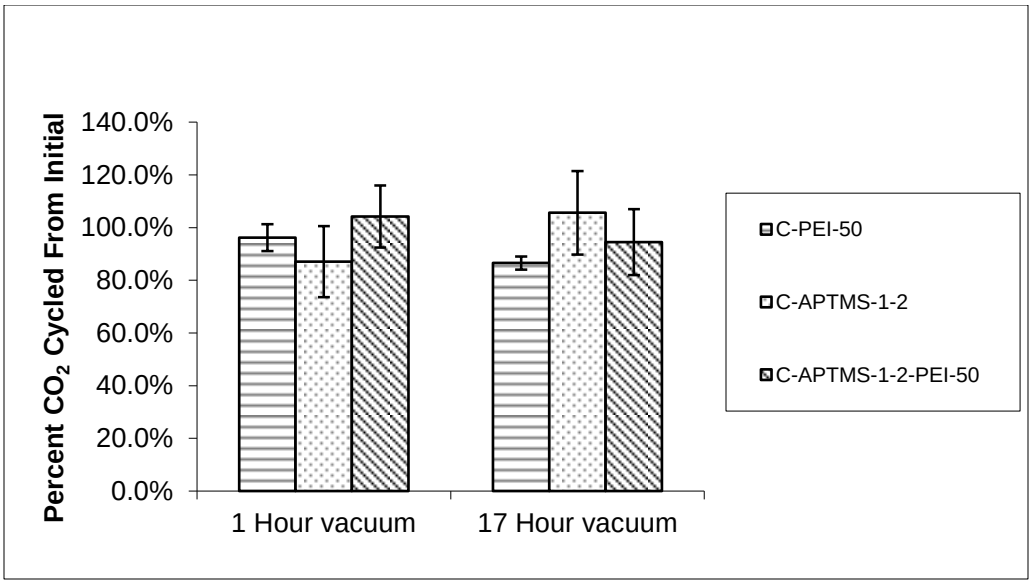

Figure 5-25: Vacuum regeneration results for 85°C vacuum desorption in the vacuum oven

In summary, vacuum desorption at 85°C and 93kPa showed some interesting results for the amine treated clays. Clay treated with APTMS was interesting in the fact that the first regeneration showed a reduction in CO_2 capacity to 87.1% of the original, but after 17 hours the CO_2 capacity went above 100% of the original capacity. This would indicate that the regeneration time of 1 hour might not be enough time for the sample to fully regenerate, and the sample is not degraded by a desorption time of 17 hours in the vacuum oven. Samples treated with PEI and the combination of PEI and APTMS had a cycle adsorption capacity near 100% after the first vacuum desorption for 1 hour, but had an average decrease in the CO_2 adsorption capacity after the 17 hour vacuum step. This indicates that there might be some loss of the amines or degradation to the sample during long vacuum regeneration at 85°C

5.6 CO_2 Adsorption at High Pressure

CO_2 adsorption at an elevated pressure was also conducted to see if an increase in pressure had any effect on the adsorption capacity of the adsorbent. If there is enhanced adsorption capacity or different properties at different pressures, there could be other possible

applications for the treated adsorbents. The procedure for the pressure vessel tests were described in the experimental procedures section. The pressure that was used was varied from 40 psi to 300 psi. 300 psi was chosen because it is close to the pressure that is used in IGCC processes. The lower pressures were chosen to determine the pressure were the adsorption of CO_2 reaches a maximum and is no longer dependent on pressure increases. A soak time of 2, 16, and 24 hours was used to determine the effect of adsorption time on the adsorption capacity and to insure that equilibrium was reached.

The results for clay treated with APTMS are given in Figure 5-26. In Figure 5-26 it can be seen that within experimental error, that, the adsorption capacity is not significantly affected by the pressure or the adsorption time. This would indicate that a two hour adsorption time is sufficient to achieve the maximum CO_2 adsorption on the sample treated with APTMS. Additionally, the CO_2 adsorption capacity for all of the different pressures and time averages to 6.93 weight percent which is only slightly higher than the average adsorption capacity of the clay treated with APTMS in the TGA at 85°C. This would indicate that the sorption of CO_2 on clay treated with APTMS is not physically absorbed but is chemical reacted onto the sample. Figures 5-26 and 5-27 are the results for untreated clay, clay treated with PEI and clay treated with APTMS+PEI.

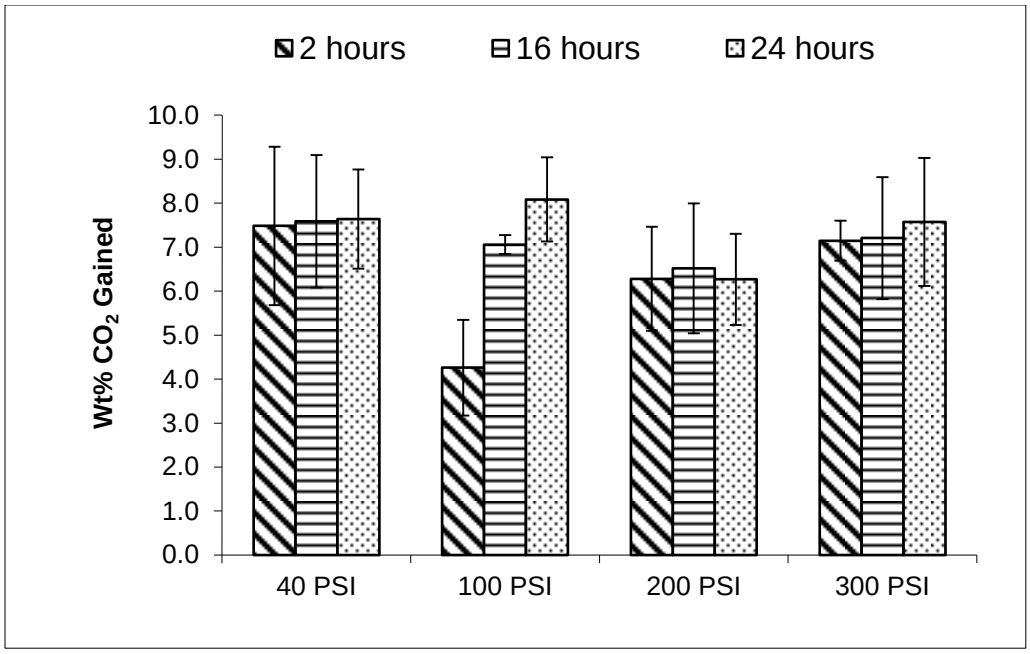

Figure 5-26: CO_2 sorption at pressure using clay treated with APTMS

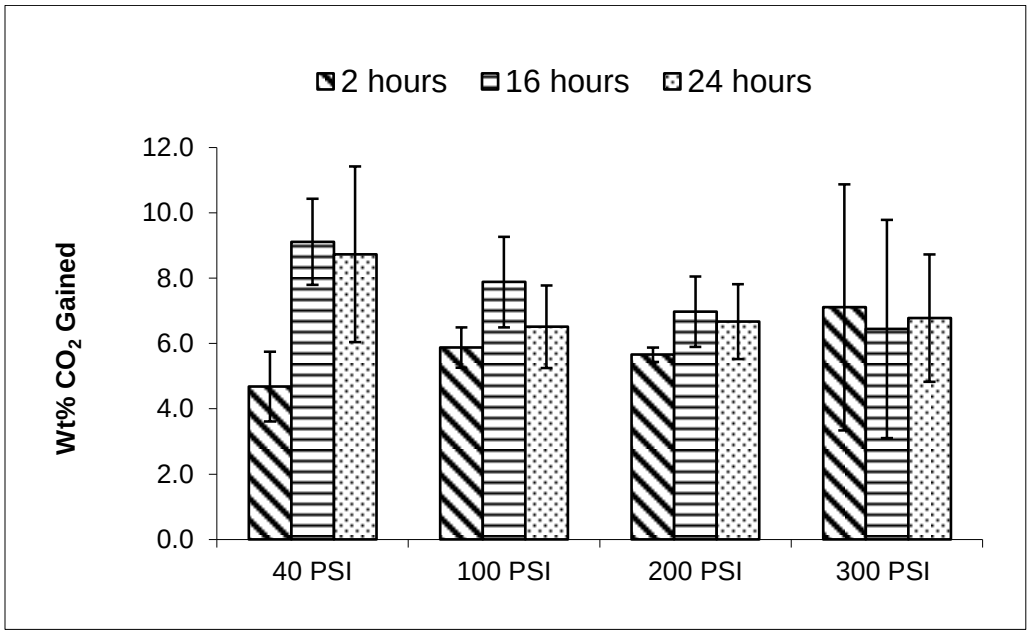

Figure 5-27: CO_2 sorption at pressure using clay treated with PEI

Figure 5-27 shows the CO_2 adsorption at pressures from 40-300psi with adsorption times of 2-24 hours. Again there is not a significant difference in the amount of the overall CO_2 adsorption capacity with the changing of pressure and soak time. This is somewhat surprising

since in the TGA adsorption profile for samples of clay treated with PEI there seemed to be some diffusion controlled reactions towards the end of the adsorption step. In Figure 5-28 the adsorption of pure CO_2 at high pressure can be seen for samples treated with the combination of APTMS and PEI. Similarly to the samples treated with only APTMS and PEI, there is not a significant difference in the adsorption capacity with the change in pressure. There is possibly a change in the CO_2 adsorption capacity at 40psi with increasing adsorption times. This would indicate that the CO_2 adsorption equilibrium might not be reached with only a 2 hour adsorption time.

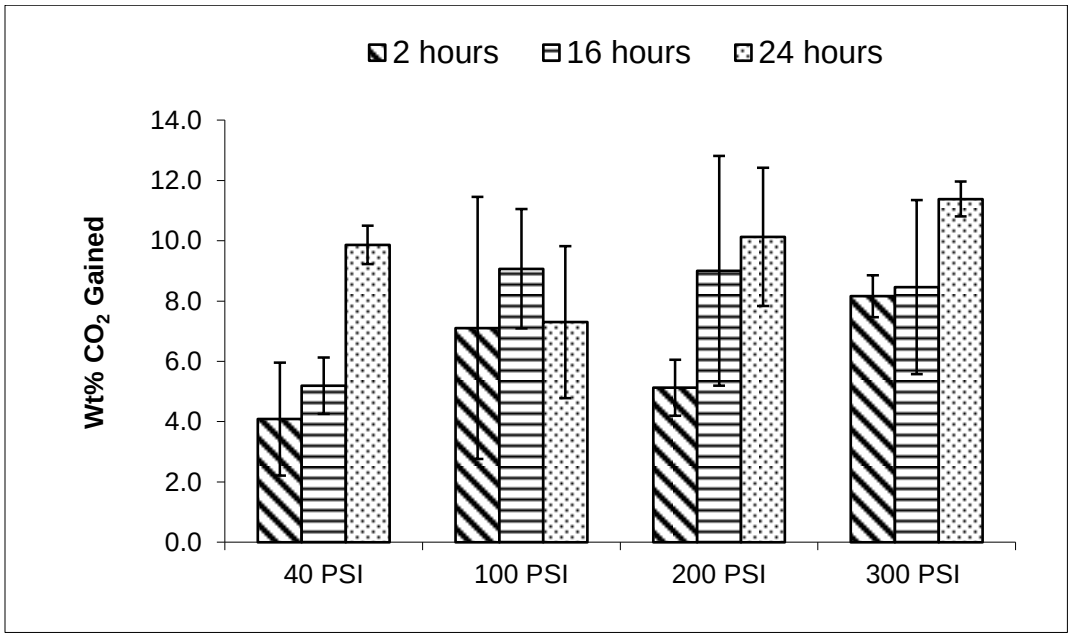

Figure 5-28: CO_2 sorption at pressure using clay treated with APTMS+PEI

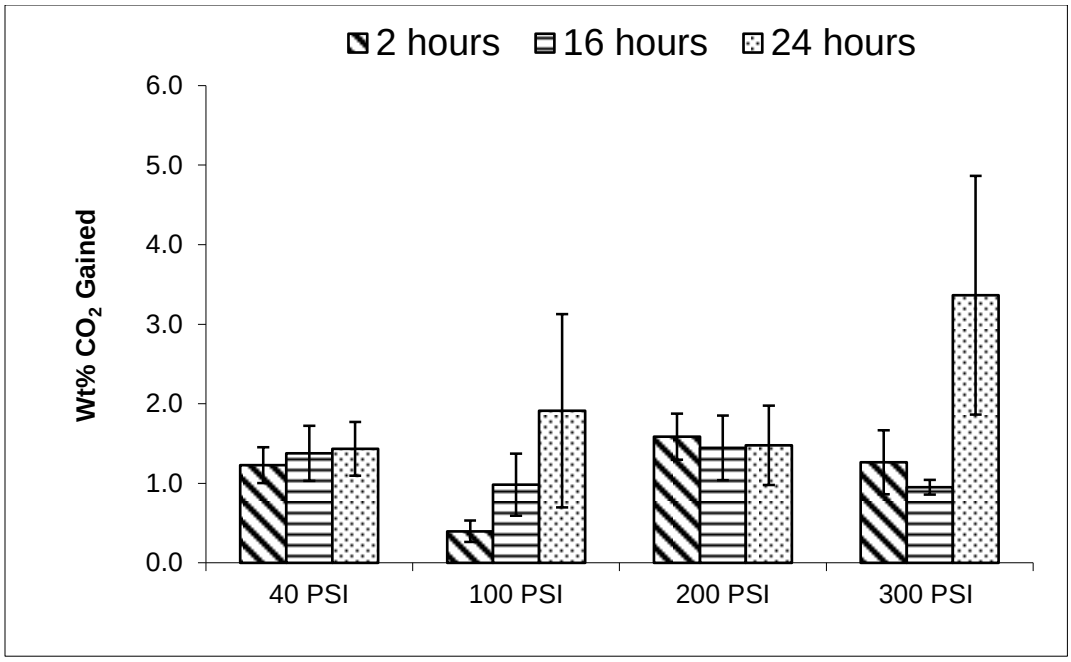

Figure 5-29: CO_2 sorption at pressure using untreated clay

Similarly to the TGA results, the untreated clay adsorbed very little CO_2; see Figure 5-29 this would suggest that the amine treatments had an important role in increasing the CO_2 adsorption capacity of the clay. The results for each treatment showed that using this method for testing the CO_2 adsorption capacity at elevated pressure, there is not significant dependence on the pressure of the CO_2 to the adsorption capacity of the adsorbent. A comparison of all the clay treatments at 24 hours is given in Figure 5-30.

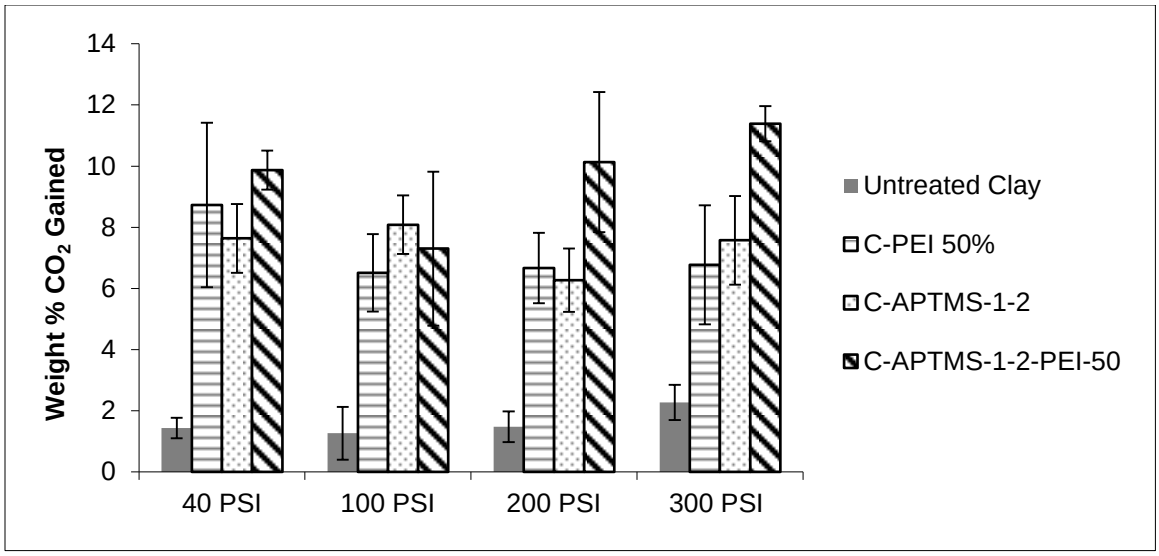

Figure 5-30: CO_2 sorption at different pressures with 24 hours adsorption time

The results shown in Figure 5-30 demonstrate that the highest average adsorption capacity is obtained with the clay treated with APTMS+PEI at 300 psi. The adsorption capacity is 11.36 weight percent and is higher than the adsorption capacity of clay treated with APTMS+PEI at 85°C, which averaged 7.2 weight percent with a maximum adsorption capacity of 9.7 weight %. The adsorption results show that there is a slight increase in the adsorption capacity of CO_2 in pure CO_2 at high pressure, but does not indicate that there is a significant increase in sorption capacity with increasing pressure. This indicates that the increase in CO_2 capacity due to the physical absorption at high pressures is small.

5.6.1 CO_2 Adsorption at High Pressure with Increasing Temperature

The TGA results suggested that there was an increase in the CO_2 adsorption capacity with an increase in temperature to 85°C. Therefore, it was decided to study the effects of temperature on the adsorption capacity at a pressure of 300psi for 24 hours. This time and pressure were chosen because 300psi is close to the adsorption pressure of an IGCC plant and a 24 hour adsorption time would help ensure that equilibrium was reached.

The detailed procedure for conducting the experiments is described in the experimental section. Using the ideal gas law, the pressure vessel was calculated to have a final pressure of 300psi. The modified ideal gas law used to calculate the pressure is shown in Equation 5-2

$$\frac{P_2}{T_2}T_1 = P_1 \qquad 5\text{-}2$$

Where P_2 is the pressure in the pressure vessel at the adsorption temperature. T_2 is the adsorption temperature studied, T_1 is the room temperature, and P_1 is the calculated pressure that is placed into the pressure vessel.

The samples were placed into the pressure vessel and the then the pressure vessel was placed into a water bath in the oven at a set temperature. The water bath was used to better maintain a constant temperature. The first temperature studied was 50°C to determine if temperature had any effect. The results of this experiment are shown in Figure 5-31.

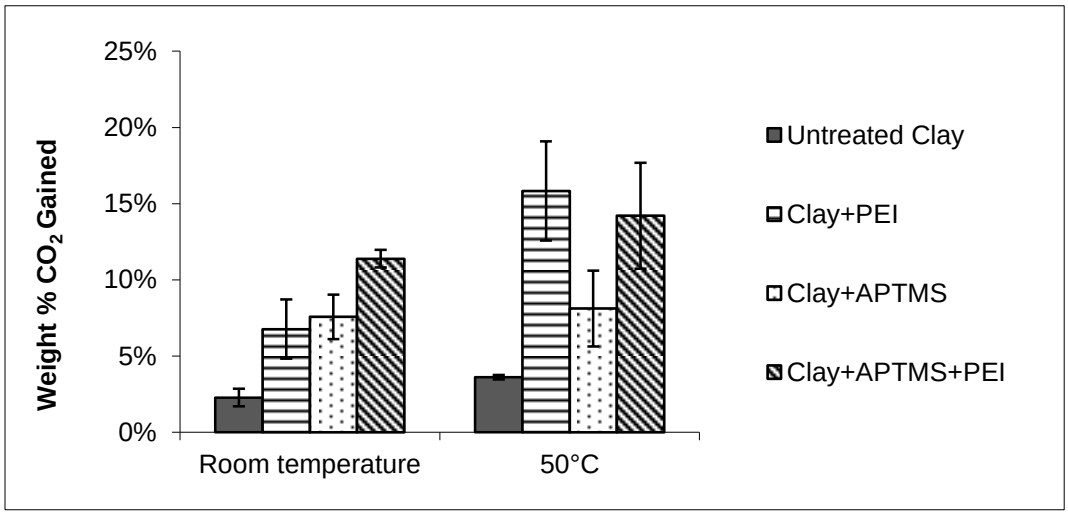

Figure 5-31: CO_2 adsorption at 300psi for 24 hours at room temperature and at 50°C

The results indicate that there is an increase in the adsorption capacity of the samples treated with PEI, and this is similar to the results obtained at atmospheric pressure using TGA.

The adsorption capacity of the untreated clay and the clay treated with APTMS was not significantly affected by the increase in temperature. Additionally, there is not a significant difference in the CO_2 adsorption capacity in the samples treated with the combination of PEI and APTMS over the samples treated with PEI. The increase in adsorption capacity for the samples treated with PEI is assumed to be due to the same reason as the increase shown in the TGA. In the literature, it is suggested that the CO_2 reacts with the surface PEI but then there is resistance to the amount of CO_2 that can diffuse into the PEI. Increasing the temperature helps expand the PEI and promote diffusion which increases the CO_2 adsorption capacity. Therefore, even at 300psi for 24 hours increasing the temperature increases the CO_2 adsorption capacity.

Since the adsorption capacity increased for samples treated with PEI, tests were conducted at 75°C and 85°C to determine if there is a higher increase in the CO_2 adsorption capacity. Figure 5-32 displays the results of the CO_2 adsorption capacities at higher temperatures using 300psi and a 24 hour adsorption time.

In Figure 5-32 it can be seen that the adsorption capacity for the untreated clay and the clay treated with APTMS had very little change in the adsorption capacity with increasing temperature. The adsorption capacity for clay treated with PEI and the combination of PEI had an increased adsorption capacity for at 50-85°C compared to room temperature. The difference in adsorption capacity between 50°C, 75°C and 85°C was small compared to the difference at room temperature. This would indicate that with increasing the adsorption temperature above 50°C there is not a significant increase in the CO_2 adsorption capacity.

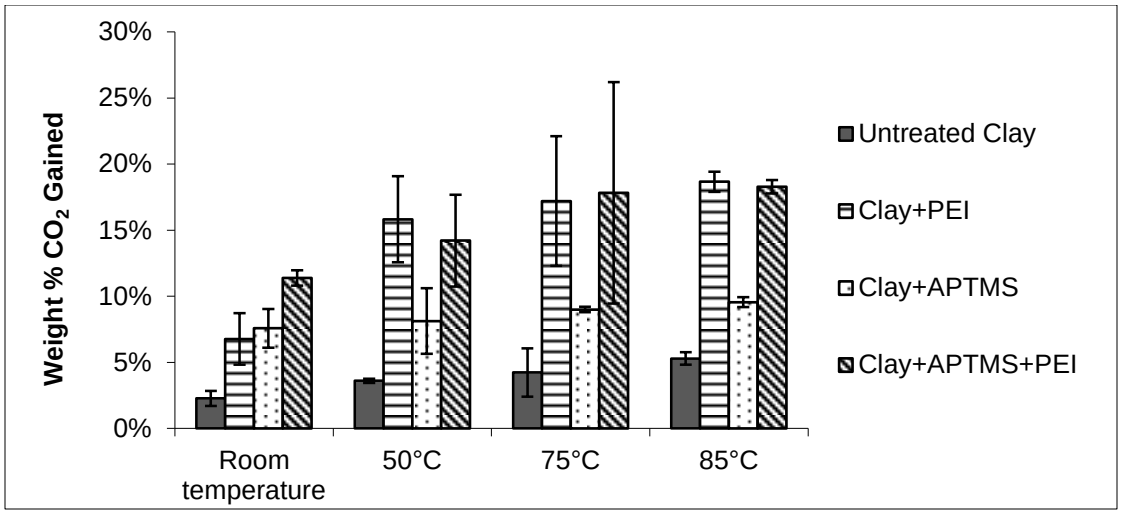

Figure 5-32: Temperature comparison at 300psi for a 24 hours adsorption time

The results for the CO_2 adsorption capacity with increasing temperatures at 300psi and a 24 hours adsorption time showed that there was an increase in the adsorption capacity for samples treated with PEI. The adsorption capacity did not significantly change for the untreated clay and the clay treated with APTMS. This was expected since there seemed to be no diffusion issues with APTMS treated samples and the untreated clay has very little CO_2 adsorption capacity. The samples treated with only PEI had approximately the same amount of CO_2 adsorption as the samples treated with the combination of APTMS and PEI. There also was not a significant difference in the adsorption capacities when increasing the temperature above 50°C. This would indicate that the increase in the diffusion of CO_2 with increasing temperature, as previously seen in the TGA results, does not have a significant effect in the high pressure results. This would suggest that at 300psi and a 24 hour adsorption time at temperatures above 50°C there is not a signification additional amount of CO_2 that can diffusive into the PEI and react with amines.

5.6.2 Regeneration Using Vacuum

Three samples of clay treated with APTMS, PEI, and APTMS+PEI were weighed and placed into the vacuum oven for 2hours at 85°C at 93kPa in order to get a baseline weight for vacuum regeneration. The samples were then removed and placed into the pressure vessel. Pure CO_2 at 300 psi was contacted with these samples for 2hours. The amount of CO_2 adsorbed was calculated by measuring the weight difference between the sample weight before and after the exposure to CO_2. The samples were then placed back into the vacuum oven to study desorption of the CO_2 in the vacuum oven. The samples were subsequently weighed and placed into the CO_2 pressure vessel. The amount of CO_2 adsorbed was then compared to the original amount of CO_2 adsorbed. Figure 5-33 shows the CO_2 adsorption capacity of the samples tested in this manner. The adsorption capacities for each treatment are in the range that was calculated during the adsorption tests. The percent weight that is desorbed in the vacuum oven compared well to the initial CO_2 adsorption, but after calculating the amount of CO_2 that is adsorbed after the vacuum regeneration onto the sample, the capacity for CO_2 adsorption was found to have gone down for all three treatments.

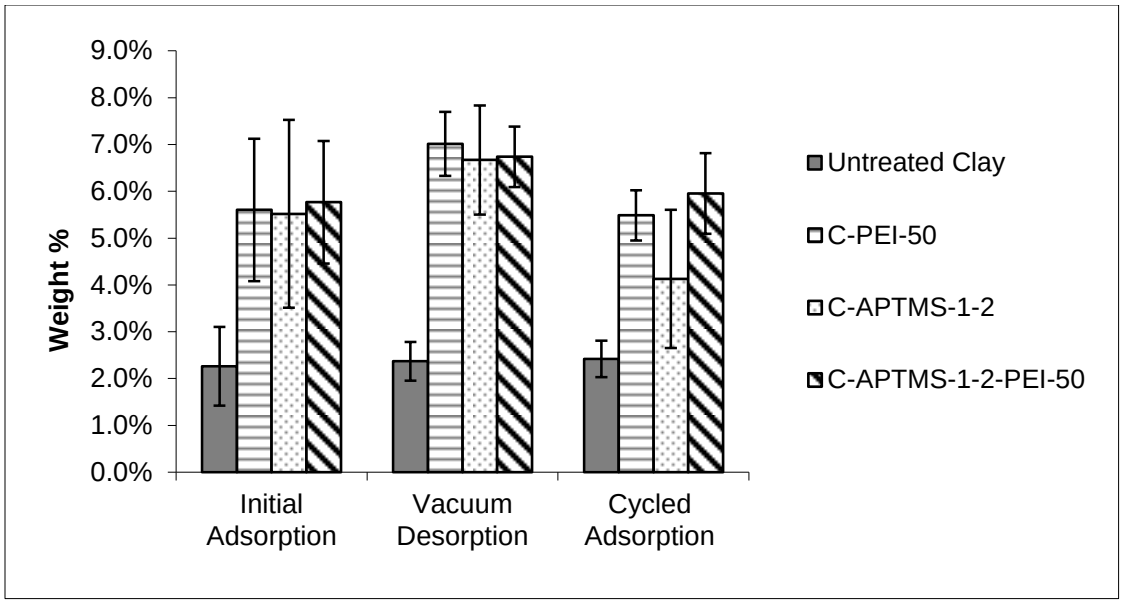

Figure 5-33: Weight percent CO_2 adsorbed at 300 psi for at least 2 hours and weight percent desorbed under vacuum at 85°C at 93kPa

In Figure 5-33 one can see that the weight desorbed was greater than the amount of weight gained during the initial CO_2 adsorption. This would indicate that all of the CO_2 was removed during the vacuum regeneration. Additionally, the second CO_2 adsorption capacity should be the same as the initial adsorption capacity. However, the second CO_2 adsorption was not equal to the initial adsorption capacity, indicating that some degradation of the sample is occurring or all of the CO_2 on the sample is not being removed. It is also interesting to note that the clay treated with the combination of APTMS and PEI preformed the best in terms of the CO_2 cycling. The decrease in the adsorption for clay treated with PEI might be because some of the PEI is being evaporated during the vacuum cycling step. The untreated clay had a small amount of CO_2 adsorption but did have the same amount of CO_2 adsorption after the vacuum regeneration.

Vacuum regeneration was also tried on the samples exposed to CO_2 at 50°C and 300psi for 24 hours. This was done to confirm that increased CO_2 adsorption capacity seen for the PEI samples at 50°C could also be regenerated. The same vacuum regeneration procedure was used as before with 1 hour desorption at 85°C in the vacuum oven. The results are shown in Figure 5-34. The concern with exposing the treated clay samples to 50°C pure CO_2 at 300psi for 24 hours was the possible formation of urea that could not be regenerated using vacuum at these conditions. This would cause a reduction in the adsorption capacity during cycles.

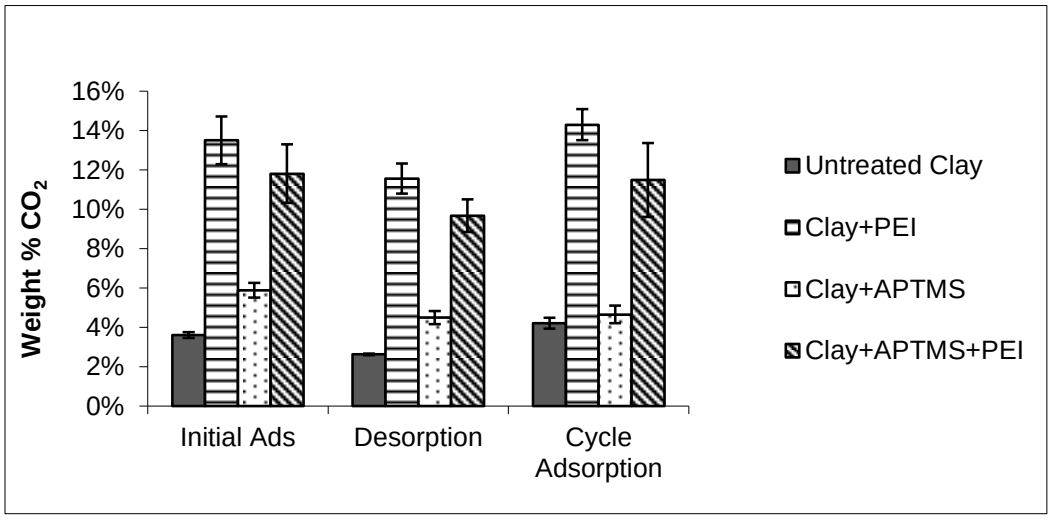

Figure 5-34: Vacuum regeneration with adsorption at 50°C at 300psi

The results shown in Figure 5-34 demonstrate that vacuum can desorb the CO_2 after exposure to 50°C pure CO_2 at 300psi for 24 hours. The adsorption capacity did not change significantly during the second adsorption after the vacuum desorption step. These results show that vacuum desorption is a possible regeneration method for samples exposed to high pressure CO_2.

5.7 Stability of the Adsorbent after Long Exposure to Water Vapor

In order for a CO_2 adsorbent to be applicable to real flue gas adsorption applications, the adsorbent must be regenerated numerous times. This has been studied in the previous sections using temperature swing adsorption (TSA) and nitrogen as a sweep gas. Using nitrogen as a sweep gas is an easy technique in the lab to study feasibility, but to have an industrially relevant adsorbent, the sweep gas has to be something that can be easily removed from CO_2 so that the CO_2 outlet stream can be pure enough for sequestration. CO_2 and low pressure steam, so far, are the two prospective sweep gases. Low pressure steam can easily be removed from the CO_2 stream after regeneration by condensing out the water vapor. The problem with using CO_2 as a sweep stream is the formation of urea instead of carbamate that has been reported to happen at high regeneration temperatures. The formation of urea is slow, but since it does not regenerate at the typical regeneration temperature, the adsorbent progressively loses CO_2 adsorption capacity.

Therefore, the effects of low pressure steam on our adsorbents should be studied. Other researchers [54] have simulated steam regeneration by using an autoclave purged with nitrogen or air and then exposing the adsorbent with steam at temperatures ranging from 105°C -180°C for 24hours to simulate many regeneration cycles. The steam was generated by placing a flask with 30ml DI water in an autoclave and heating to the desired temperature. The results showed a significant decrease in the CO_2 adsorption capacity even at the lowest temperature of 105°C. The adsorbent was mesoporous silica made in house that was similar to commercial MCM-48 and SBA-15 but had thinner pore walls, which is one of the reasons that

was offered for the reduction of the pore volume, surface area and CO_2 adsorption capacity after steam treatment. [54]

The present was carried out by placing the samples in an environmental chamber at 66-67°C and ~98.4 relative humidity for 24 hours. The lower temperature was considered to be less severe than 105°C, but it is unknown what the degradation of the sample will be if condensation occurs on the sample. The other researchers who had conducted their experiments in an autoclave reported no apparent condensation on the sample bottles or samples.

The experiment used approximately 40mg of sample, and it was placed into the environmental chamber for 24 hours. The bottles were then removed from the chamber after 24 hours and weighed shortly thereafter; the samples had to be moved into a different lab with a balance. The bottles had no lids and were bound together in a bundle using a rubber band. Six different samples were used in this study each having a duplicate for repeat analysis. The samples included clay reacted with APTMS, clay impregnated with PEI loadings of 33%, 50%, 66%, and clay reacted with APTMS and then impregnated with PEI 50% loading. Two samples of clay-APTMS were immediately tested in the TGA without drying. The remaining samples were placed in a vacuum oven at 60°C overnight to dry.

All of the bottles had obvious condensation on and in the bottle, indicating that not only did water vapor come into contact with the samples but also liquid water. The samples that had PEI in them were actually sitting in a pool of water. The clay reacted with APTMS samples looked damp, but there was no standing water. The amount of water appeared to increase with

increased PEI loading, meaning that the cloisite-PEI-33 had the least amount of water while the PEI-66 appeared to have the most. The liquid water being in contact with the clay-APTMS samples was a concern because of the possibility that the powdered samples would turn into a solid clump of material affecting the mass transfer to the amine sites and possibly requiring another grinding step in a mortar and pestle. Removing the dried clay-APTMS samples from the bottles and putting them into the TGA crucible broke up the sample into a powder without any intentional crushing. The two wet samples that were not dried before the TGA experiment broke apart easily into a powder when touched after the adsorption experiment indicating that the sample did not strongly agglomerate together, which would probably have greatly reduced the accessibility of the amine sites. The C-PEI-50 and C-PEI-33 sample did form a solid clump of material in the bottle, but this was partially broken up in the process of transferring it to the TGA pan. The C-PEI-66 also formed a solid mass of material, but when transferring the sample to the TGA pan, the solid was more of a dry paste-like consistency than a powder. This is one of the reasons why almost all of our work has been done using 50% PEI loaded samples instead of 66% PEI loaded samples. The C-APTMS-PEI-50 sample formed a solid mass of material that had to be broken to be removed from the bottle and placed into the TGA pan.

CO_2 adsorption was studied by ramping the instrument at 5°C per minute in N_2 to 100°C for 30 minutes then reducing the temperature to 85°C for adsorption in pure CO_2 in the Thermo Cahn TGA. Table 5-6 shows the results for the CO_2 adsorption TGA experiment. For the clay treated with APTMS, the CO_2 adsorption capacity was greatly reduced after being exposed to the 66-67°C and ~98% relative humidity environment chamber. Sample 1AD and 1AJ, clay reacted with APTMS, CO_2 adsorption capacities reduce to an average of 65% of their original

capacity. Since the wet sample had a significant amount of water in the sample, the sample weight for the CO_2 weight percent calculation was taken when the sample weight reached an approximate equilibrium during the initial N_2 desorption step at 100°C.

The sample weight is manually put into the Thermo Cahn TGA and not measured by the TGA before the run begins, this may cause some error due to the sample drying in the N_2 purge that is running through the reactor while the experiment is being set up. This most likely would not cause a big error when the samples have been dried and have been sitting in a sealed bottle before running the experiments. However, with a very water-saturated sample that may be rapidly drying in the N_2 purge, there could be more error.

The clay treated with PEI samples were expected to perform worse than the clay treated with APTMS because PEI is soluble in water and is not expected to be covalently attached to the sample, but electrostatically attached to the negative surface of the clay. Clay loaded with 33% PEI exposed to the 66°C water vapor adsorbed 99 percent of its initial carbon dioxide adsorption capacity. This is unexpected intuitively, but there have been other reports that show that mesoporous silica impregnated with PEI showed similar results when exposed to water vapor. Clay loaded with 66% PEI showed an increase in its adsorption capacity. The C-PEI-50 sample showed a slight decrease but was better than the C-APTMS samples. The C-APTMS-PEI sample also had a similar adsorption capacity to the samples not exposed to the environmental chamber. Although the adsorption capacity was not as high as other C-APTMS-PEI samples made in the past. Table 5-6 shows the data collected for the samples after exposure to the environmental chamber. Figure 5-35 is a comparison of the initial adsorption capacity with the

weight capacity of the samples after the exposure in the environmental chamber for samples of clay treated with 50% PEI, APTMS and APTMS+PEI. Figure 5-36 is a comparison of the 3 different loadings of PEI onto the clay. From Figures 5-35 and 5-36 it can be seen that the sample of clay treated with APTMS performed the worst of all of the treatments. Figures 5-37-38 are some representative TGA graphs for the data collected.

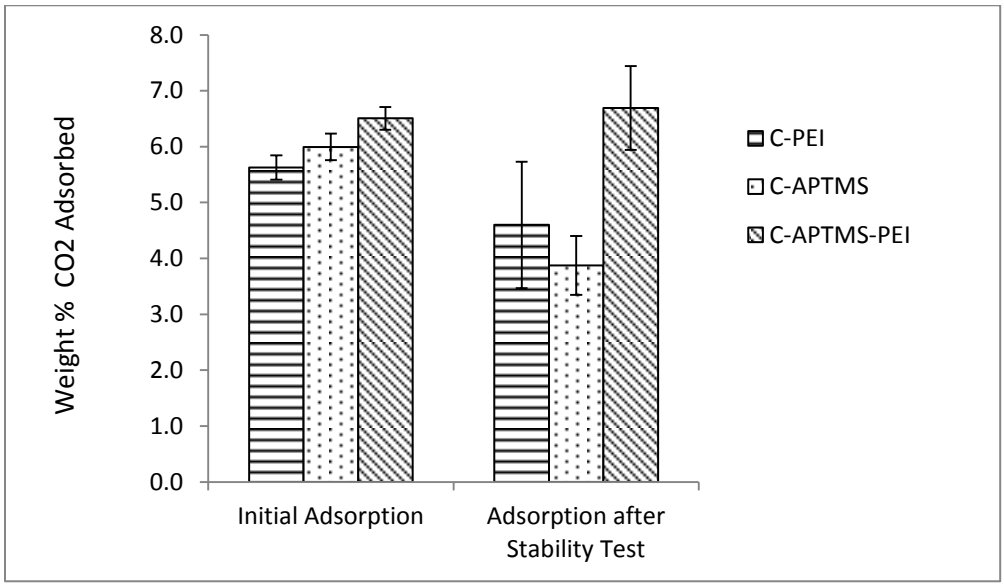

Figure 5-35: Comparison of amine treatments on CO_2 adsorption

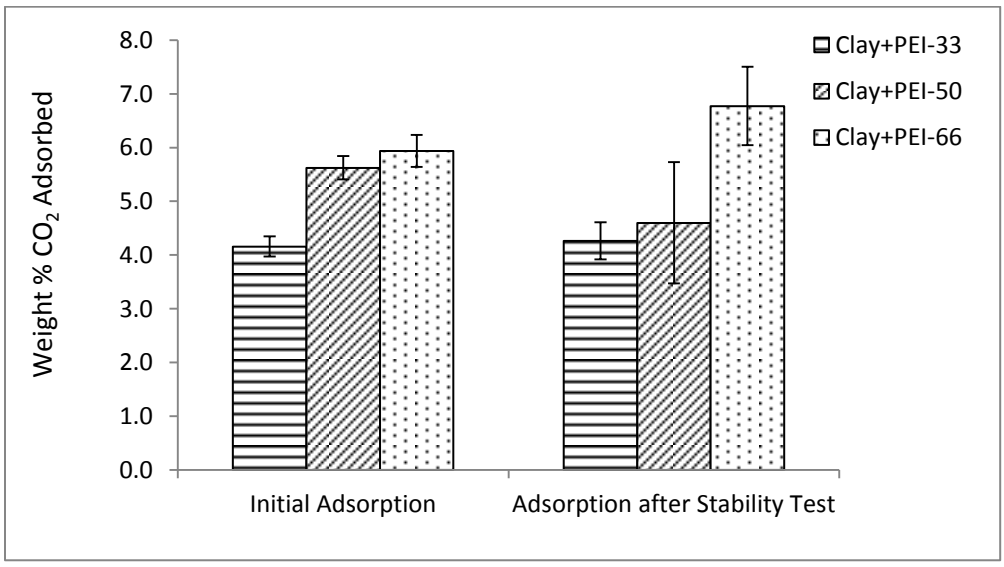

Figure 5-36: Comparison of the PEI loading on CO_2 adsorption

Table 5-6: CO_2 adsorption capacity after exposure to the environmental chamber

Sample	Weight (mg)	Weight (After 66-67°C Env. Chamber) 24 hr	60°C vacuum dried weight	After 66-67°C Env. Chamber CO_2 Capacity
C-APTMS (1AD)	37.735	79.237 mg (210 wt%)	NA Did not Dry	3.4 wt%
C-APTMS (1AD)	45.016	84.445 mg (188 wt%)		3.9 wt%
C-APTMS (1AJ)	42.306	80.023 mg (189 wt%)	NA Did not Dry	3.6 wt%
C-APTMS (1AJ)	44.653	86.751 mg (194 wt%)	41.320 mg (93 wt%)	4.6 wt%
C-PEI-33 (1AE)	30.124	91.295 mg (303 wt%)	30.713 mg (102 wt%)	4.51 wt%
C-PEI-33 (1AE)	38.536	113.353 mg (294 wt%)	39.444 mg (102 wt%)	4.02 wt%
C-PEI-50 (1AG)	45.696	135.532 mg (297 wt%)	42.082 mg (92 wt%)	5.4 wt%
C-PEI-50 (1AG)	53.434	153.625 mg (288 wt%)	51.190 mg (96 wt%)	3.8wt%
C-PEI-66	36.719	136.532 mg (370 wt%)	37.257 mg (101 wt%)	7.29wt%
C-PEI-66	41.459	142.174 mg (343 wt%)	41.897 mg (101 wt%)	6.26wt%
C-APTMS-PEI (2N)	34.554	123.316 mg (357 wt%)	34.002 mg (98 wt%)	6.16wt%
C-APTMS-PEI (2N)	38.112	157.267 mg (413 wt%)	36.935 mg (97 wt%)	7.22wt%

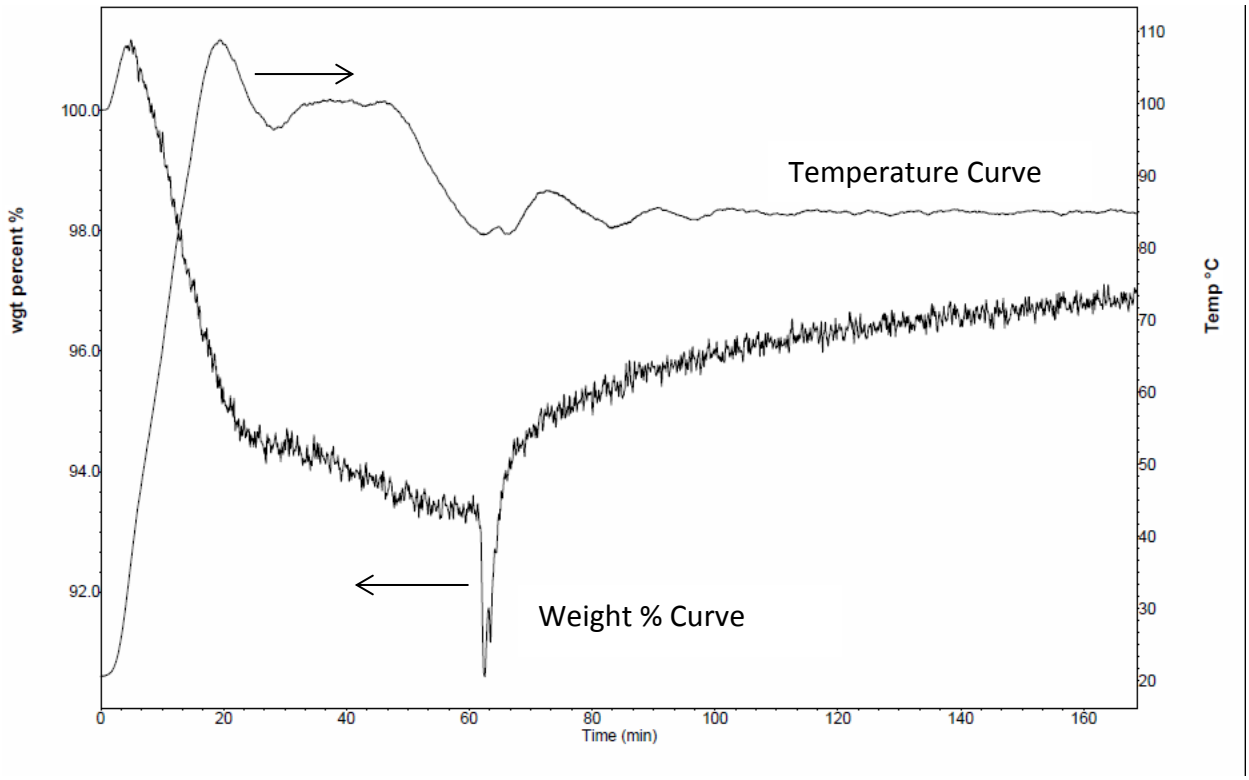

Figure 5-37: CO_2 adsorption of clay loaded with 66% PEI after exposure to the environment chamber

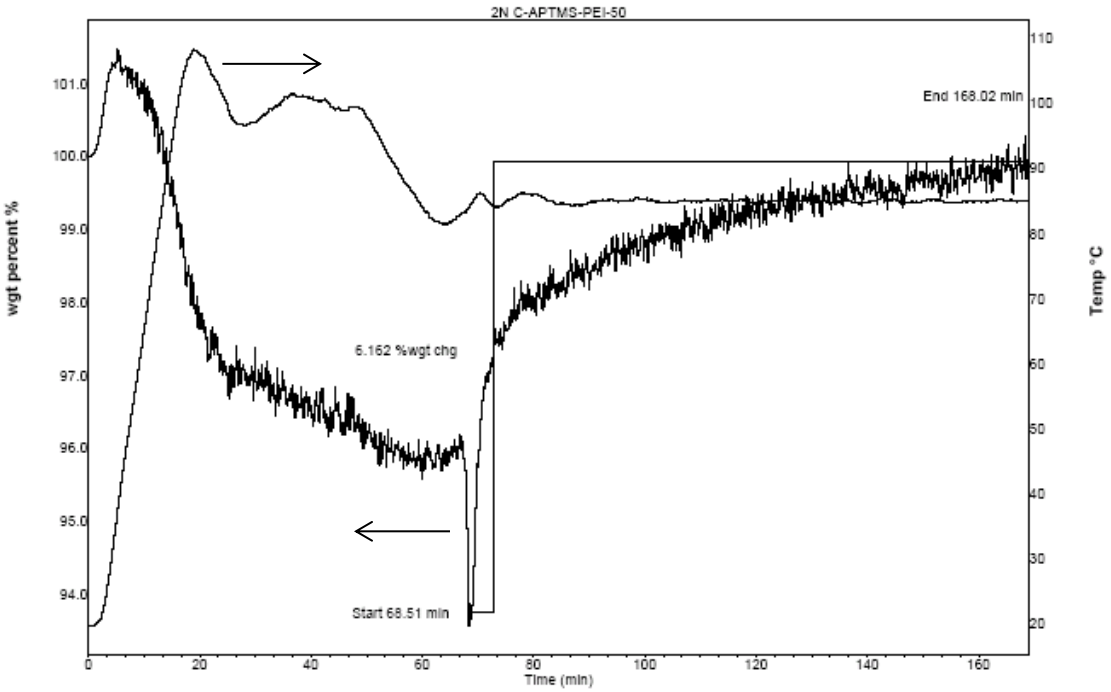

Figure 5-38: CO_2 adsorption for clay treated with APTMS and PEI after exposure to the environment chamber

From Figures 5-37-38, it can be seen that the same CO_2 adsorption profile is observed for the adsorption of CO_2 before and after exposure to the environmental chamber at 66-67°C and 98%RH for 24 hours. This was also true for all of the other samples tested. The data collected here suggest that the use of steam for the regeneration of samples treated with only APTMS would not be an ideal way for regeneration. Although the decrease in adsorption capacity for samples treated with APTMS could have been due to the condensation of water directly onto the sample, which probably would not occur to the degree that it did in the environmental chamber when using low pressure steam. The stability of samples treated with PEI and APTMS+PEI showed good resilience to the environmental chamber and therefore low-pressure steam might be a good candidate for regeneration of these samples.

5.8 Activation Energy Results

The stability of amines on solid supports is a big concern for the applicability of the amine solid adsorbents in commercial applications. Therefore the activation energy of the degradation of APTMS and PEI on montmorillonite was studied using a TGA technique described in a paper by Friedman. [66] Additionally, other papers on TGA activation energy assumed a very general kinetic equation. [67], [68] The method is used for decomposition kinetics of polymers using different heating rates through its decomposition region. After heating the material at different heating rates, the temperatures for a constant decomposition level are determine. Equation 5-3 is a general kinetic equation used to calculate activation energy.

$$\left(-\frac{1}{\omega_o}\right)\left(\frac{d\omega}{dt}\right) = Ae^{-\frac{\Delta E}{RT}} f\left(\frac{\omega}{\omega_o}\right) \quad 5\text{-}3$$

Where ω = weight of organic material, ω_o = original weight, t = time (in hours), *A* = pre-exponential factor of rate constant (per hour), ΔE = activation energy of rate constant, (in calories/mole) *R* = gas constant (1.987 cal. /°K. mole), *T* = absolute temperature, and $f\left(\frac{\omega}{\omega_o}\right)$ = a function of the weight of organic material. [66] By taking logarithms of both sides of Equation 5-3, one can obtain Equation 5-4.

$$\ln\left[\left(-\frac{1}{\omega_o}\right)\left(\frac{d\omega}{dt}\right)\right] = \ln A + \ln f\left(\frac{\omega}{\omega_o}\right) - \frac{\Delta E}{RT} \quad 5\text{-}4$$

It is assumed that $f\left(\frac{\omega}{\omega_o}\right)$ is a constant for constant values of $\left(\frac{\omega}{\omega_o}\right)$. Values of $\left(-\frac{1}{\omega_o}\right)\left(\frac{d\omega}{dt}\right)$ and $\frac{1}{T}$ were determined for each $\left(\frac{\omega}{\omega_o}\right)$ for each TGA experimental run and plotted against each other. The slope of each line is equal to $-\frac{\Delta E}{R}$, while the intercept is ln $[Af\left(\frac{\omega}{\omega_o}\right)]$. Flynn, et. al. used a similar equation, Equation 5-5, and graphed the negative logarithm of the heating rate (-log(*B)*) versus 1/T.

$$E \cong -4.35\ (d\log B)/(d\frac{1}{T}) \quad \textbf{5-5}$$

Were *B* is the ramping or heating rate for each TGA run. A sample of clay treated with PEI was first tested using heating rates of 5, 10, 15, and 20°C per minute in pure nitrogen. Figure 5-39 shows the TGA graph of sample clay treated with PEI at these heat rates. Figure 5-40 shows a plot of –log *B* vs. 1/*T* from the data in Figure 5-39

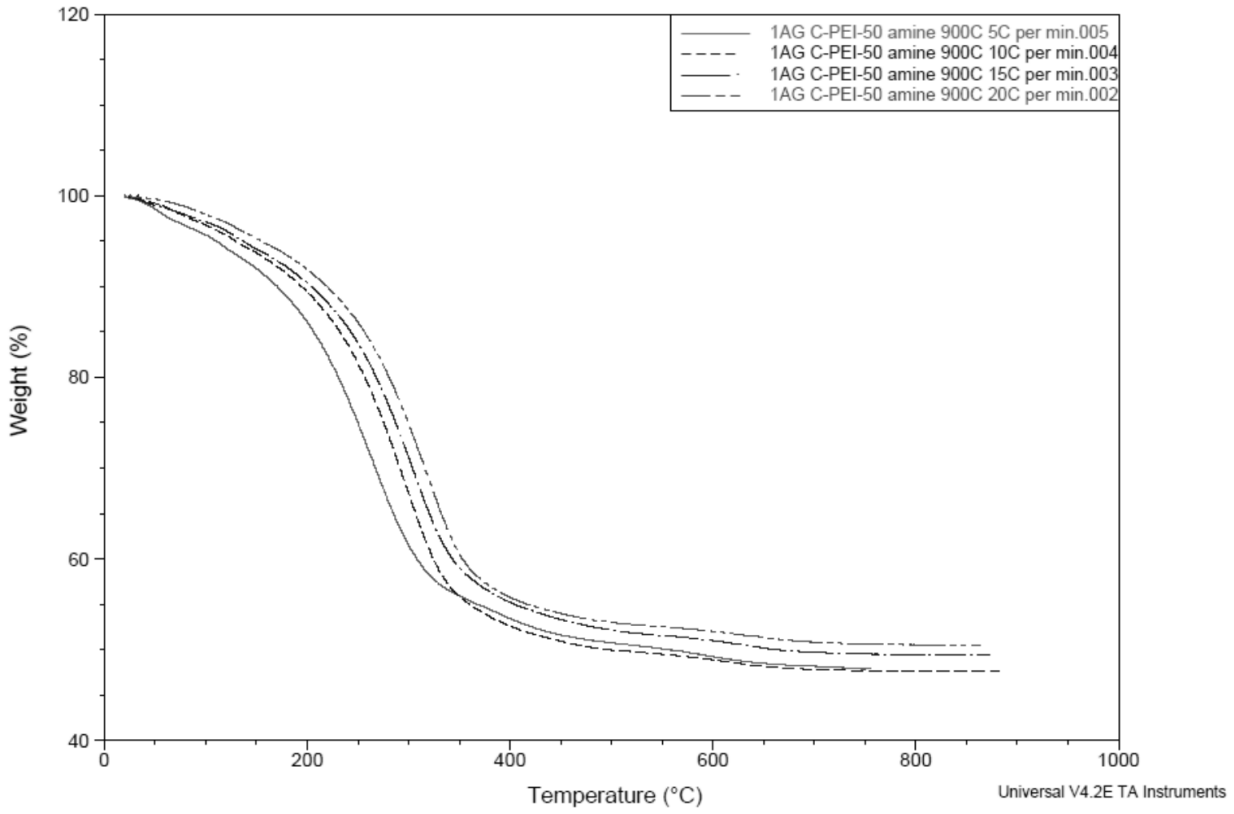

Figure 5-39: TGA overlay graph of sample clay treated with PEI

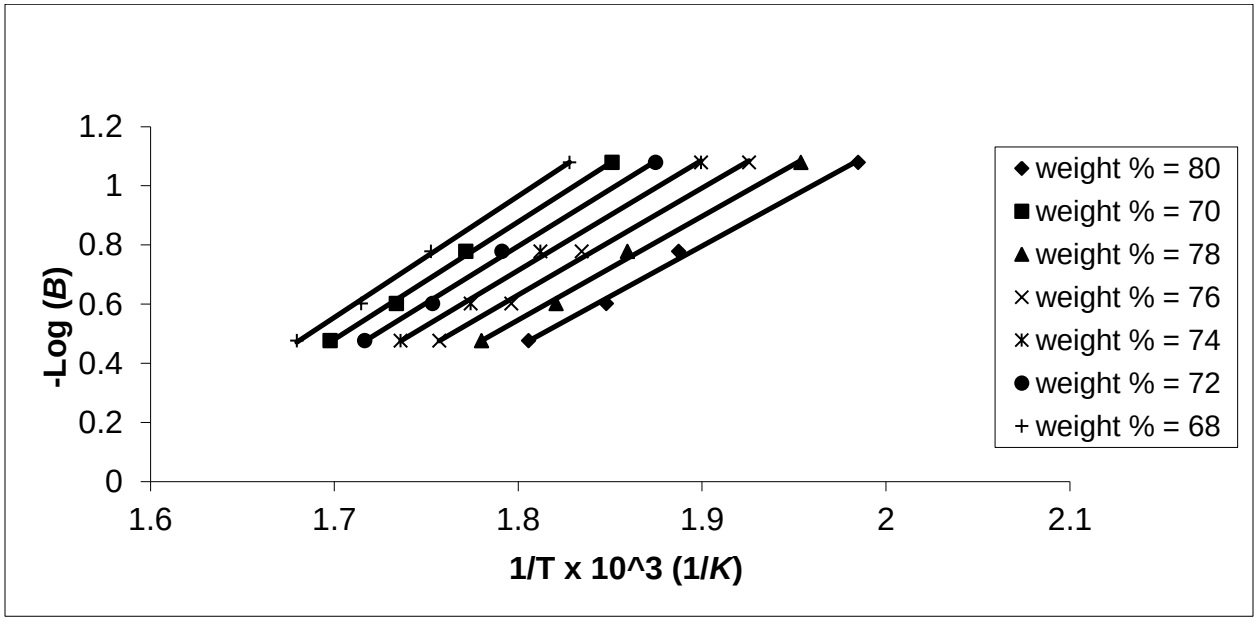

Figure 5-40: Logarithm of heating rate vs. reciprocal absolute temperature

From Figure 5-39 values of 1/T were calculated at different weight percentages during the constant weight loss process. By using the equation by Flynn, the activation energy can be calculated at each weight percent for an average value of 16.26 Kcal/mole with a standard deviation of 1.1. Figure 5-41 is a graph of the activation energy versus residual fraction $\left(\frac{\omega}{\omega_o}\right)$

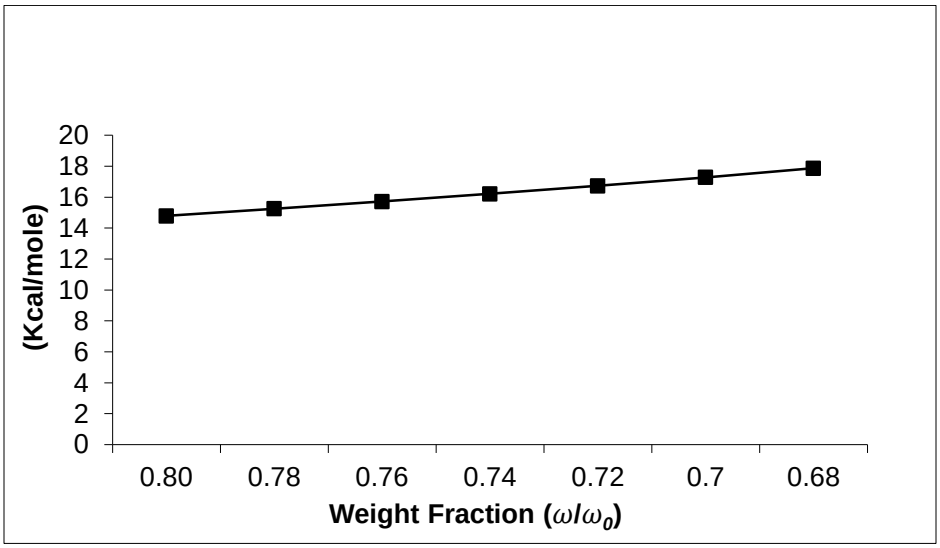

Figure 5-41: Activation energy of clay treated with PEI versus weight fraction

Figure 5-42 is an overlay graph of clay treated with APTMS. The TGA data did not form a very ideal decomposition graph and the calculated activation energy had a very big standard deviation. The calculated decomposition activation energy was 45.4 Kcal/mole with a standard deviation of 20.1 Kcal/mole.

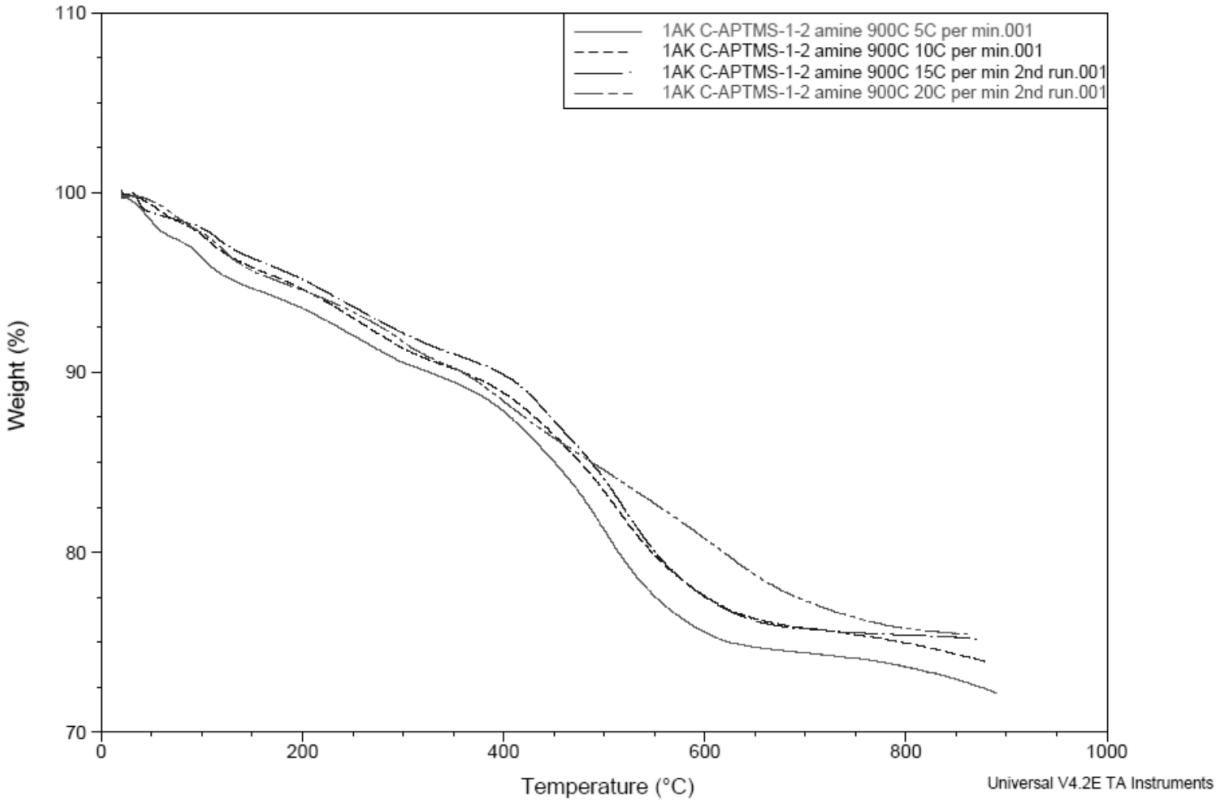

Figure 5-42: Clay treated with APTMS overlay TGA graph

Figure 5-43 is a graph of the decomposition activation energy versus the residual weight fraction.

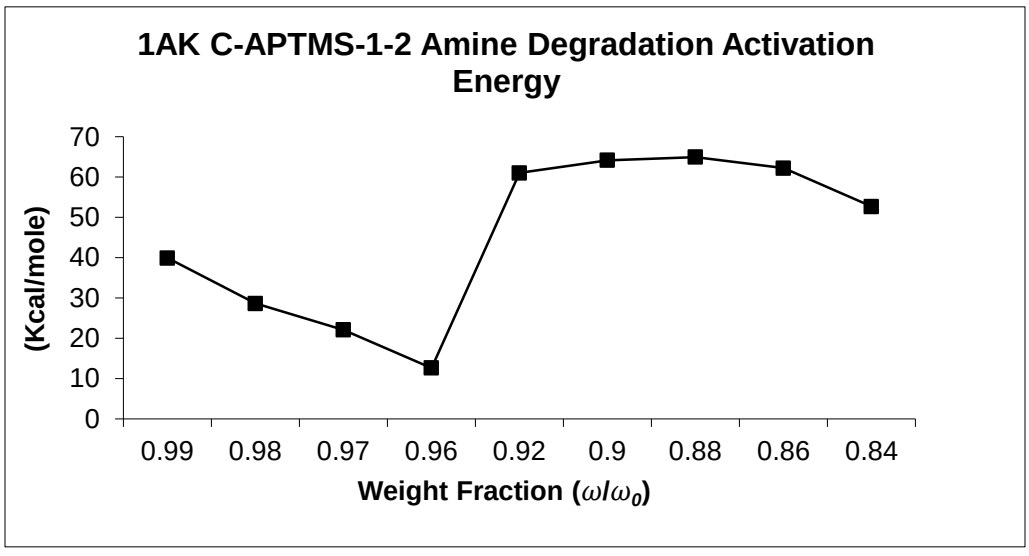

Figure 5-43: Clay treated with APTMS activation energy versus weight fraction

Figures 5-42 and 5-43 show that this method for calculating the activation energy for the degradation of APTMS on clay is poor.

Clay treated with the combination of APTMS and PEI was also studied using this method. Similar to the clay treated with APTMS, the clay treated with the combination of APTMS and PEI did not give good results for an accurate calculation of the degradation activation energy.

The goal of this study was not only to better understand the degradation of the amine on the clay, but also try to use this technique to study the desorption of CO_2 from the adsorbents. Therefore, the activation energy of desorption of CO_2 was studied using a similar procedure to the decomposition of the amines. The TGA procedure for the desorption of CO_2 was to react CO_2 to the adsorbent at 85°C then cool the sample in CO_2 to 30°C. Once the sample was at 30°C the reaction gas was switched to nitrogen and the heating rate was varied to achieve graphs similar to the decomposition graphs. Figure 5-44 is a TGA overlay graph of desorption of CO_2 on clay treated with APTMS. The curves were adjusted to be equal at the start of decomposition.

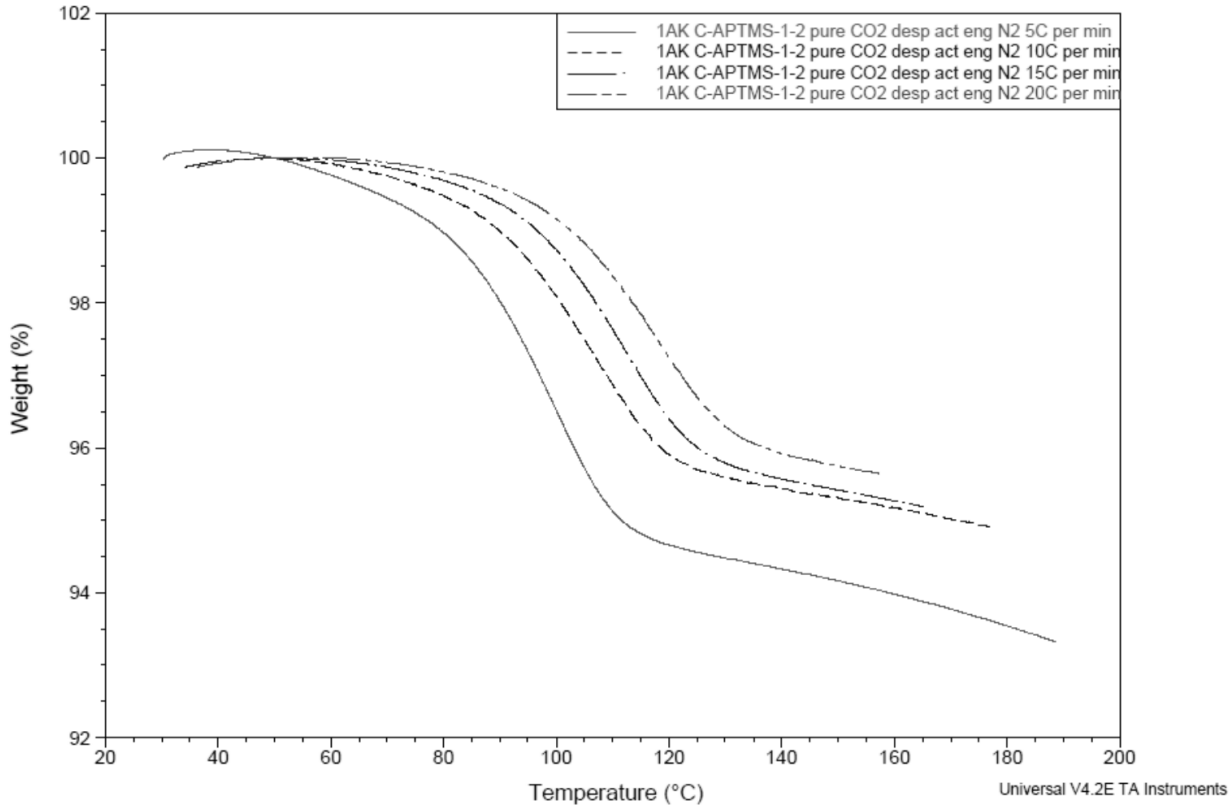

Figure 5-44: Desorption of CO_2 on clay treated with APTMS in nitrogen

By using the same procedure to calculate activation energy as before, the activation energy was 15.4 Kcal/mole with a standard deviation of 0.76 Kcal/mole. While the calculated standard deviation is small, it can be seen that the ending weight percent for the different heating rates is significantly different. This is not expected since the same amount of CO_2 is eventually expected to desorb, independent of the heating of the heating rate. Therefore, this procedure to calculate desorption activation energy for CO_2 did not seem very accurate.

The degradation activation of polymers using this TGA technique has been conducted for many years. The results obtained using this technique on the adsorbents studied did not seem to give very accurate results. Additionally, trying the use this technique to study desorption of CO_2 also seemed to give inconclusive results.

Chapter 6

6. Conclusions and Future Work

6.1 Conclusions

The research completed in this project shows that untreated nanoclay adsorbs very little CO_2 at atmospheric pressure and at pressures up to 300psi at various temperatures. Clay treated with APTMS and PEI was able to adsorb significant CO_2. Additionally, the amine treated clay was able to adsorb CO_2 at different pressures and temperatures, even when using a gas mixture of 10% CO_2 and 90% N_2. The highest adsorption capacities at atmospheric pressure were observed to occur at temperatures between 75°C and 100°C. This phenomenon has been seen in the literature using PEI and is attributed to diffusion limitations at lower temperatures.

The combination of APTMS reacted to the edge hydroxyl groups and PEI attached to the clay surface showed an increased adsorption capacity at 85°C in the TGA at atmospheric pressure over samples treated with PEI or APTMS alone. The adsorption capacity at high pressures and room temperature also showed an increased adsorption capacity for the combination for APTMS and PEI. At increased temperatures and high pressure, samples treated with PEI showed a big increase in CO_2 adsorption, while samples treated with APTMS did not have a significant increase in CO_2 adsorption capacity. Similar to CO_2 adsorption at atmospheric pressure, this was attributed to the reduction in diffusion resistance when the sample is heated.

FTIR, TGA, and SEM studies showed that APTMS and PEI were successfully attached to the nanoclay. The attachment of amines to the nanoclay reduced the surface area according to the BET surface area analysis. The surface area of the dry untreated clay was significantly lower than the expected surface area for completely separated platelets. The APTMS treated samples also showed a decrease in the BET surface area over the untreated clay. It is suspected that if the clay platelets were completely separated during CO_2 adsorption the CO_2 adsorption capacity would increase because more amine groups would be easily available for reacting to CO_2.

The regeneration of amine treated adsorbents was initially studied using pure nitrogen, and showed that the sorbents could be regenerated in nitrogen at 100°C. Over ten cycles there was a small of loss of CO_2 adsorption capacity for all of the treated samples. This indicated the possibility for cycling of the sorbents. Other regeneration schemes using pure and humid CO_2 at 155°C also showed that regeneration using these sweep gases was possible. Loss of the CO_2 adsorption capacity was observed when using pure CO_2 at 155°C and indicated that the ability for the cycling of the adsorbent over hundreds or thousands of cycles should be investigated further. Vacuum regeneration of the adsorbents also indicated that this could be a possible mechanism for cycling. Vacuum desorption also showed that there is some loss of CO_2 adsorption capacity over multiple cycles.

The stability of the adsorbents in water vapor at mild temperatures was studied and indicated that the adsorption capacity of APTMS treated samples could be greatly reduced with long exposures to water vapor at mild temperatures. It is important to note that liquid

water was observed on these samples and could have possibly affected the CO_2 adsorption capacity more than water vapor. The samples treated with PEI surprisingly showed little to no degradation after exposure to water vapor at mild temperatures. Although this is surprising, this has also been seen in the literature.

In summary, a nanoclay treated with commercially available amines has been shown to adsorb CO_2. Although the CO_2 adsorption capacity is not as high as the highest reported amine treated adsorbents, it is still within the range being employed for scale up studies. The advantage of these adsorbents is the use a support that is relatively cheap and available in huge quantities. This work has shown that the possibility of CO_2 capture from a coal-fired power plant using an amine treated nanoclay is possible.

6.2 Future Work

Future work for this project would be cycling tests using humid CO_2 at 155°C over hundreds of cycles to determine the stability or degradation rate of the adsorbent. Additionally, the regeneration over hundreds of cycles using vacuum should be further investigated.

The degradation due to SO_x and NO_x is a big concern for solid amine adsorbents over thousands of adsorption and desorption cycles. The degradation due to these acid gases is expected to slightly degrade the solid amine adsorbents developed in this study. The rate of degradation and stability of the adsorbents when exposed to these acid gases should be studied. To study these properties, an actual or simulated coal-fired slipstream should be used as an adsorption gas.

The stability of the adsorbents to water vapor was tested using an environmental chamber that could not get to temperatures of low pressure steam. Since low pressure steam could be a likely candidate for regeneration of solid amine adsorbents, the stability of the adsorbents should be examined using low pressure steam or similar conditions. Additionally, cycling experiments using steam would be interesting.

Determining the energy for desorption of CO_2 using different cycling techniques is an important property needed to design a commercial process. Therefore, futures studies are needed to determine the energy need to desorb CO_2 from the adsorbents studied. Use more conclusive characterization tests to determine if a reaction of CO_2 with the attached amine occurs as predicted.

References:

[1] Plasynski, "Progress and New developments in Carbon Capture and Storage," *Critical Reviews in Plant Sciences,* vol. 28, no. 3, pp. 123-138, 2009.

[2] International Energy Agency, "CO_2 Emissions from fuel Combustion," International Energy Agence and the Organisation for Economic Co-operation and Development, Paris, 2011.

[3] L. Parker and P. Folger, "Capturing CO_2 from Coal-Fired Power Plants: Challenges for a Comprehensive Strategy," Congressional Research Service Reports, Washington, DC, 2010.

[4] U.S. Energy Information Administration, "Electricity generation from coal and natural gas both increased with summer heat," U.S. Department of Energy, Washington, DC, 2012.

[5] W. Liu, "Critical Material and Process Issues for CO_2 Separation from Coal-Powered Plants," *Minerals, Metals and Materials Society,* vol. 61, no. 4, pp. 36-44, 2009.

[6] J. Ciferno, J. Litynski, S. Plasynski, J. Murphy, G. Vaux, R. Munson and J. Marano, "DOE/NETL Carbon Dioxide Capture and Storage RD&D Roadmap," US DOE National Energy Technology Laboratory, Pittsburgh, 2010.

[7] D. Connell, "Carbon Dioxide Capture Options for Large Point Sources in the Midwestern United States," 2005.

[8] J. Bradshaw, S. Bachu, D. Bonijoly, R. Burruss, S. Holloway, N. P. Christensen and O. M. Mathiassen, "CO_2 storage capacity estimation: issues and development of standards," *International Journal of Greenhouse Gas Control,* vol. 1, pp. 62-68, 2007.

[9] USDOE/National Energy Technology Laboratory, "Carbon Dioxide Enhanced Oil Recovery," USDOE/ National Energy Technology Laboratory, 2010.

[10] USDOE/National Energy Technology Laboratory, "Carbon Sequestration Atlas of the United States and Canada Third edition," United States Department of Energy/ National Energy Technology Laboratory, 2010.

[11] H. W. Pennline, D. R. Luebke, B. I. Morsi, Y. J. Heintz, K. L. Jones and J. B. Ilconich, "Carbon Dioxide Capture and Separation Techniques for Advanced Power Generation Point Sources," U.S. Department of Energy/NETL, Pittsburgh, 2006.

[12] C. M. White, B. R. Strazisar, E. J. Granite, J. S. Hoffman and H. W. Pennline, "Separation and Capture of CO_2 from Large Stationary Sources and Sequestration in Geological Formations," *Journal of Air and Waste Management Association,* vol. 53, no. 6, pp. 645-715, 2003.

[13] A. Yazaydin and R. Snurr, "Screening of Metal-Organic Framewroks for Carbon Dioxide Capture from Flue Gas Using a Combined Experimental and Modeling Approach," *Journal of American Chemical Society,* vol. 131, pp. 18198-18199, 2009.

[14] D. Britt, H. Furukawa, B. Wang, T. G. Glover and O. M. Yaghi, "Highly efficient separation of carbon dioxide by a metal-organic framework replete with open metal sites," *Proc Natl Acad Sci USA,* vol. 106, pp. 20637-20640, 2009.

[15] S. R. Caskey, A. G. Wong-Foy and A. J. Matzger, "Dramatic Tuning of Carbon Dioxide Uptake via Metal Sustitution in a Coordination Polymer with Cylindrical Pores," *Journal of the American Chemical Society,* vol. 130, pp. 10870-10871, 2008.

[16] D. Wu, Q. Yang, C. Zhong, D. Liu, H. Huang, W. Zhang and G. Maurin, "Revealing the

Structure-Property Relationships of Metal-Organic Frameworks for CO_2 Capture from Flue Gas," *Langmuir*, vol. 28, pp. 12094-12099, 2012.

[17] S. A. S. Talesh, S. Fatemi, S. Hashemi and M. Ghasemi, "Effect of Si/Al Ratio on CO_2-CH_4 Adsorption and Selectivity in Synthesized SAPO-34," *Separation Science and Technology*, vol. 45, pp. 1295-1301, 2010.

[18] D. Ko, r. Siriwardane and L. T. Biegler, "Optimization of a Pressure-Swing Adsorption Process Using Zeolite 13X for CO_2 Sequestration," *Ind. Eng. Chem. Res.* , vol. 42, pp. 3393-48, 2003.

[19] M. Tatlier and A. Erdem-Senatalar, "Fractal dimension of zeolite surfaces by calculation," *Chaos, Solitons and Fractals*, vol. 12, pp. 1145-1155, 2001.

[20] F. Brandani and D. M. Ruthven, "The Effect of Water on teh Adsorption of CO_2 and C_3H_8 on Type X Zeolites," *Ind. Eng. Chem. Res.* , vol. 43, pp. 8339-8344, 2004.

[21] B. Castellani, M. Filipponi, S. Rinaldi and F. Rossi, "Capture of Carbon Dioxide Using Gas Hydrate Technology," in *The 25th International Conference on Efficiency, Cost, Optimization, Simulation and Environmental Impact of Energy Systems*, Peruglia, Italy, 2012.

[22] H. Yang, Z. Xu, M. Fan, F. Gupta, R. B. Slimane, A. E. Bland and I. Wright, "Progress in carbon dioxide separtion and capture: A review," *Journal of Environmental Sciences*, vol. 20, no. 1, pp. 14-27, 2008.

[23] L.-S. Fan and F. Li, "Chemical Looping Technology and Its Fossil Energy Conversion Applications," *Industrial & Engineering Chemistry Research*, vol. 49, no. 21, pp. 10200-10211, 2010.

[24] C. A. Scholes, S. E. Kentish and G. W. Stevens, "Carbon Dioxide Separation through Polymeric Membrane Systems for Flue Gas Applications," *Recent Patens on Chemical Engineering*, vol. 1, pp. 52-66, 2008.

[25] J. C. Hicks, J. H. Drese, D. J. Fauth, M. L. Gray, G. Qi and C. W. Jones, "Designing Adsorbents for CO_2 Capture From Flue Gas-Hyperbranched Aminosilicas Capable of Capturing CO_2 Reversibly," *Journal of the American Chemical Society*, vol. 130, no. 10, pp. 2902-2903, 2008.

[26] M. T. Ho, G. W. Allinson and D. E. Wiley, "Reducing the Cost of CO_2 Capture from Flue Gases Using Pressure Swing Adsorption," *Industrial & Engineering Chemistry Research*, vol. 47, no. 14, pp. 4883-4890, 2008.

[27] J. H. Drese, S. Choi, R. P. Lively, W. J. Koros, D. J. Fauth, M. L. Gray and C. W. Jones, "Synthesis-Structure-Property Relationships for Hyperbranced Aminosilica CO_2 Adsorbents," *Advanced Functional Materials*, vol. 19, pp. 3821-3832, 2009.

[28] L. Gray, Y. Soong, K. Champagne, H. Pennline, J. Baltrus, R. S. Jr., R. Dhatri, S. Chuang and T. Filburn, "Improved immobilized carbon dioxide capture sorbents," *Fuel Processing Technology*, vol. 86, no. 14-15, pp. 1449-1455, 2005.

[29] X. Xu, C. Song, R. Wincek, J. M. Andresen, B. G. Miller and A. W. Scaroni, "Separation of CO_2 from Power Plant Flue Gas Using a Novel CO_2 "Molecular Basket" Adsorbent," *Energy and Fuels*, vol. 13, pp. 1463-1469, 2002.

[30] X. Xu, C. Song, J. M. Andresen, B. G. Miller and A. W. Scaroni, "Preparation and characterization of novel CO_2 "molecular basket" adsorbents based on polymer-modifed

mesoporous molecular sieve MCM-41," *Microporous and Mesoporous Materials,* vol. 62, pp. 29-45, 2003.

[31] X. Xu, C. Song, B. G. Miller and A. W. Scaroni, "Influence of Moisture on CO_2 Separation from Gas Mixture by a Nanoporous Adsorbent Based on Polyethylenimine-Modified Molecular Sieve MCM-41," *Industrial and Engineering Chemisty Research,* vol. 21, no. 44, pp. 8113-8119, 2005.

[32] X. Xu, C. Song, B. G. Miller and A. W. Scaroni, "Adsorption separation of carbon dioxide from flue gas of natural gas-fired boiler by a novel nanoporous "molecular basket" adsorbent," *Fuel Processing Technology,* vol. 86, pp. 1457-1472, 2005.

[33] X. Wang, X. Ma, V. Schwartz, J. C. Clark, S. H. Overbury, S. Zhao, X. Xu and C. Song, "A solid molecular basket sorbent for CO_2 capture from gas streams with low CO_2 concentration under ambient conditions," *Physical Chemisty Chemical Physics,* vol. 14, pp. 1485-1492, 2012.

[34] P. J. Harlick and A. Sayari, "Applications of Pore-Expanded Mesoporous Silicas. 3. triamine silane grafting for Enhanced CO_2 adsorption," *Industrial & Engineering Chemistry Research,* vol. 9, no. 45, pp. 3248-3255, 2006.

[35] A. Sayari and P. J. Harlick, "Applications of Pore-Expanded Mesoporous Silica. 5. Triamine Grafted Material with Exceptional CO_2 dynamic and Equilibrium Adsorption Performance," *Industrial & Engineering Chemistry Research,* vol. 46, pp. 446-458, 2007.

[36] Y. Belmabkhout, R. Serna-Guerrero and A. Sayari, "Adsorption of CO_2-Containing Gas Mixtures over Amine-Bearing Pore-Expanded MCM-41 Silica: Application for Gas Purification," *Industrial & Engineering Chemistry Research,* vol. 49, pp. 359-365, 2010.

[37] Y. Belmabkhout, R. Serna-Guerrero and A. Sayari, "Adsorption of CO_2-containing gas mixtures over amine-bearing pore-expanded MCM-41 silica: application for CO_2 separtion," *Chemistry and Materials Science,* vol. 17, no. 2, pp. 395-401, 2011.

[38] J. C. Hicks, J. H. Drese, D. J. Fauth, M. L. Gray, G. Qi and C. W. Jones, "Designing Adsorbents for CO_2 Capture from Flue Gas-Hyperbranched Aminosilicas Capable of Capturing CO_2 Reversibly," *Journal of the American Chemical Society,* vol. 130, pp. 2902-2903, 2008.

[39] J. H. Drese, S. Choi, R. P. Lively, W. J. Koros, D. J. Fauth, M. L. Gray and C. W. Jones, "Synthesis-Structure-Property Relationships for Hyperbranched Aminosilica CO_2 adsorbents," *Materials Views,* vol. 19, no. 23, pp. 3821-3832, 2009.

[40] W. Li, S. Choi, J. H. Drese, M. Hornbostel, G. Krishnan, P. M. Eisenberger and C. W. Jones, "Steam-Stripping for Regeneration of Supported Amine-Based CO_2 Adsorbents," *ChemSusChem,* vol. 3, no. 8, pp. 899-903, 2010.

[41] X. Yan, L. Zhang, Y. Zhang, G. Yang and Z. Yan, "Amine-Modified SBA-15: Effect of Pore Structure on the Performance for CO_2 Capture," *Industrial & Engineering Chemistry Research,* vol. 50, pp. 3220-3226, 2011.

[42] N. Hiyoshi, K. Yogo and T. Yashima, "Adsorption of Carbon Dioxide on Amine Modified SBA-15 in the Presence of Water Vapor," *Chemistry Letters,* vol. 33, pp. 510-511, 2004.

[43] A. Sayari, Y. Belmabkhout and R. Serna-Guerrero, "Flue gas treatment via CO_2 adsorption," *Chemical Engineering Journal,* vol. 171, no. 3, pp. 760-774, 2011.

[44] X. Xu, C. Song, J. M. Andresen, B. G. Miller and A. W. Scaroni, "Novel Polyethylenimine-

Modified Mesoporous Molecular Sieve of MCM-41 Type as High-Capacity Adsorbent for CO_2 Capture," *Energy & Fuels,* vol. 16, pp. 1463-1469, 2002.

[45] P. Bollini, S. Choi, J. H. Drese and C. W. Jones, "Oxidative Degradation of Aminosilica Adsorbents Relevant to Postcombustion CO_2 capture," *Energy & Fuels,* vol. 25, pp. 2416-2425, 2011.

[46] O. Leal, C. Bolivar, C. Ovalles, J. J. Gracia and Y. Espidel, "Reversible adsorption of carbon dioxide on amine surface-bonded silica gel," *Inorganica Chimica Acta,* vol. 240, pp. 183-189, 1995.

[47] G. P. Knowles, J. V. Graham, S. W. Delaney and A. L. Chaffee, "Aminopropyl-functionalized mesoporous silicas as CO_2 adsorbents," *Fuel Processing Technology,* vol. 86, pp. 1435-1448, 2005.

[48] G. P. Knowles, S. W. Delaney and A. L. Chaffee, "Diethylenetriamine[propyl(silyl)]-Functionalized (DT) Mesoporous Silicas as CO_2 Adsorbents," *Industrial & Engineering Chemistry Research,* vol. 45, no. 8, pp. 2626-2633, 2006.

[49] C. Knofel, J. Descarpentries, A. Benzaouia, V. Zelenak, S. Mornet, P. Llewelyn and V. Hornebecq, "Functionalised micro-/mesoporous silica for the adsorption of carbon dioxide," *Microporous and Mesoporous Materials,* vol. 99, no. 1-2, pp. 79-85, 2007.

[50] H. Y. Yang and F. T. Huang, "Amine-Grafted MCM-48 and Silica Xerogel as Superior Sorbents for Acidic Gas Removal from Natural Gas," *Industrial & Engineering Chemistry Research,* vol. 42, no. 12, pp. 2427-2433, 2003.

[51] W. Linfang, M. Lei, W. Aiquin, L. Qian and Z. Tao, "CO_2 adsorption on SBA-15 Modified by Aminosilane," *Chinese Journal of Catalysis,* vol. 28, no. 9, pp. 805-810, 2007.

[52] N. Hiyoshi, K. Yogo and T. Yashima, "Adsorption characterisitcs of carbon dioxide on organically functionalized SBA-15," *Microporous and Mesoporous Materials,* vol. 84, pp. 357-365, 2005.

[53] P. Bollini, S. Choi, J. H. Drese and C. W. Jones, "Oxidative Degradation of Aminosilica Adsorbents Relevant to Postcombustion CO_2 capture," *Energy & Fuels,* vol. 25, pp. 2416-2425, 2011.

[54] W. Li, P. Bollini, S. A. Didas, S. Choi, J. H. Drese and C. W. Jones, "Structural Changes of Silica Mesocellular Foam Supported Amine-Functionalized CO_2 adsorbents Upon Exposure to Steam," *Applied Materials & Interfaces,* vol. 2, no. 11, pp. 3363-3372, 2010.

[55] O. Leal, C. Bolivar, C. Ovalles, J. J. Gracia and Y. Espidel, "Reversible adsorption of carbon dioxide on amine surface-bonded silica gel," *Inorganica Chimica Acta,* vol. 240, pp. 183-189, 1995.

[56] R. A. Khatri, S. S. C. Chuang, Y. Soong and M. Gray, "Thermal and Chemical Stability of Regenerable Solid Amine Sorbent for CO_2 Capture," *Energy & Fuels,* vol. 20, pp. 1514-1520, 2006.

[57] A. Sayari and Y. Belmabkhout, "Isothermal versus Non-isothermal Adsorption-Desorption Cycling of Triamine-Grafted Pore-Expanded MCM-41 Mesoporous Silica for CO_2 Capture from Flue Gas," *Energy & Fuels,* vol. 24, pp. 5273-5280, 2010.

[58] J. H. Drese, S. Choi, S. A. Didas, P. Bollini, M. L. Gray and C. W. Jones, "Effect of support structure on CO_2 adsoorption properties of pore-expanded hyperbranced aminosilicas," *Microporous and Mesoporous Materials,* vol. 151, pp. 231-240, 2012.

[59] A. Heydari-Gorji, Y. Belmabkhout and A. Sayari, "Polyethylenimine-Impregnated Mesoporous Silica: Effect of Amine Loading and Surface Alkyl Chains on CO_2 Adsorption," *Langmuir,* vol. 27, pp. 12411-12416, 2011.

[60] A. Sayari and Y. Belmabkhout, "Stabilization of Amine-Containing CO_2 Adsorbents; Dramatic Effect of Water Vapor," *Journal of the American Chemical Society,* vol. 18, no. 132, pp. 6312-6314, 2010.

[61] T. Drage, A. Arenillas, K. Smith and C. Snape, "Thermal stability of polyethylenimine based carbon dioxide adsorbents and its influence on selection of regeneration strategies," *Microporous and Mesoporous Materials,* vol. 116, pp. 504-512, 2008.

[62] C. Biqiong, J. R. G. Evans, H. C. Greenwell, P. Boulet, P. V. Coveney, A. A. Bowden and A. Whiting, "A critical appraisal of polymer-clay nanocomposites," *Chemical Society Reviews,* vol. 37, pp. 568-594, 2008.

[63] F. Hussain and M. Hojjati, "Polymer-matrix Nanocomposites, Processing, Manufacturing and Application: an Overview," *Composite Materials,* vol. 40, pp. 1511-1575, 2006.

[64] F. Bergaya and B. Theng, Handbook of Clay materials, Elsevier, 2006, pp. 1-109.

[65] K. Wang, L. Wang, J. Wu, L. Chen and C. He, "Preparation of Highly Exfoliated Epoxy/Clay Nanocomposites by "Slurry Compounding": Process and Mechanisms," *American Chemical Society,* vol. 21, pp. 3613-3618, 2005.

[66] H. L. Friedman, "Kinetics of Thermal Degradation of char-forming plastics from thermogravimetry. Application to a phenolic plastic," *Polymer Science,* no. 6, pp. 183-195, 1964.

[67] J. H. Flynn and L. A. Wall, "A Quick, direct method for the determination of activation energy from thermogravimetric data," *Journal of Polymer Science Part B; Polymer Letters,* vol. 4, no. 5, pp. 323-328, 1966.

[68] S. Gill and S. P., "Decomposition Kinetics using TGA," TA Instruments, New Castle, DE, 1994.

[69] O. Monticelli, Z. Musina, A. Frache, F. Bellucci, G. Camino and S. Russo, "Influence of compatibilizer degradation on fromation and properties of PA6/organoclay nanocomposites," *Polymer Degradation and Stability 92 ,* vol. 92, pp. 370-378, 2007.

[70] J. L. Bishop, C. M. Pieters and J. O. Edwards, "Infrared Spectroscopic Analyses on the Nature of Water in Montmorillonite," *Clays and Clay Minerals,* vol. 42, no. 6, pp. 702-716, 1994.

[71] A. Danon, P. C. Stair and E. Weitz, "FTIR Study of CO_2 Adsorption on Amine-Grafted SBA-15: Elucidation of Adsorbed Species," *Physical Chemistry,* vol. 115, pp. 11540-11549, 2011.

[72] X. Wang, V. Schwartz, J. C. Clark, X. Ma, S. H. Overbury, X. Xu and C. Song, "Infrared Study of CO_2 Sorption over "Molecular Basket" Sorbent Consisting of Polyethylenimine-Modified Mesoporous Molecular Sieve," *Physical Chemistry,* vol. 17, no. 113, pp. 7260-7268, 2009.

[73] A. C. C. Chang, S. S. Chuang, M. Gray and Y. Soong, "In-situ Infrared Study of CO_2 Adsorption on SBA-15 Grafted with (Aminopropyl)triethoxsilane," *Energy & Fuels,* vol. 17, pp. 468-473, 2003.

Appendix A: Tabulated Data for Graphs

Table A-1: Data for Figure 4-5, Comparison of "dry method" versus "slurry method"

Concentration (g APTMS/ g Clay)	0.4	0.8
"Dry Method" Percent Amine (wt.%)	14.8	17.4
"Dry Method" Standard Deviation (STDEV) (wt.%)	0.1	0.9
"Slurry Method" Percent Amine (wt.%)	19.8	19.1
"Slurry Method" STDEV (wt.%)	1.6	1.1

Table A-2: Data for Figure 4-6, Percent amine grafted versus the concentration of APTMS "slurry method"

Concentration (g APTMS/ g Clay)	0.4	0.6	0.8	1.0	1.2
Percent Amine (wt.%)	14.2	13.6	12.0	16.7	15.7
STDEV (wt.%)	1.6	1.1	1.6	0.2	1.9

Table A-3: Data for Figure 4-8, Comparison of amount amine grafted versus treatment

	Weight Percent Amine	STDEV (wt.%)
C-PEI-50	37.4	1.5
C-APTMS-1-2	15.7	1.9
C-APTMS-PEI	40.5	2.1

Table A-4: Data for Figure 5-5, Carbon dioxide adsorption capacity as a function of adsorption temperature at atmospheric pressure in the TGA

Adsorption Temperature	50°C	75°C	85°C	100°C	125°C	150°C
Untreated Clay (wt.%)	0.2	0.6	0.7	1.0	1.1	0.7
Untreated Clay (STDEV wt.%)	0.1	0.3	0.4	0.3	0.3	0.5
C-PEI (wt.%)	2.4	6.0	6.2	6.3	3.9	1.3
C-PEI (STDEV wt.%)	0.6	1.2	0.9	0.9	1.7	0.8
C-APTMS (wt.%)	4.6	5.2	6.1	4.3	4.5	4.1
C-APTMS (STDEV wt.%)	1.2	2.0	0.9	1.3	1.9	1.6
C-APTMS-PEI (wt.%)	2.3	3.7	7.5	5.7	5.4	3.0
C-APTMS-PEI (STDEV wt.%)	1.1	1.5	1.9	1.7	0.1	0.2

Table A-5: Data for Figure 5-6, Time versus percent CO_2 adsorbed based on a 90 minute adsorption run

Percent Adsorption	50%	75%	90%	95%
C-PEI (minutes)	1.1	8.2	32.2	53.8
C-PEI (STDEV minutes)	0.6	3.2	5.7	5.6
C-APTMS (minutes)	0.7	2.2	8.1	18.7
C-APTMS (STDEV minutes)	0.2	1.0	5.6	12.1
C-APTMS-PEI (minutes)	2.0	11.7	33.8	58.8
C-APTMS-PEI (STDEV minutes)	1.9	7.4	3.7	7.7

Table A-6: Data for Figure 5-9, CO_2 adsorption for clay loaded with PEI at 85°C

PEI	Mn 423	Mn 1200	Mn 60,000
CO_2 adsorption (wt.%)	6.2	6.0	1.6
STDEV (wt.%)	0.9	0.7	0.8

Table A-7: Data for Figure 5-10, Comparison of PEI loading versus CO_2 adsorption capacity at 85°C

PEI loading	33%	50%	66%
CO_2 adsorption (wt.%)	4.0	6.2	5.3
STDEV (wt.%)	0.4	0.9	1.1

Table A-8: Data for Figure 5-12, CO_2 adsorption capacity in pure CO_2 and 10% CO_2 balanced with nitrogen

	C-PEI	C-APTMS	C-APTMS-PEI
Pure CO_2 (wt.%)	6.2	6.1	7.5
Pure CO_2 (STDEV wt.%	0.9	0.9	1.9
10% CO_2 (wt.%)	5.9	5.1	6.5
10% CO_2 (STDEV wt.%)	0.6	2.3	3.1

Table A-9: Data for Figure 5-13, Percent regeneration using pure nitrogen at 100°C

	CO_2 adsorption (wt.%)	1st Cycle CO_2 adsorption (wt.%)	Percent regeneration based on 1st cycle adsorption
C-PEI (wt.%)	5.8	5.5	94.0%
C-PEI (STDEV wt.%)	0.9	0.7	4.3%
C-APTMS (wt.%)	6.0	6.0	101.2%
C-APTMS (STDEV wt.%)	1.1	1.0	2.6%
C-APTMS-PEI (wt.%)	7.6	7.3	97.2%
C-APTMS-PEI (STDEV wt.%)	2.0	1.9	3.9%

Table A-10: Data for Figure 5-14, CO_2 adsorption capacity over 10 cycles

Cycle	0	1	2	3	4	5	6	7	8	9	10
C-PEI (wt.%)	6.2	5.8	5.7	5.6	5.6	5.1	5.4	5.4	5.3	5.3	5.2
C-PEI (STDEV wt.%)	0.1	0.1	0.1	0.1	0.1	0.7	0.1	0.1	0.0	0.1	0.0
C-APTMS (wt.%)	6.7	6.6	6.6	6.6	6.6	6.7	6.6	6.6	6.6	6.6	6.6
C-APTMS (STDEV wt.%)	1.4	1.4	1.3	1.3	1.3	1.2	1.3	1.3	1.3	1.3	1.3
C-APTMS-PEI (wt.%)	8.5	8.4	8.3	8.3	8.3	8.2	8.2	8.2	8.1	8.1	8.0
C-APTMS-PEI (STDEV wt.%)	0.3	0.4	0.4	0.5	0.5	0.5	0.6	0.6	0.7	0.7	0.7

Table A-11: Data for Figure 5-18, Percent CO_2 cycled using pure CO_2 at 155°C for 30 minutes for regeneration

Cycle	1	2	3
C-PEI (Percent CO_2 cycled)	84%	78%	77%
C-PEI (STDEV)	5%	6%	9%
C-APTMS (Percent CO_2 cycled)	101%	91%	79%
C-APTMS (STDEV)	7%	10%	9%
C-APTMS-PEI (Percent CO_2 cycled)	100%	93%	85%
C-APTMS-PEI (STDEV)	7%	10%	11%

Table A-12: Data for Figure 5-20, Percent CO_2 cycled using humid CO_2 at 155°C for 30 minutes for regeneration

Cycle	1	2
C-PEI (Percent CO_2 cycled)	95%	92%
C-PEI (STDEV)	5%	6%
C-APTMS (Percent CO_2 cycled)	96%	95%
C-APTMS (STDEV)	8%	9%
C-APTMS-PEI (Percent CO_2 cycled)	96%	92%
C-APTMS-PEI (STDEV)	3%	7%

Table A-13: Data for Figure 5-25, Vacuum regeneration results for 85°C vacuum desorption in the vacuum oven

	1 hour vacuum	17 hour vacuum
C-PEI (Percent CO_2 cycled)	96%	87%
C-PEI (STDEV)	5%	3%
C-APTMS (Percent CO_2 cycled)	87%	106%
C-APTMS (STDEV)	14%	16%
C-APTMS-PEI (Percent CO_2 cycled)	104%	95%
C-APTMS-PEI (STDEV)	12%	13%

Table A-14: Data for Figures 5-26-30, Pure CO_2 adsorption at pressure

Pressure (PSI)	**40**	**40**	**40**	**100**	**100**	**100**	**200**	**200**	**200**	**300**	**300**	**300**
Time (hours)	**2**	**16**	**24**	**2**	**16**	**24**	**2**	**16**	**24**	**2**	**16**	**24**
C-PEI (wt.%)	4.7	9.1	8.7	5.9	7.9	6.5	5.7	7.0	6.7	6.4	6.4	6.8
C-PEI STDEV	1.1	1.3	2.7	0.6	1.4	1.3	0.2	1.1	1.1	2.8	3.3	1.9
C-APTMS (wt.%)	7.5	7.6	7.6	4.3	7.1	8.1	6.3	6.5	6.3	6.0	7.2	7.6
C-APTMS STDEV	1.8	1.5	1.1	1.1	0.2	1.0	1.2	1.5	1.0	1.8	1.4	1.5
C-APTMS-PEI (wt. %)	4.1	5.2	9.9	7.1	9.1	7.3	5.1	9.0	10.1	7.3	8.5	11.4
C-APMTS-PEI STDEV	1.9	0.9	0.6	4.3	2.0	2.5	0.9	3.8	2.3	0.8	2.9	0.6
Untreated Clay (wt.%)	0.9	1.4	1.4	0.4	1.0	1.3	1.6	1.4	1.5	2.0	1.0	2.3
Untreated Clay STDEV	0.6	0.3	0.3	0.1	0.4	0.9	0.3	0.4	0.5	0.8	0.1	0.6

Table A-15: Data for Figures 5-31-32, Pure CO_2 adsorption at pressure and temperature

Adsorption for 24 hours at 300 PSI	Room Temperature	50°C	75°C	85°C
C-PEI (wt.%)	6.8	15.8	17.2	18.7
C-PEI STDEV	1.9	3.3	4.9	0.8
C-APTMS (wt.%)	7.6	8.1	9.0	9.6
C-APTMS STDEV	1.5	2.5	0.2	0.4
C-APTMS-PEI (wt. %)	11.4	14.2	17.8	18.3
C-APMTS-PEI STDEV	0.6	3.5	8.4	0.5
Untreated Clay (wt.%)	2.3	3.6	4.2	5.3
Untreated Clay STDEV	0.6	0.1	1.8	0.5

Table A-16: Data for Figure 5-33, CO_2 adsorption and vacuum desorption results

Pure CO_2 adsorption at 300 PSI and 2 Hours	Initial Adsorption	Vacuum Desorption	Cycled Adsorption
C-PEI (wt.%)	5.6	7.0	5.5
C-PEI (STDEV wt.%)	1.5	0.7	0.5
C-APTMS (wt.%)	5.5	6.7	4.1
C-APTMS (STDEV wt.%)	2.0	1.2	1.5
C-APTMS-PEI (wt.%)	5.8	6.7	6.0
C-APTMS-PEI (wt.%)	1.3	0.6	0.9
Untreated Clay (wt.%)	2.3	2.4	2.4
Untreated Clay STDEV	0.8	0.4	0.4

Table A-17: Data for Figure 5-34, CO_2 adsorption and vacuum desorption results

Pure CO_2 adsorption at 300 PSI, 2 Hours and 50°C	Initial Adsorption	Vacuum Desorption	Cycled Adsorption
C-PEI (wt.%)	13.5	11.6	14.3
C-PEI (STDEV wt.%)	1.2	0.8	0.8
C-APTMS (wt.%)	5.9	4.5	4.7
C-APTMS (STDEV wt.%)	0.4	0.3	0.4
C-APTMS-PEI (wt.%)	11.8	9.7	11.5
C-APTMS-PEI (wt.%)	1.5	0.8	1.9
Untreated Clay (wt.%)	3.6	2.6	4.2
Untreated Clay STDEV	0.1	0.0	0.3

Table A-18: Data for Figures 5-35-36, CO_2 adsorption before and after water stability test

Water stability test	Initial Adsorption	Adsorption After Stability Test
C-PEI-33 (wt.%)	4.2	4.3
C-PEI-33 (STDEV wt.%)	0.2	0.4
C-PEI-50 (wt.%)	5.6	4.6
C-PEI-50 (STDEV wt.%)	0.2	1.1
C-PEI-66 (wt.%)	5.9	6.8
C-PEI-66 (STDEV wt.%)	0.3	0.7
C-APTMS (wt.%)	6.0	3.9
C-APTMS (STDEV wt.%)	0.2	0.5
C-APTMS-PEI (wt.%)	6.5	6.7
C-APTMS-PEI (wt.%)	0.2	0.8